ISSN 1346-7328
国総研資料 第104号
平 成 1 5 年 3 月

国土技術政策総合研究所資料

TECHNICAL NOTE of
National Institute for Land and Infrastructure Management

No. 104 March 2003

建築構造物の耐震安全性の向上に関する日欧共同研究
第７回合同推進会議

The 7th Management Panel on Collaboration Research Activities about Building Structural Engineering between JRC-IPSC, NILIM & BRI
30-31 May 2002, at Tsukuba City, JAPAN

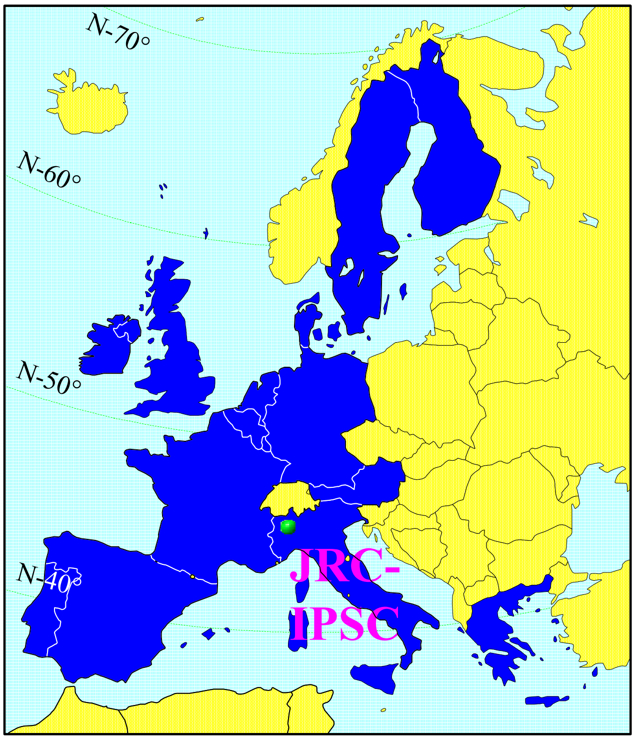

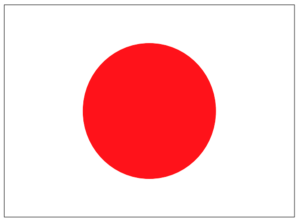

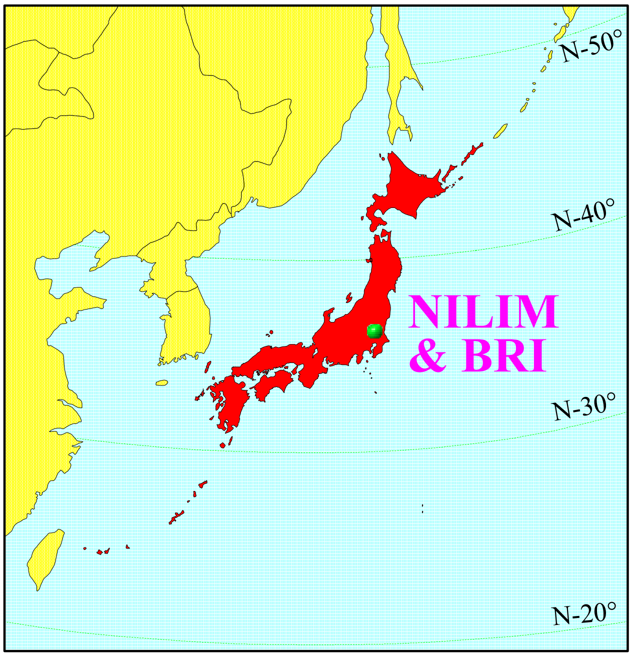

国土交通省　国土技術政策総合研究所

National Institute for Land and Infrastructure Management
Ministry of Land, Infrastructure and Transport, JAPAN

はしがき

建築構造物の耐震安全性の向上に関する日欧共同研究は、1995 年 11 月に、当時の建設省建築研究所及び欧州連合・共同研究センター・安全工学研究所(現在、市民保護安全研究所)が、以下の６項目についての研究協力協定を締結して以来、実施されている。

(1)日欧の耐震基準の相互比較

(2)性能概念に基づく耐震設計法の開発と検証

(3)直下型地震等の構造物への影響評価

(4)免震・制振適用に関する基本概念の構築

(5)既存建築構造物の脆弱性評価手法・補修補強工法の開発

(6)耐震性評価のための実大構造物実験手法

なお、2001 年に建設省建築研究所が組織改革され、建築研究所が独立行政法人となり、あわせて国土交通省の内部研究機関として国土技術政策総合研究所が設置されたことにより、日本側では、両研究所が連携して、本共同研究を行っている。

本共同研究では、日欧双方の研究所において得られた研究成果を情報交換し、更に、その後の研究方針を調整するため、日欧双方が参加して合同推進会議を実施している。合同推進会議は、１年に１回、日本と欧州で交互に、開催しており、1996 年から 2001 年までに、つくば市またはイタリア共和国イスプラにおいて、６回開催された。

第７回合同推進会議は、2002 年 5 月 30 日～31 日に、つくば市において開催された。会議では、ピロティーを有する建築物の地震時挙動に関する検討、既存建築物の耐震性向上に関する研究プロジェクト等が報告され、今後の活動方針について議論された。

本資料は、第７回合同推進会議での報告・討議内容を記録したものである。

Preface

The Collaboration Research Activities about Building Structural Engineering between EU and Japan is initiated in the “Record of Discussion” on December 1995 in the field of the earthquake engineering for building structures between the past Safety Technology Institute (the latest Institute for the Protection and Security of the Citizen), Joint Research Centre, European Union (JRC-IPSC) and the past Building Research Institute, Ministry of Construction, Japan. The “Record of Discussion” included the following 6 items.

(ITEM 1) : Comparison of the seismic performance of building structures designed according to the current European and Japanese Norms (comparison)

(ITEM 2) : Development and validation of new design methods based on performance concepts (performance concepts)

(ITEM 3) : Study of seismic action, such as impulsive type of ground motion in near source areas or long-duration long-period motion in the far field over soft soil (seismic action)

(ITEM 4) : Study of the concepts of base isolation and seismic response control for building structures (base isolation)

(ITEM 5) : Vulnerability assessment, repair and strengthening of existing building structures (repair)

(ITEM 6) : Development of large scale experimental method (pseudo dynamic)

In 2001, Building Research Institute was reorganized to become an Independent Administrative Institution named as Building Research Institute (BRI), and the new national research institute in Ministry of Land, Infrastructure and Transport was organized as National Institute for Land and Infrastructure Management (NILIM). Therefore, in Japan the both of BRI and NILIM execute this Collaboration Research Activities.

At this Collaboration Research Activities, the Management Panels are held by the both of EU and Japan in order to exchange the research results and discuss the future plan. The Management Panels are supposed to be held once a year at EU or Japan respectively, and they were already held 6 times at Tsukuba, Japan or at Ispra, Italy from 1996 to 2001.

The 7th Management Panel was held in 30 and 31 May 2002 at Tsukuba city in Japan. The presentation topics were Sub-Structure Pseudo Dynamic Testing on Soft First Story, Seismic Performance Assessment & Rehabilitation: SPEAR, and others. The future plan was discussed and the resolutions were adopted.

This technical note is a record of the 7th Management Panel.

国土技術政策総合研究所資料 Technical Note of NILIM
第１０４号 2003 **年** 3 **月** No.104 March 2003

建築構造物の耐震安全性の向上に関する日欧共同研究 第７回合同推進会議

The 7th Management Panel on Collaboration Research Activities about Building Structural Engineering between JRC-IPSC, NILIM & BRI

概要

以下の研究機関により実施されている建築構造に関する日欧共同研究の第７回合同推進会議が、2002 年 5 月 30 日～ 31 日に、つくば市において開催された。

- 欧州連合・共同研究センター・市民保護安全研究所
- 国土交通省国土技術政策総合研究所
- 独立行政法人建築研究所

会議では、これまでの研究活動状況等が報告され、今後の活動方針について議論された。

本資料は、第７回合同推進会議での報告・討議内容を記録したものである。

ｷｰﾜｰﾄﾞ ： 日欧共同研究、建築構造物、合同推進会議

Synopsis

The 7th Management Panel on Collaboration Research Activities between the following Institutes was held in 30 and 31 May 2002 at Tsukuba, Japan .

- the Institute for the Protection and Security of the Citizen, Joint Research Centre, EUROPEAN UNION (JRC-IPSC),
- National Institute for Land and Infrastructure Management, Ministry of Land, Infrastructure and Transport, JAPAN (NILIM),
- Building Research Institute, JAPAN (BRI)

The past activities related to the collaboration research were confirmed and the future plans of the collaboration works were made.

This technical note is a record of the 7th Management Panel.

Key Words ： Collaboration Research Activities, EU, JAPAN, Building Structural Engineering, Record of Management Panel

Table of contents

Member

<u>JRC-IPSC side:</u>

Fabio TAUCER	:Structural Mechanics Unit.

<u>NILIM side:</u>

Junichi MURAKAMI	:Deputy of Director General,
Mikio FUTAKI	:Director of Building Department,
Mizuo INUKAI	:Senior Researcher, Standards and Accreditation System Division, Building Department,

<u>BRI side:</u>

Hiroyuki YAMANOUCHI	:Chief Executive,
Toshibumi FUKUTA	:Director of International Institute of Seismology and Earthquake Engineering,
Masaomi TESHIGAWARA	:Chief Research Engineer, Department of Structural Engineering,
Masanori IIBA	:Chief Research Engineer, Department of Structural Engineering,
Hiroshi KURAMOTO	:Associate Professor, International Cooperation Center of Engineering Education Development, Toyohashi University of Technology,
Hiroshi FUKUYAMA	:Chief Research Engineer, Department of Structural Engineering,
Hiroto KATO	:Senior Research Engineer, Department of Structural Engineering,
Koichi KUSUNOKI	:Senior Research Engineer, Department of Structural Engineering,

AGENDA ON 30&31 MAY, 2002 AT NILIM & BRI

30 May(Thu)

9:30 9:35	Opening at Meeting room of NILIM ANNEX 4F
10:00-10:10	Introduction of members, confirmation of agenda
10:10-10:50	Session 1 Experimental Results on Stress-Strain Relation of Ti-Ni Shape Memory Alloy Bars and Their Application to Seismic Control of Buildings by T. Fukuta
10:50-11:30	Session 2 Experimental Study on Torsional Vibration Behavior of Steel Frame Specimen with Eccentricity by H. Kato
12:00-13:30	Friendship luncheon hosted by NILIM & BRI
13:30-14:00	Greeting to Director General
14:00-14:45	Session 3 Seismic Performance of Retrofitted RC Slab Connected with Strengthening Frame by M. Inukai
14:45-15:20	Session 4 Posterior Time-Step Adjustment Technique in Substructuring Pseudo-Dynamic Test by K. Kusunoki
15:20-15:50	Session 5 Mass-eccentric Effect on response of Base Isolation System for Houses by M. Iiba
18:00-20:00	Dinner

31 May(Fri)

9:30-10:15	Session 6 Sub-Structure Pseudo Dynamic Testing on 12 story Reinforced Concrete Frame with Soft First Story by H. Kuramoto
10:15-11:00	Session 7 European Laboratory For Structural Assessment (ELSA) by F. Taucer
11:00-12:00	Session 8 Smart Structural System Large Scale Shaking Test by M. Teshigawara
12:00-14:00	Luncheon hosted by NILIM & BRI
14:00-14:30	Session 9 Safety Assessment for Earthquake Risk Reduction: An EU Research and Training Network by F. Taucer
14:30-15:00	Session 10 Seismic Performance Assessment & Rehabilitation: SPEAR by F. Taucer
15:00-15:30	Session 11 Japanese Design And Construction Guidelines For Seismic Retrofit of Building Structures With FRP Composites by H. Fukuyama
15:30-16:00	Session 12 Discussion about Future plan and Possible collaboration
16:00-16:30	Visit to laboratory
16:30-16:45	Confirmation of resolutions
16:45-17:00	Adoption of final resolutions
18:00-20:00	Friendship dinner hosted by BRI

SUMMARY, RESOLUTION AND RECOMMENDATIONS OF THE SEVENTH MANAGEMENT PANEL ON COLLABORATION RESEARCH ACTIVITIES BETWEEN JRC-IPSC J-NILIM AND J-BRI
(Tsukuba, Ibaraki, Japan, May 30 & 31, 2002)

The seventh management panel on collaboration research activities between JRC-IPSC(Institute for the Protection and Security of the Citizen, the former JRC-ISIS), J-NILIM(National Institute for Land and Infrastructure Management) and J-BRI(Building Research Institute) was held in Tsukuba on May 30 and 31, 2002, for the purpose of confirming the past activities related to the collaboration research, exchanging the related research information and discussing the future plan of the collaboration works. The past research results presented and discussed in a most friendly and cordial atmosphere. The cooperative activities in the future were discussed, and the summary, resolutions and recommendations were agreed.

1. PARTICIPANTS TO THE MEETING

From JRC-IPSC
Fabio TAUCER
From J-BRI
Toshibumi FUKUTA, Masaomi TESHIGAWARA, Hiroshi FUKUYAMA, Hiroto KATO, Masanori IIBA, Kouichi KUSUNOKI,
Hiroshi KURAMOTO(former researcher of BRI, Toyohashi Univ. of Technology)
From J-NILIM
Mikio FUTAKI, Mizuo INUKAI

2. SUMMARY OF MEETING

The research results were presented and discussed on the collaborative research items as written below.

(ITEM 1) : Comparison of the seismic performance of building structures designed according to the current European and Japanese Norms (comparison)
(ITEM 2) : Development and validation of new design methods based on performance concepts (performance concepts)
(ITEM 3) : Study of seismic action, such as impulsive type of ground motion in near-source areas or long-duration long-period motion in the far field over soft soil (seismic action)
(ITEM 4) : Study of the concepts of base isolation and seismic response control for building structures (base isolation)

(ITEM 5) : Vulnerability assessment, repair and strengthening of existing building structures (repair)
(ITEM 6) : Development of large scale experimental method (pseudo dynamic)

JRC-IPSC side
- Presentation of the research activities, structure and organization of the ELSA laboratory. (F. Taucer)
- Safety Assessment for Earthquake Risk Reduction (SAFERR): Overview (F. Taucer)
- Seismic Performance Assessment and Rehabilitation (SPEAR): Overview (F. Taucer)

J-NILIM and J-BRI side
- Experimental Results on Stress-Strain Relation of Ti-Ni Shape Memory Alloy Bars and their Application to Seismic Control of Buildings (T. Fukuta)
- Experimental Study on Torsional Vibration Behavior of Steel Frame Specimen with Eccentricity (H. Kato)
- Seismic Performance of Retrofitted RC Slab Connected with Strengthening Frame (M. Inukai)
- Posterior Time-Step Adjustment Technique in Substructuring Pseudo-Dynamic Test (K. Kusunoki)
- Mass-eccentric Effect on Response of Base Isolation System for Houses (M. Iiba)
- Japanese Design and Construction Guidelines for Seismic Retrofit of Building Structures with FRP Composites (H. Fukuyama)
- Sub-Structure Pseudo Dynamic Testing on 12 Storey Reinforced Concrete Frame with Soft First Storey (H. Kuramoto)
- Smart Structural Systems Large Scale Test (M. Teshigawara)

Under the above considerations, the future plan of the collaborative activities was discussed.

3. RESOLUTION

1) Both sides consider that the meeting was successful and fruitful.

2) Both sides re-affirm that the exchange of detailed information about the results of the past activities was effective and should be continued at an increased level.

3) Both sides discussed the future areas of collaboration for research, namely: i) the renewal of existing building structures and ii) the harmonization of testing methods directed towards the development of performance based design methodologies. For this

purpose effective exchange of information during the next months will be maintained by electronic mail, fax, telephone, etc.

4. RECOMMENDATIONS

1) Both sides will make any necessary actions for continuing collaboration on the present agreement.

2) The materials and papers introduced in the meeting are bound as proceedings of the seventh management panel.

3) The collaboration between J-BRI, J-NILIM and JRC-IPSC, acting as main communication links of the Japanese and European research parties, will be continuously pursued.

Tsukuba, Japan, May 31, 2002

Fabio TAUCER, M. Eng..
Chairman, Management Panel EU Side
Structural Mechanics Unit
Institute for the Protection and Security of the Citizen
Joint Research Centre (JRC-IPSC),
European Commission

Mikio FUTAKI, Dr. of Eng.
Chairman, Management Panel Japanese Side
Building Department
National Institute for Land and,
Infrastructure Management (J-NILIM)
Ministry of Land, Infrastructure and
Transport, Japan

SUMMARY, RESOLUTION AND RECOMMENDATIONS OF THE SEVENTH MANAGEMENT PANEL ON COLLABORATION RESEARCH ACTIVITIES BETWEEN JRC-IPSC J-NILIM AND J-BRI
(Tsukuba, Ibaraki, Japan, May 30 & 31, 2002)

The seventh management panel on collaboration research activities between JRC-IPSC(Institute for the Protection and Security of the Citizen, the former JRC-ISIS), J-NILIM(National Institute for Land and Infrastructure Management) and J-BRI(Building Research Institute) was held in Tsukuba on May 30 and 31, 2002, for the purpose of confirming the past activities related to the collaboration research, exchanging the related research information and discussing the future plan of the collaboration works. The past research results presented and discussed in a most friendly and cordial atmosphere. The cooperative activities in the future were discussed, and the summary, resolutions and recommendations were agreed.

1. PARTICIPANTS TO THE MEETING

From JRC-IPSC
Fabio TAUCER
From J-BRI
Toshibumi FUKUTA, Masaomi TESHIGAWARA, Hiroshi FUKUYAMA, Hiroto KATO, Masanori IIBA, Kouichi KUSUNOKI,
Hiroshi KURAMOTO(former researcher of BRI, Toyohashi Univ. of Technology)
From J-NILIM
Mikio FUTAKI, Mizuo INUKAI

2. SUMMARY OF MEETING

The research results were presented and discussed on the collaborative research items as written below.

(ITEM 1) : Comparison of the seismic performance of building structures designed according to the current European and Japanese Norms (comparison)
(ITEM 2) : Development and validation of new design methods based on performance concepts (performance concepts)
(ITEM 3) : Study of seismic action, such as impulsive type of ground motion in near-source areas or long-duration long-period motion in the far field over soft soil (seismic action)
(ITEM 4) : Study of the concepts of base isolation and seismic response control for building structures (base isolation)

(ITEM 5) : Vulnerability assessment, repair and strengthening of existing building structures (repair)

(ITEM 6) : Development of large scale experimental method (pseudo dynamic)

JRC-IPSC side

- Presentation of the research activities, structure and organization of the ELSA laboratory. (F. Taucer)
- Safety Assessment for Earthquake Risk Reduction (SAFERR): Overview (F. Taucer)
- Seismic Performance Assessment and Rehabilitation (SPEAR): Overview (F. Taucer)

J-NILIM and J-BRI side

- Experimental Results on Stress-Strain Relation of Ti-Ni Shape Memory Alloy Bars and their Application to Seismic Control of Buildings (T. Fukuta)
- Experimental Study on Torsional Vibration Behavior of Steel Frame Specimen with Eccentricity (H. Kato)
- Seismic Performance of Retrofitted RC Slab Connected with Strengthening Frame (M. Inukai)
- Posterior Time-Step Adjustment Technique in Substructuring Pseudo-Dynamic Test (K. Kusunoki)
- Mass-eccentric Effect on Response of Base Isolation System for Houses (M. Iiba)
- Japanese Design and Construction Guidelines for Seismic Retrofit of Building Structures with FRP Composites (H. Fukuyama)
- Sub-Structure Pseudo Dynamic Testing on 12 Storey Reinforced Concrete Frame with Soft First Storey (H. Kuramoto)
- Smart Structural Systems Large Scale Test (M. Teshigawara)

Under the above considerations, the future plan of the collaborative activities was discussed.

3. RESOLUTION

1) Both sides consider that the meeting was successful and fruitful.

2) Both sides re-affirm that the exchange of detailed information about the results of the past activities was effective and should be continued at an increased level.

3) Both sides discussed the future areas of collaboration for research, namely: i) the renewal of existing building structures and ii) the harmonization of testing methods directed towards the development of performance based design methodologies. For this

purpose effective exchange of information during the next months will be maintained by electronic mail, fax, telephone, etc.

4. RECOMMENDATIONS

1) Both sides will make any necessary actions for continuing collaboration on the present agreement.

2) The materials and papers introduced in the meeting are bound as proceedings of the seventh management panel.

3) The collaboration between J-BRI, J-NILIM and JRC-IPSC, acting as main communication links of the Japanese and European research parties, will be continuously pursued.

Tsukuba, Japan, May 31, 2002

Fabio TAUCER, M. Eng..
Chairman, Management Panel EU Side
Structural Mechanics Unit
Institute for the Protection and Security of the Citizen
Joint Research Centre (JRC-IPSC),
European Commission

Toshibumi FUKUTA, Dr. of Eng.
Chairman, Management Panel Japanese Side
Production Engineering Department
Building Research Institute (J-BRI),
Ministry of Construction, Japan

Appendix 1

Section 1 Experimental Results on Stress-Strain Relation of Ti-Ni Shape Memory Alloy Bars and Their Application to Seismic Control of Buildings

presented by T. Fukuta

Experimental Results on Stress-Strain Relation of Ti-Ni Shape Memory Alloy Bars and their Application to Seismic Control of Buildings

Toshibumi Fukuta[1] & Masanori Iiba[2]

[1] International Institute of Seismology & Earthquake Engineering, Building Research Institute, Tsukuba, Japan
[2] Department of Structural Engineering, Building Research Institute, Tsukuba, Japan.

ABSTRACT

The mechanical property of Ti-Ni shape memory alloy (SMA) for tension and compression was investigated under super-elasticity. The test results demonstrated that the stress-strain curve for compressive stress is completely different from that for tensile stress, irrespective of whether the load is static or dynamic in nature. Super-elasticity was clearly evident under tensile strain of up to around 5%, but not under compressive strain, due to residual strain. Based on these results, SMA bars were examined to apply to the brace-type response-control devices for houses in their super-elasticity phase. It was found out that SMA has an effect to restore lateral drift of the structures to zero.

1. INTRODUCTION

SMA is a unique material that, when subject to stress, exhibits a “memory shape” effect linked to temperature and also undergoes changes in basic properties such as super-elasticity. These characteristics could potentially be applied to buildings to allow a degree of control over the building’s behavior in response to external forces, opening up new possibilities in building design. Although the tensile characteristics of thin wire have already been reported in experiments on the stress-strain relationship, temperature change, and strain rate under super-elastic conditions, little is known about how SMA behaves when subjected to compression. This study was designed to determine experimentally the stress-strain relationship in SMA bars in super-elastic alloy phase when subjected to compressive and tensile forces. Based on these results, SMA device of brace type response control for houses was examined by analysis.

2. Stress Strain Relation of SMA Bar

The alloy composition (Ti-Ni-Co alloy) and manufacturing conditions were carefully selected so that the test specimen would exhibit super-elastic properties at room temperature. Figure 1 schematically shows material phase and transformation temperatures as measured using a differential scanning calorimeter. The specimen with diameter 7 mm was fabricated from a bar of diameter 17 mm (Figure 2). The ambient temperature was around 26° C during the experiment. The readings from the two facing strain gauges were monitored to watch whether the test piece was centrally loaded. The readings deviated from one another only very slightly during the experiment. Similarly, eccentricity under the compression load did not reach significant levels. The load waveform used a triangular displacement-time relationship for both static and dynamic loads.

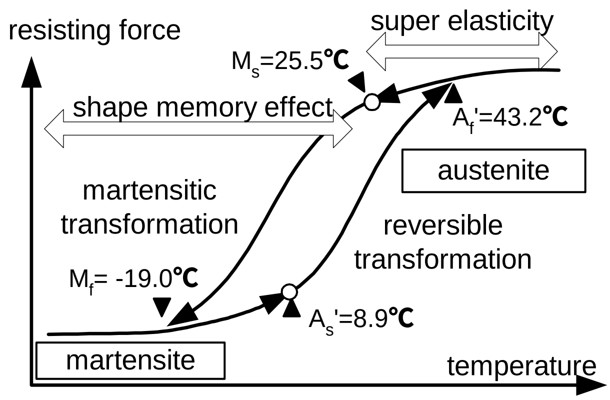

Figure 1. Transformation temperature & material phase

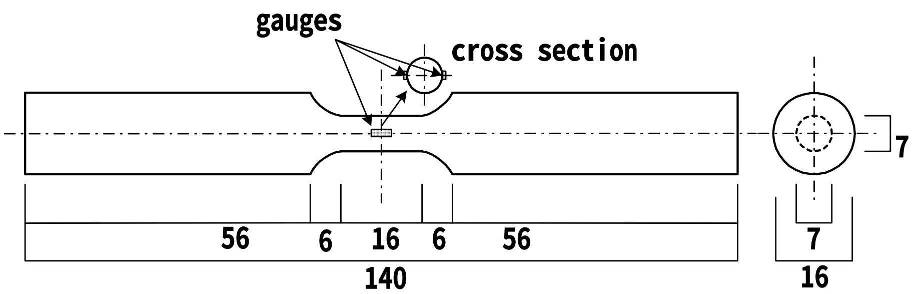

Figure 2. Test specimen

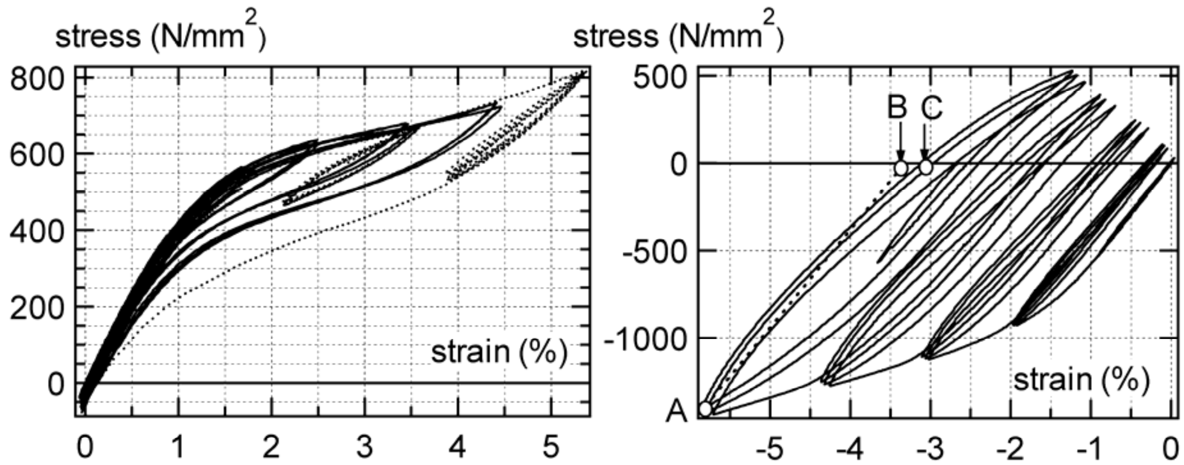

a) in tension **b)** in compression

Figure 3. Comparison of Stress-strain curves for tension test and compressive one

Figure 3-a) shows the stress-strain relationship for the static tensile test. The experiment began with three repetitions at each level (0%–1%, 0% –2%, etc.), as shown by the solid line. The specimen was then placed in a hot water bath at 50° C (hotter than the temperature at the end of the reverse transformation) for ten minutes, and repetitions were performed during unloading (at 0% – 2%, 2% –

4%, etc.). The strain generally returned to zero after each loading, clearly indicating super-elastic properties. Strain hardening can be observed from around 4% strain, where the curve gradient starts increasing. A very small amount of residual strain was observed after removal of the strain (approximately 4.5%).

Figure 3-b) shows the stress-strain curve under compression. Since the load was controlled by the distance between the two chucks of the loading machine, the paths of the stress-strain curve took were not exactly the same for all the sets of tests, because of the residual strain that remained in the test piece after removal of the load. The curve for compression forces differs in shape from the tension curve in Figure 3-a). The strain value shows no sign of the super-elasticity which would cause it to revert to zero upon removal of the load. The residual strain in fact resembles the stress-strain relationship for cold-formed carbon steel. Line AB is parallel to the initial stiffness, then strain BC shows a strain reversion.

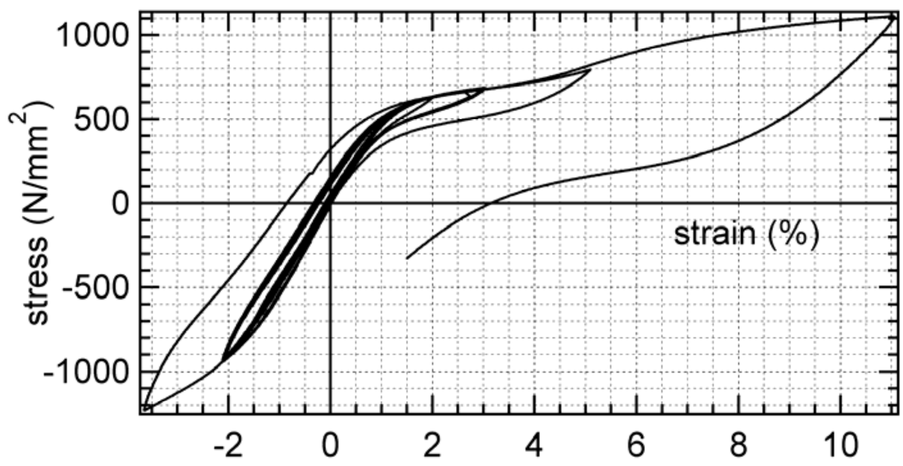

Figure 4. Stress-strain relationship for static tensile-compressive tests

Figure 4 shows the results of the tensile-compressive tests. The stress-strain relationship differs in many respects (yield strength, rigidity of plateau area after yielding, final strain value after removal of load) between the tension and the compression tests. Residual strain was observed after compression, but this could be negated almost completely by then applying a tensile strain that was greater (in absolute terms) than the compression strain that caused the residue.

Table 1. Average strain rate

strain amplitude	1st 10 cycles	2nd 10 cycles	3rd 10 cycles	4th 10 cycles
±1%	0.828	3.89	16.5	-
±2%	0.798	3.90	16.5	27.1
±4%	0.973	4.69	21.5	37.1

Unit : %/sec.

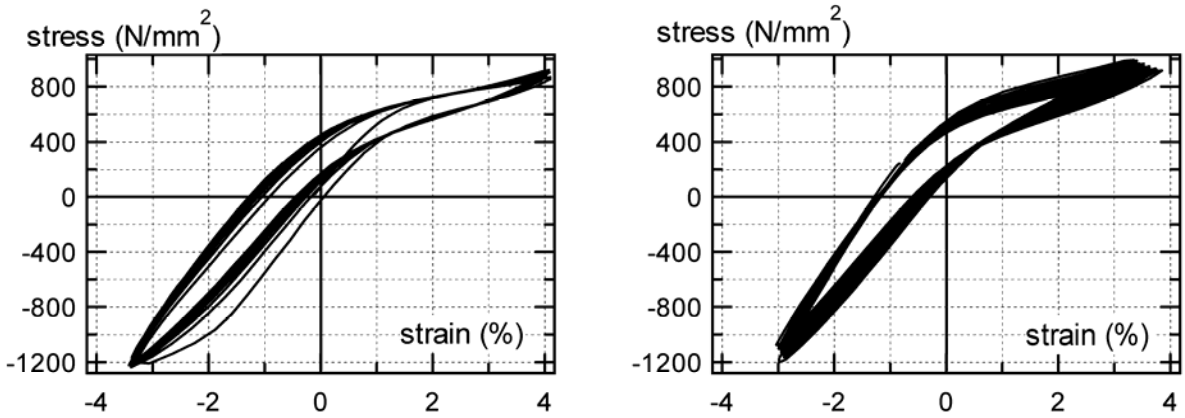

a) strain rate 0.973%/sec. b) strain rate 21.5%/sec.

Figure 5. Stress-strain relations under dynamic loading

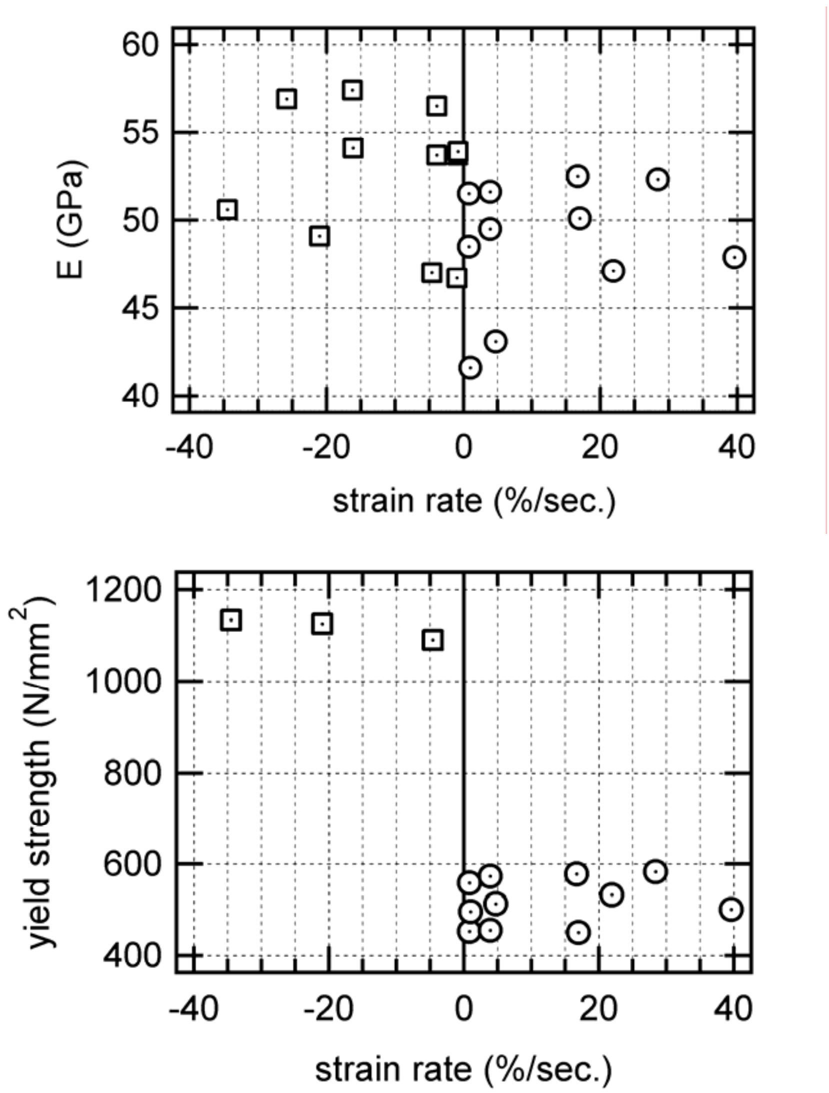

Figure 6. Effect of strain rate on Young’s modulus & yield strength

Under dynamic loading, the load waveform was triangular. The amplitude was varied at ±1%, ±2%, and ±4%, in that order. Three or four different loading frequencies were used at each amplitude (see Table 1). Ten repetitions were performed for each set of conditions. Therefore, a 110 repeated strain applied to a test specimen. Figure 5 represents results of stress-strain curves under cyclic loading. Overall shapes of curves are similar to those under static loading. Figure 6 presents effects of strain rate on Young's modulus and yield strength defined as 0.2 % offset value. The obvious relation cannot be notified between strain rate and these values. Yield strength in compression is almost two times of tension yielding under the strain rate tested.

3. SMA Device for Residential Houses

SMA bars clearly show super-elasticity in tension and not in compression. If SMA bars are used as a tension member, it would effectively control a displacement response of structures and return their lateral drift to zero after earthquakes. Then, a response control device with SMA bars is designed for low-storied houses as the followings: 1) SMA devices carry lateral forces, and beam-to-column frame supports vertical loads, 2) the size of SMA bars is designed so that the device has its required stiffness and strength, 3) SMA bars are effective only in tension. 4) elastic design is applied to the other part of the device under the yield strength of SMA bars (see Figure 7).

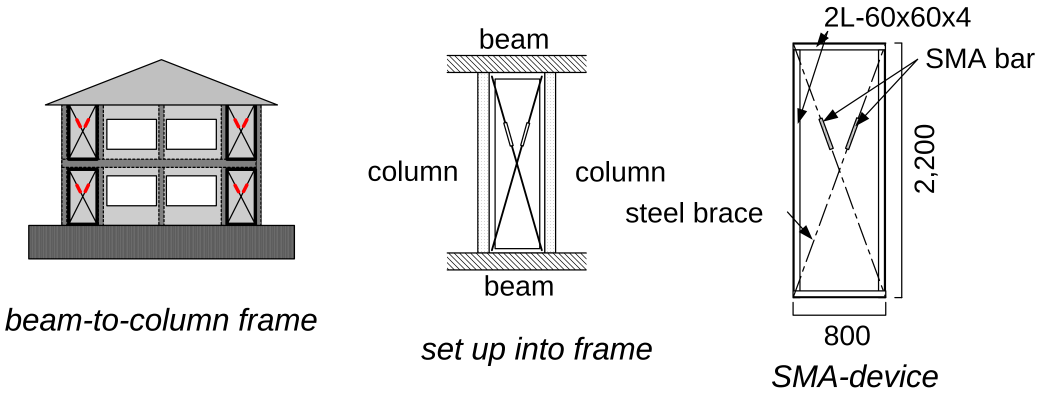

Figure 7. SMA device and its set up into a beam-to-column frame

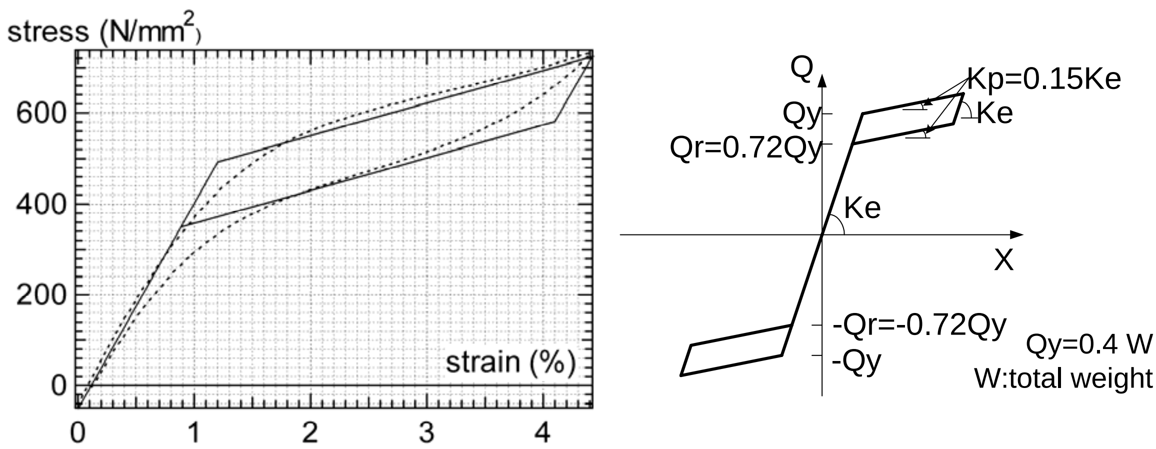

a) Stress-strain curve of SMA bars **b)** Restoring characteristic model

Figure 8. Restoring characteristic model of a structure with SMA devices

In order to conform the performance of SMA devices under sever earthquakes, the response of a structure with SMA devices was analyzed to El Centro NS wave of 340 gals maximum input. It is assumed that beam-to-column joints of the frame are pin-joint, the frame of the device behaves in elastic and the braces work only in tension. Therefore the restoring force characteristic of the structure can be assumed to be similar to stress-strain curve of SMA, as shown in Figure 8-b). This multi-linear model is based on the material test result of SMA in Figure 8-a). A single degree of freedom model with 0.5 second natural period, 5% viscous damping and lateral yield shear Qy of 40% of total weight was selected as an analytical model, which represents low-storied houses. The response is drawn in Figure 9 in comparison with the system of bi-linear restoring force characteristics. The analysis demonstrates that SMA devices return lateral drift of the structure to zero, on the contrary bi-linear system has some amount of story drift after the quake. But the maximum lateral displacement of the structure with SMA devices is about 1.5 times of the bi-linear model, because of lack of energy dissipation.

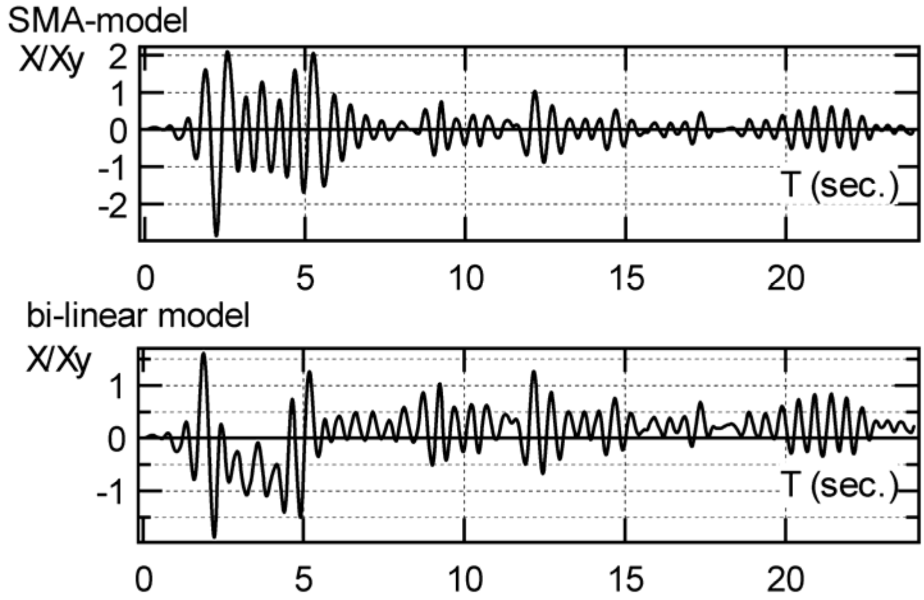

Figure 9. Time history of response of SMA-model & bi-linear model

4. CONCLUSIONS

This study looked at the stress-strain relationship for a columned specimen of diameter 7 mm taken from a bar of diameter 17 mm. The experiment was conducted with the specimen at the super-elastic alloy phase temperature. The specimen was subjected to static and dynamic compressive and tensile stress. The test results demonstrated that the stress-strain curve for tensile stress is completely different from that for compressive stress, irrespective of whether the load is static or dynamic in nature. Super-elasticity was clearly evident under tensile strain of up to around 5%, but not under compressive strain, due to the presence of residual strain. The yield strength in compression is almost two times of tension yielding under the strain rate tested. SMA devices were designed to control seismic response of wooden houses. Their performance was examined to return story drift of structures to zero after earthquakes, effectively.

ACKNOWLEDGEMENTS

This study was carried out by the Effector Section (led by University of Tokyo professor Takashi Fujita) of the Super-Intelligent Construction Systems Development project (headed by University of Tokyo professor Shunsuke Otani), a joint research project between Japan and the United States. The authors wish to convey their thanks to all involved.

REFERENCES

Funakubo T. and et al. (1984) *Shape Memory Alloy.* Sangyotosho, Tokyo

Tamai H. and Kitagawa Y. (2000) Pseudo elastic behavior of shape memory alloy wire and its application to seismic resistance member for building. *Proceedings of the IWCMM10*, Galway, Ireland

Appendix 2

Section 2 *Experimental Study on Torsional Vibration Behavior of Steel Frame Specimen with Eccentricity*

presented by H.Kato

Fifth International Congress on Advances in Civil Engineering, 25-27 September 2002
Istanbul Technical University, Istanbul, Turkey

Experimental Study on Torsional Vibration Behavior of Steel Frame Specimen with Eccentricity

Hiroto KATO, Koichi KUSUNOKI

Department of Structural Engineering, Building Research Institute, Tsukuba, Japan

Toshibumi FUKUTA

International Institute of Seismology and Earthquake Engineering,
Building Research Institute, Tsukuba, Japan

Fumitoshi KUMAZAWA

Faculty of Engineering, Shibaura Institute of Technology, Tokyo, Japan

Abstract

Torsional response can destructively effect the seismic capacity of structures. Many damaged buildings due to torsional vibration were observed after sever earthquakes. However, it cannot be said that the mechanism of the damage due to the torsional vibration had been clearly investigated. The main purpose of this paper is to reproduce the torsional response with the pseudo dynamic test technique. One-span, one-bay and two-story steel structures were tested. Three structures that had different eccentric ratios were designed for the pseudo dynamic tests. Furthermore, shaking table tests on three structures were conducted to verify the validity of the pseudo dynamic tests. From the shaking table and the pseudo dynamic tests, it was confirmed that the pseudo dynamic test can adequately reproduce the response of structure with eccentricity; eccentricity was not as effective on the maximum horizontal displacement at center of gravity, but the maximum rotational angle was increased according to its eccentricity.

1 Introduction

There have been many buildings damaged due to torsional response during severe earthquakes. However, it cannot be said that the mechanism of the damage due to the torsional response has been clearly investigated. One of the main purposes of this study is to reproduce the torsional response of structures with eccentricity by the pseudo dynamic (PSD) test, and to investigate the mechanism of the damage due to the torsional vibration. In order to verify the validity of the PSD test, the shaking table tests were also conducted (Kato and Kusunoki, 2001). This paper presents the outlines of earthquake response tests and the outcomes from the experimental study.

2 Outlines of Specimens

The specimens were one-span, one-bay and two-story steel structures as shown in Fig.1. Rigid slabs made of reinforced concrete provided the inertia force for the shaking table tests, and were used as the loading beam for the PSD test. The weight of each slab was 76.9kN for the first floor and 78.0kN for the second floor. The eccentricity was provided only on the first story by adjusting column positions as shown in Fig.1 a). Two of four columns were located closer to the center of the slab than others. The natural period of the specimens need to be nearly the same to neglect the effects of the frequency characteristics of the input motion. However, it is not easy to provide structures with various stiffness eccentricities that have the same natural period. Therefore the method of adjustment of column positions on the first story mentioned above was applied for the test in order to make the natural periods of test structures almost constant.

H-Shaped steel was used for columns (H-125x125x6.5x9 for the first story and H-100x100x6x8 for the second story). The clear height of column between top and bottom base plates was 1,500mm as shown in Fig. 2. Material test results are shown in Table 1. Table 2 shows the strength of column, the story shear and the story shear coefficients. The story shear coefficient for the first story was 1.43 and 1.85 for the second story.

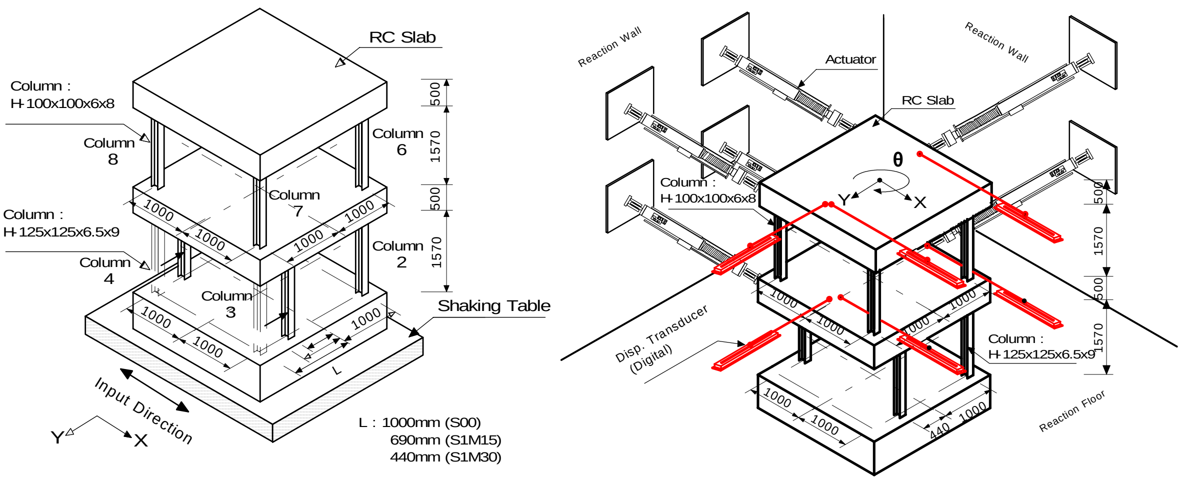

a) Shaking Table Test
b) Pseudo Dynamic Test

Fig.1 Setup of Specimen

Table 1 Material Test Results

	H-125 (First story)	H-100 (Second story)
Yield Strength (N/mm^2)	304.4/301.7	347.8/340.1
Tensile Strength (N/mm^2)	431.9/435.5	475.6/473.6
Strain Fracture (%)	26.4/27.3	25.8/25.5

Left-side value is for flange, right-side value for web

Table 2 Strength of Specimen

	Yielding Moment (kN*m)	Story Shear at Yielding (kN)
First story	41.4/14.3 [2.9]	220.8/76.3 (1.43)
Second story	26.6/9.3 [2.9]	141.9/49.5 (1.85)

Left-side value is for X Direction, right-side value for Y Direction
[ ] the ratio of yielding moment on X Direction to Y Direction
( ) Story Shear Coefficient

Test parameters are the values of eccentric ratio in the direction of X. The X-axis is the direction of the input motion, as shown in Fig.1 a). The eccentric ratio of 0.0, 0.15 and 0.30 were applied in the X direction. Here, the eccentric ratio is defined as a function of distance between center of gravity and rigidity (Eq.1), which is prescribed in the Building Standard Low Enforcement Order of Japan, and represents how easily a structure can vibrate torsionaly (JBC/Japan Building Center, 2001).

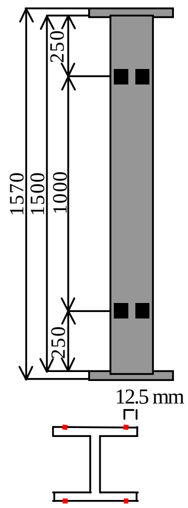

Fig. 2 Column

$$R_e = \frac{e}{r_e} \tag{1}$$

e : Eccentric Distance. The distance between center of gravity and rigidity

r_e : Radius of Spring Force.

$$r_{ex} = \sqrt{K_R / K_x}\ ,\ \ r_{ey} = \sqrt{K_R / K_y}$$

K_R : Torsional Stiffness.

K_x, K_y : Horizontal Stiffness to The Direction of X and Y

In structural design of building with eccentric ration larger than 0.15, design external force should be made to increase up to 1.5 times in accordance with the values of eccentric ratio. An eccentric ratio of zero means that the structure has no eccentricity. The test parameters are shown in Table 3. The number of specimens are six, three were prepared for the PSD tests (P00, P1M15 and P1M30).In addition, three specimens (S00, S1M15 and S1M30) were used for the shaking table tests in order to compare the reproduced behaviors between the PSD test and those of the shaking table tests. In order to achieve the specific eccentricity, columns were shifted by the distance shown in Table 3 from the location for the structure without eccentricity.

The test structure was assumed to be 1/2 scaled model of a real size structure. However, no prototype structure in real size was designed because the main purpose of this research was to investigate the basic effect of the torsional response on structural damages, not to observe the response of a specific structure. Because of this, the horizontal strength of column was assumed simply to be proportional to the area of section. Scale factors for each item are listed in Table 4 (Kumazawa, 1996). Single underlined items are the items that cannot be scaled down, and double underlined items are the items of which scale factor does not have proper relationship with the real size structure.

Table 3 Names of Specimens and Test Parameters

		Shifted Distance from Uniform Arrange (mm)	Names of Specimens	
			Shaking Table Test	Pseudo Dynamic Test
Eccentric Ratio in X direction	0.00	0	S00	P00
	0.15	310	S1M15	P1M15
	0.30	560	S1M30	P1M30

Table 4 Scale Factors

Physical Phenomena			
Length	1/2	Area	1/4
Volume	1/8	<u>Gravity Acceleration</u>	1.0
Specific gravity	1.0	Mass	1/8
Rotational inertia	1/32	Time	1/2
Column			
<u>Young's modulus</u>	1.0	Axial strain	1.0
<u>Curvature</u>	2.0	<u>Twisting strain</u>	2.0
Horizontal strength	1/4	Horizontal stiffness	1/2
Yield deformation	1/2	Rotational stiffness	1/8
Response of Structure			
Natural period	1/2	Horizontal acceleration	2.0
Horizontal velocity	1.0	Horizontal deformation	1/2
Rotational acceleration	1.0	Rotational velocity	1.0
Rotational deformation	1.0		

Strains of steel columns were measured with strain gauges put on the flange at both ends of columns as shown in Fig. 2 (black rectangular marks show strain gauge locations). Four strain gauges were put at one end, eight gauges were used for one column, and totally strains at 64 different points were measured during the PSD and the shaking table tests.

Three displacement transducers were used to measure response bi-directional horizontal displacement and rotational angle of each floor as shown in Fig.1 b). Two transducers were for X-direction and rotation, and one was for Y-direction. Two additional transducers were used to measure slip displacement at bottom of basement during the shaking table tests.

Three accelerometers were used to measure response acceleration during each floor at the shaking table test. Two were for Y-direction and rotation, and one was for X-direction. One accelerometer was placed on the center of the basement to measure actual input motion to a specimen.

3 Input Motions

The North-South component of JMA-Kobe (Kobe Observatory of Japan Meteorological Agency) recorded at the Hyogo-Ken-Nanbu earthquake in 1995 was used for the input motion, of which time axis was scaled down by 1/2 according to the scale factor. The input earthquake wave and the response acceleration magnification with various damping coefficient are shown in Fig.3. Five different normalized peak acceleration waves of 200, 450, 900, 1640 and 2400cm/sec^2 were inputted in order of level. Peak accelerations in a real size are 100, 225, 400, 820 and 1200 cm/sec^2 because of scale factors. The shaking table tests were conducted with these input motions prior to the PSD tests, and recorded acceleration at the basement of each specimen was used for the input motion to the PSD tests.

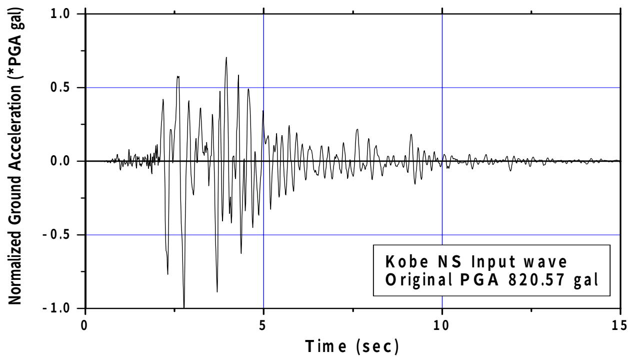

a) Earthquake Acceleration

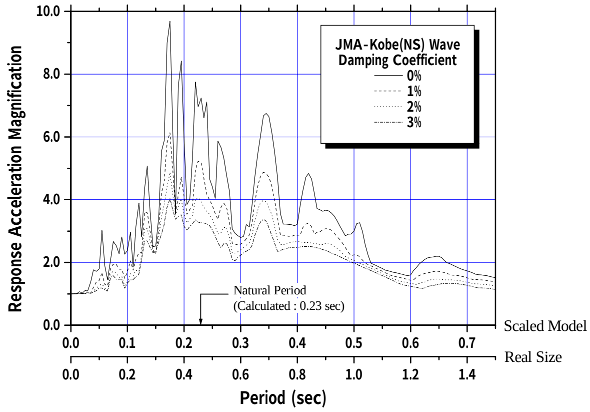

b) Response Acceleration Magnification

Fig. 3 Input Acceleration Wave

4 Test Results and Discussions

4.1 Fundamental Characteristics of Specimens

In order to measure natural periods and damping coefficients of specimens, responses with the white noise input were measured at the shaking table tests. On the other hand, since a stiffness matrix was needed for the PSD tests to assume a damping matrix, unit loading tests, that small amount of force was loaded at each floor and in each direction, were carried out just after setting up each specimen. Then, all responses for each force were measured, and the flexibility matrix was generated. The natural periods were calculated with the flexibility matrix and the mass matrix for each specimen. Measured natural periods were listed in Table 5. The damping coefficients could be assumed as 1% from the shaking table test with the white noise. The damping coefficients of 1% proportional to the initial stiffness were assumed for the PSD tests.

The natural periods in both X and Y direction of the shaking table and the PSD tests are almost the same, however, those of torsional response are a little different. Since the natural periods of the shaking table tests were calculated with transfer function at the white noise input, the accuracy of the natural period of the torsional response is not so high because it is higher modes.

Table 5 Natural Periods (sec)

Specimen	X Direction	Y Direction	Torsion
P00	0.264	0.401	0.201
P1M15	0.264	0.390	0.217
P1M30	0.276	0.393	0.226
S00	0.260	0.410	0.220
S1M15	0.280	0.410	0.240
S1M30	0.280	0.410	0.250

4.2 Comparison of Results of PSD Tests and Shaking Table Tests

Responses of Specimens

The response displacements at center of gravity on roof floor in the X direction and rotational angles of the first story of which the input level was 1640cm/sec^2, are shown in Fig.4. In the figure, solid lines show the results of the PSD tests and broken lines are those of the shaking table tests. It can be said that the response displacements of P1M15 and P1M30 agreed very well with those of the shaking table tests, which include maximum response displacements. And the rotational angles of those specimens also show rather well correspondence. However, the response displacement of P00 was evidently larger than that of S00, the behaviors of both did not coincide. From Fig. 4, the maximum response displacements at center of gravity of employed specimens are almost in agreement, in spite of difference of eccentric ratios. Meanwhile the response rotational angles of specimens with eccentricity grow with increasing of eccentric ratio, as against those of P00 and S00 are very small. It was observed that the eccentricity of specimen was inclined to have an influence on the rotational response.

The relationship between story shear force and inter-story drift in the first story of the PSD for the same input level are compared with those of the shaking table tests in Fig.5. Though the behaviors of P1M15 and P1M30 agreed well with those of the shaking table tests, the result of P00 was different from that of S00, especially the initial stiffness of the shaking table test was a little higher than that of the PSD test. Because of the difference of stiffness, the response of the PSD test did not agree with that of the shaking table test. The reason why the stiffness of S00 and P00 were different needs further investigation. From these results, it will be said that the PSD test can adequately reproduce the dynamic response of specimen, if the stiffness of specimen is in agreement.

The orbits at center of gravity in the first story of the PSD tests are illustrated in Fig.6. The results of P1M15 and P1M30 show drifts in Y direction, it is understood that the effects of eccentricity promote the deflection of perpendicular direction where input motions were not given.

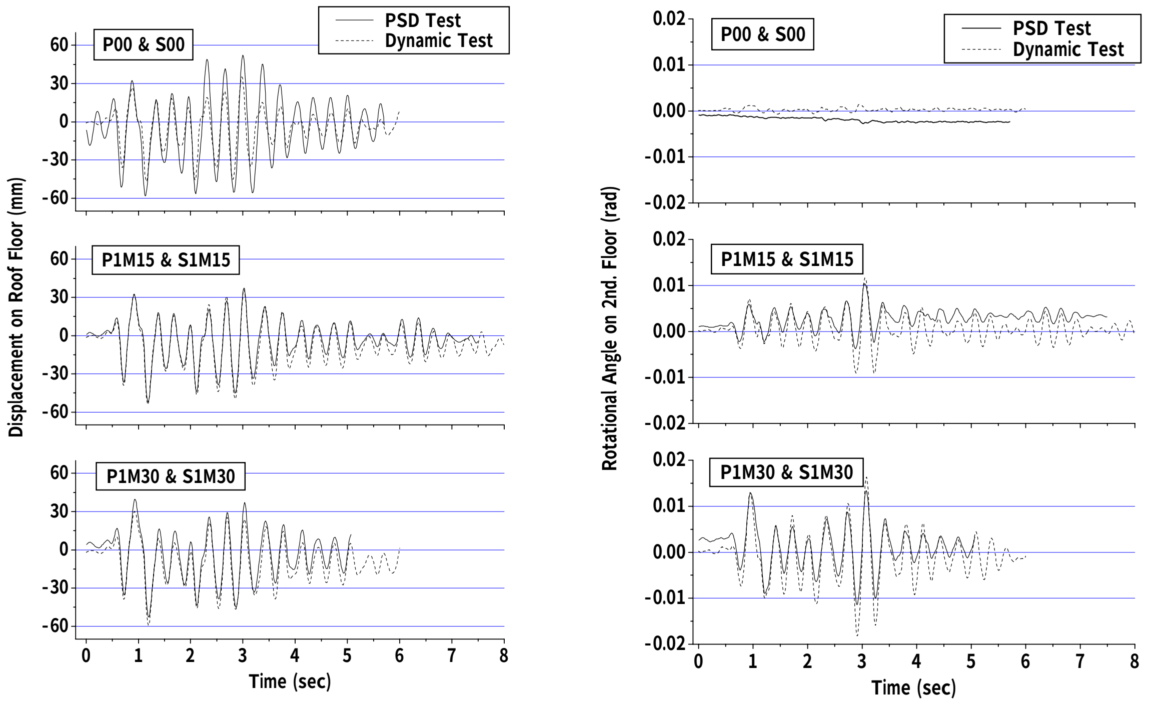

a) Displacement Responses (Roof Floor)   b) Rotational Angle Responses (First Story)

Fig.4 Dynamic Responses of Specimens for 1640cm/sec^2 Input

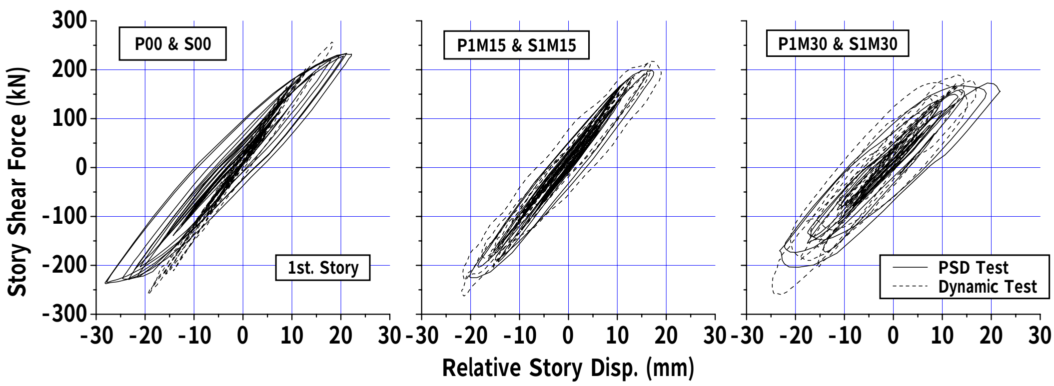

Fig.5 Story Shear Force and Story Drift Relationship (1640cm/sec^2 Input)

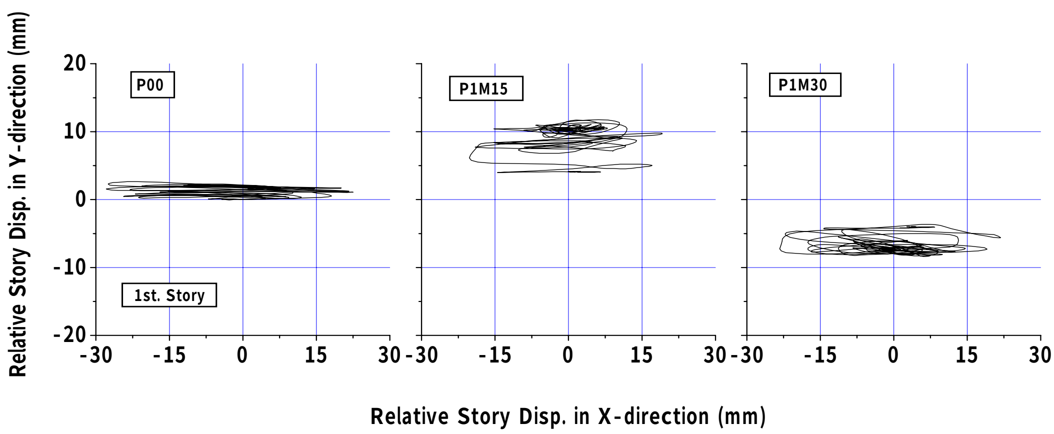

Fig.6 Orbits of Center of Gravity of PSD Specimens (1640cm/sec^2 Input)

Maximum Responses

Figure 7 a) shows maximum response displacements at center of gravity of the first story in the X direction for each input level. As mentioned before, P00 and S00 are quite different especially for relatively large input levels. P1M15 and P1M30 agree well with S1M15 and S1M30 regardless of input level. It can be seen that there is the tendency to slightly increase the maximum response displacement at center of gravity with increasing of the eccentric ratio. Figure 7 b) shows maximum torsional response angle of the first story for each input level. Maximum torsional response angle of P1M30 at input level of 1640 cm/sec^2 was 28% smaller than that of S1M30. Maximum torsional response angle is the relative angle to the basement and residual torsional angle could be accumulated. Maximum angle of P1M30 at input level of 2400 cm/sec^2 was also 27% smaller than that of S1M30. Maximum torsional response angle increased according to the eccentric ratio. For example, the ratios of maximum angle to P1M15 at input level of 1640 cm/sec^2 were 1.15 (P1M30).

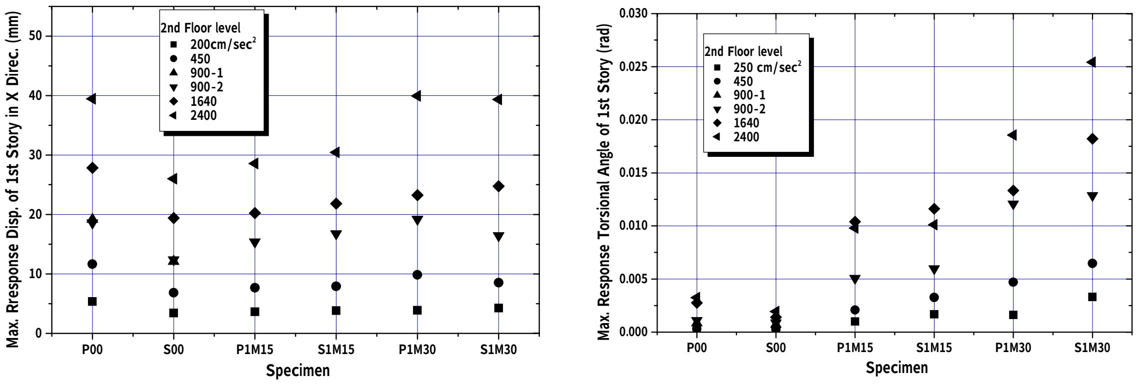

a) Disp. of 1st Story   b) Torsional Angle of 1st Story

Fig.7 Maximum Responses (1640cm/sec^2 Input)

Responses of Individual Columns

Since the tendency of promoting torsional vibration by eccentricity of specimen was observed as mentioned above, the responses of individual columns will be indicated below. Figure 8 shows the response displacement of eccentric and non-eccentric bays with those at center of gravity of P1M30 at input level of 1640 cm/sec^2. The displacement of eccentric bay are larger than that of center of gravity, on the other hand the one of non-eccentric bay show opposite trend. The ratio of maximum response of eccentric bay to that at center of gravity was about 1.4; the one of non-eccentric bay was 0.6. Those outcomes make clear that the eccentric bay is forced to be deformed largely, in spite of the displacements at center of gravity of each specimens were not so different as shown in Fig.4 a).

The restoring characteristics of individual columns in the first story of specimens with eccentricity are illustrated in Fig.9. Here, Column 2 is in non-eccentric bay and Column 3 is in eccentric bay as shown in Fig.1 a). The abscissa of the graph is deformation of column and the ordinate shows shear force obtained from measured strain of column. The restoring characteristics of the PSD and the shaking table tests adequately agreed with each other, it is conformed that the both results correspond in the level of structural elements. The Columns 3 have a spindle-shaped hysteresis loops, it means that the columns had been yield and reached in plastic range. On the other hand, the Columns 2 show elastic restoring characteristics, those had remained in elastic range. The phenomena which areas of hysteresis loops of P1M30 and S1M30 are larger than those of P1M15 and S1M15, show the possibility that structural element in eccentric bay will be suffered heavy damage in large earthquake excitations.

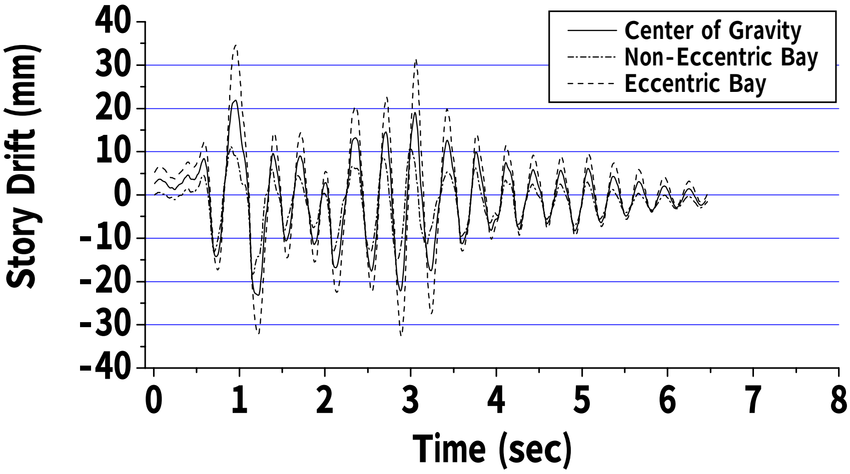

Fig.8 Comparison of Displacement Response in Each Streets of Specimen
(1st story of P1M30, 1640cm/sec^2 Input)

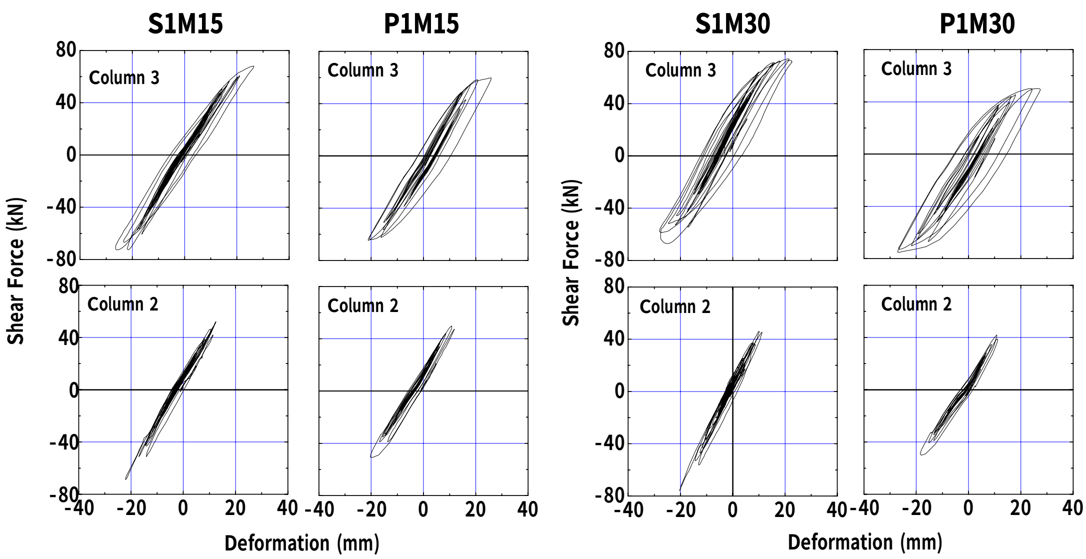

a) Eccentric Ratio 0.15 b) Eccentric Ratio 0.30

Fig.9 Restoring Characteristics of Individual Columns (1640cm/sec^2 Input)

5 Concluding Remarks

In order to investigate the mechanism of damage due to torsional response, a series of PSD tests on the specimens with eccentricity were conducted. Furthermore, in order to verify the validity of the PSD test, the shaking table tests on the same specimens were conducted. The outcomes from this experimental study are summarized as follows;

1. The pseudo dynamic test technique with torsional response was newly developed. If the stiffness of specimen can be given properly, the pseudo dynamic test can reproduce the dynamic response of eccentric specimen with sufficient accuracy.
2. The displacement response at center of gravity of specimens was not so influenced by the values of eccentric ratio.
3. Torsional response angle increases evidently according to the eccentric ratio.
4. There is the possibility that structural elements in eccentric bay will be suffered heavy damage in large earthquake excitations.

Acknowledgement

The authors express their appreciation to Messrs Yuuichi Hirosaki (graduate student in Shibaura Institute of Technology), Kenji Ashida (Nohara Co. Ltd.), Isao Fujimoto, Yasuhiro Kiuchi and Yutaka Komatsu (The Center for Better Living) for their contribution to conduct this experimental research.

References

JBC/Japan Building Center (2001). Guideline for Technical Standard Related to Building Structure, (in Japanese)

Kato H. and Kusunoki K., et al. (2001). Study on earthquake response characteristics of frame structures with eccentricity (Part 1– 3). Summaries of Technical Papers of AIJ Annual Meeting, (in Japanese)

Kumazawa F. (1996). Study on Response Characteristics of Small Scaled Reinforced Concrete Structures. Ph. D Thesis, University of Tokyo (in Japanese)

Appendix 3

Section 3 *Seismic Performance of Retrofitted RC Slab Connected with Strengthening Frame*

presented by M.Inukai

SEISMIC PERFORMANCE OF RETROFITTED RC SLAB CONNECTED WITH STRENGTHENING FRAME

Mizuo INUKAI[1)], Takashi KAMINOSONO[2)]
Motoyuki TOHARA[3)], Tadashi KIMURA[3)], Hironobu IMAMURA[3)]

Key Words: 1995 Hyogoken Nanbu Earthquake, new retrofit method, existing building, reinforced concrete slab, non-shrinkage mortar, apartment house

1. Purpose

Since the 1995 Hyogoken Nanbu Earthquake, the retrofits for the old buildings are done but there are few research activities about the retrofit method for middle high rise apartment houses. Generally, the retrofit is executed for office buildings, school buildings and so on which the users can move out during the retrofit construction works.

It means that it is needed to develop a new retrofit method which the resident people can use their buildings continuously during this retrofit works. In apartment houses, there are always few residents who cannot accept the temporary remove during retrofit construction works.

In 1998, the research activities was done about the retrofit of the high rise apartment house with Steel Reinforced Concreter Structure which was designed by the old seismic code before 1981. These activities proposed that the retrofit method should use the strengthening frame with Reinforced Concrete Structure outside of the existing structure [1]. And the researches were not made about the construction method for the continuous use or the connecting method between the existing structure and the strengthening frame.

Therefore, this research paper describes the experimental study about the seismic performance of the reinforced concrete slabs retrofitted by the non-shrinkage mortar. This slab is connected between the existing reinforced concrete frame structure and the strengthening frame.

2. Model building

The model building is 11 storeys apartment house [1]. The lower 7 storeys is the Steel Reinforced Concrete Structure, and the upper than it is the Reinforced Concrete Structure. The number of spans in the span direction (X-direction) is 1 and one in the ridge direction (Y-direction) is 14 (Fig.1, Table 1). This model building was designed by the old seismic code before 1981. According to the seismicity assessment [1], the maximum *Is* index [2] on each floor was from 03. to 0.8, and especially the maximum *Is* index on 5-10 floor was less than 0.6. That means the building needs some retrofit.

Table 1 Model Building

Size	11 storeys with pent house of 3 storeys
Structure type	-Steel Reinforced Concrete (Lower than 1 meter high on 7th floor) -Reinforced Concrete (Upper than it)
Material	-Concrete (Compressive strength: 20(N/mm^2)) (Lower than floor beam on 3rd floor) -Light Concrete (Compressive strength 20(N/mm^2)) (Upper than column on 3rd floor) -Steel bars: SR235,SD295,SD345 -Steel: SS400

1) Senior Research Engineer, Building Department, National Institute for Land and Infrastructure Management, Ministry of Land, Infrastructure and Transport. Tsukuba-shi, Ibaraki-ken, 305-0802, Japan)
2)Associate Director, ditto.
3)Urban Development Corporation

The retrofit plan in 1998 proposed the required strength to get the enough *Is* index which is more than 0.6. And the retrofit method should use the strengthening frame on the outside of the corridor and the verandah of the building by connecting with the existing structure using prestress steel bars. This strengthening frame should have 7 spans among the 14 spans and the existing slab in 3 spans should be retrofitted by the RC slab. The problem of this method is that almost reinforce concrete slabs should be retrofitted for their shear force transfer performance between strengthening frames beside the outside frames. The strengthening frame is designed to support the strength shortage of the existing frames. This shortage of strength should be transferred from the existing frames to strengthening frames finally to foundations or ground.

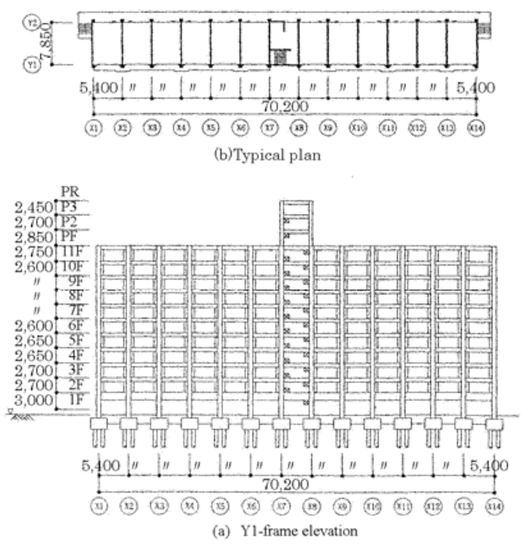

Fig.1 Model building

The existing slabs of this building are cantilever with beams at their end.

In this research paper, we used the Anchors to set up the retrofit slabs underneath the existing slabs. That is because the Anchors don't need the construction workers to enter into some private spaces without any anchorage wholes which go through the beams. This retrofit construction works need only the public spaces, for example, corridor, or verandah. So, it is useful to build strengthening frames beside the outside frames.

In order to decrease the period of the construction works, we use half-precast slabs for the retrofit slabs. And we considered that the columns of the strengthening frame should be precast RC members and the beams should be cast-in-place RC members. That is because the beams of the strengthening frame need some large tolerance about the position of the anchorage wholes to connect with the existing members which do not have enough accuracy about the position of the steel bars. We used half-precast slabs because we can shorten the formworks in the public spaces which sometimes interrupt the walks or the emergency escapes for residents (Fig. 2).

Therefore, it is possible to use continuously the apartment house during the retrofit construction works. And we need the experiments about this retrofit method and its seismic property.

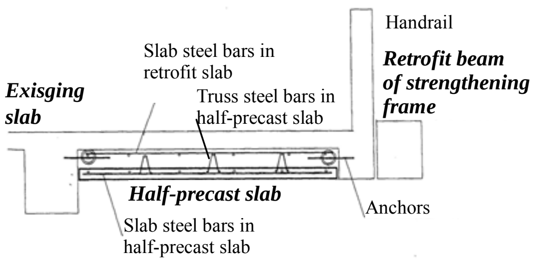

Section of corridor in public space

Fig.2 Overview of Retrofit slab

3. Specimens

The specimens are shown in Table 2 and Fig.3. The specimens are made of existing slab in depth of 110mm and retrofit slab in depth of 100mm which is cast by non-shrinkage mortar which is between existing slab and half-precast slab in depth of

Table2 Specimens (unit:mm)

Specimen	Size	Existing Slab	Retrofit Slab		Half-Precast Slab	
Flret-0m (no-retrofitted)	Full-scale Slab	Length:2,000 Width :1,300 Depth : 110 Slab steel bar 1 (Span-direction) D13@200 double Slab steel bar 2 (Ridge-direction) D10@200 double	—		—	
Flret-1m (retrofitted)			Length 1,000	Width:1,300 Depth: 100 Slab Steel bar (Both directions) D10@200 Anchors D16@200 Insert depth: 130 Whole diameter:20 Anchorage length: 480	Length 1,000	Width:1,260 Depth: 60 Slab steel bar (Both directions) D10@200 double Truss steel bar ϕ13-ϕ6-ϕ6-H65
Flret-2m (retrofitted)			Length 2,000		Length 2,000	

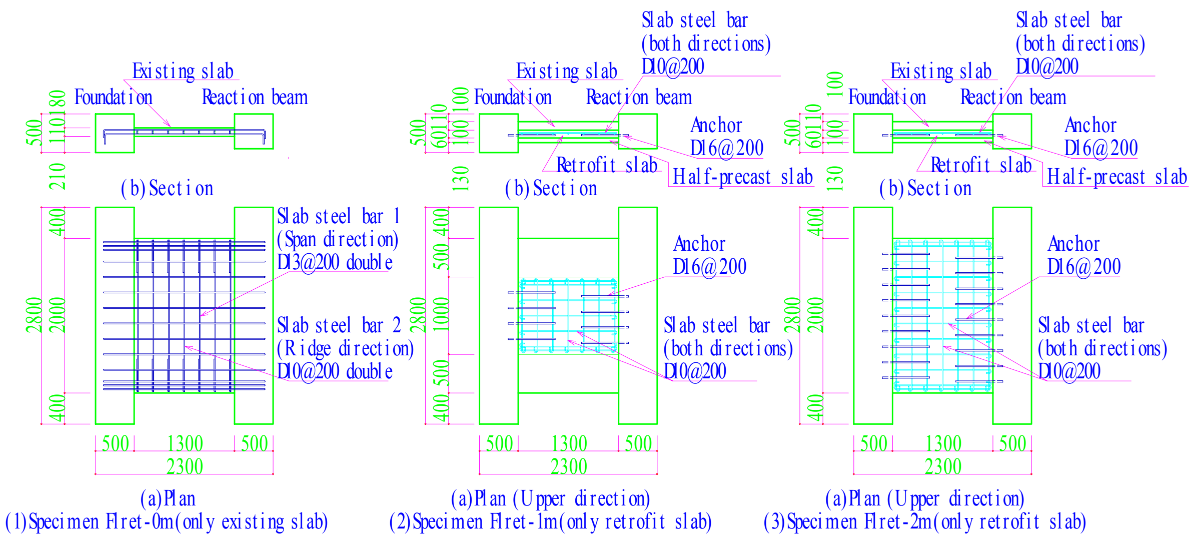

Fig.3 Steel bar arrangement

60mm. The half-precast slab has a function to be forms for fresh concrete. The total depth of these specimens is 270 mm which is the same as the depth of the beams at the end of the existing slabs. The scale is full-scale because we have to use the drill machine for anchors underneath the existing slabs. The minimum size between the bottom end of the existing slab and the center of anchors is 65mm.

In order to assess the effect of the retrofit and the length of retrofit slabs, the parameter of the specimens is the length of retrofit slab which is 0m, 1m and 2m.

The existing slab has steel bars D10@200double in the ridge direction (Y-direction) and D13@200double in the span direction (X-direction). In the model building, slab steel bar is D10@200double in both directions. The existing slab steel bars are increased because we considered that the specimens should be collapsed in shear mode and should have some effect of the next existing slab in the ridge direction.

As for the making of the specimen with retrofit slab, at first, we made a existing slab, a reaction beam and a foundation. 1 week later, we cast a retrofit slab after the cast of anchors D16@200 on the reaction beam and the foundation underneath the existing slab, retrofit slab steel bars D10@200 in both directions, half-precast slab with a truss of round steel bars of ϕ13-ϕ6-ϕ6 and which height is 65mm, and non-shrinkage mortar between the existing slab and the half-precast slab.

When anchors are cast, anchorage wholes in depth of 130mm and in diameter of

20mm are prepared before the casting of concrete in the foundation and the reaction beam. The anchorage material for D16@200 is the capsule type adhesives made of glass tube. One tube is inserted into the anchorage whole, and an anchor steel bar D16 with a section end 45 degrees cut is inserted into an anchorage whole with rotations by a drill machine. The anchorage length from the surface of the foundation or the beam to the other end of anchors D16 is 480mm. We used a low noise drill machine for the residents of the apartment house.

The diameter of anchor 16mm is the maximum size which is possible to cast under the corridor slab in width of 1,300mm because the required anchorage length is 30 x diameter (=480mm), the required insert length is 130mm, and the length of a drill machine is about 400mm. Total length is just less than 1,300mm. The space between anchors 200mm is the required minimum size.

Non-shrinkage mortar should be filled in all volume of the retrofit slab. That is why we made a filling test before casting which is executed by the Prestressed Concrete Construction Company (Photo 1). The wooden forms for the 4 headers and the bottom, and the acrylic plate for the top were prepared for the filling test. The vinyl tubes are inserted from the one end of this filling test specimen to the opposite end, and non-shrinkage mortar is cast from the opposite end. The vinyl tubes inserted in the opposite end is the air exit for filling. After the mortar reached the one end, the specimen is left for cure in one day. The next day, we confirmed that the mortar is filled enough just underneath the acrylic plate.

The material properties are shown in Table 3 and Table 4.

4. Experiment

The loading test is made with the slab horizontal (Photo 2). By this loading

Table3 Material properties of Concrete and Mortar

Part to be used	σc	Ec	εc
Concrete of slab in not-retrofitted specimen	31.3	3.33	1,775
Concrete of existing slab in retrofitted specimens	33.5	3.07	1,943
Mortar of retrofit slab	60.1	2.17	5,411
Concrete of half-precast slab	40.6	2.80	2,248

Notes) σc: Compressive strength(N/mm^2)
Ec: Young modulus x10^4(N/mm^2)
εc: Strain at compressive strength x10^{-6}(mm/mm)

Table 4 Material properties of Steel bars and Anchors

Part to be used	Size (Nominal name)	σt	Es	εs	σo
Existing slab	D13(SD295A)	349	1.79	1,951	493
	D10(SD295A)	338	1.79	1,889	468
Retrofit slab	D10(SD295A)	361	1.75	2,060	505
Anchor	D16(SD295A)	343	1.81	1,892	484

Notes) σt: Yield strength(N/mm^2)
Es: Young modulus x10^5(N/mm^2)
εs: Strain at yielding x10^{-6}(mm/mm)
σo: Tensile strength(N/mm^2)

Photo 1 Filling test of non-shrinkage mortar

Reaction frame
Specimen
Oil jack

Photo 2 Loading test

test, we can know that the retrofit slab or the half-precast slab would fall down or not.

The foundation is fixed to the reaction floor and the reaction frame, and the reaction beam is supported by the roller supports. 2 oil jacks on the 2 ends of the reaction beam load the horizontal force in plane of a slab like a cantilever beam loading.

During the loading, when the slab steel bar in the span direction is yielding, another prestress steel bars are installed near the ends of the slab to escape from the flexural failure mode.

5. Results

The horizontal force – displacement relationship is shown Fig.4. The maximum horizontal force is 913kN of specimen Flret-0m, 1,037kN of Flret-1m, and 1,341kN of Flret-2m. The failure mode is shear failure for all of 3 specimens.

As for the retrofitted specimens, Flret-1m and Flret-2m, the retrofit slab is separated from the existing slab at the displacement more than 20mm and do not fall down to the ground.

As for the specimen Flret-1m, in the half-precast slab, many flexural cracks and shear cracks take place. At the foundation, the same crack as the cone failure of anchors take place.

As for the specimen Flret-2m, in the half-precast slab, any cracks do not take place.

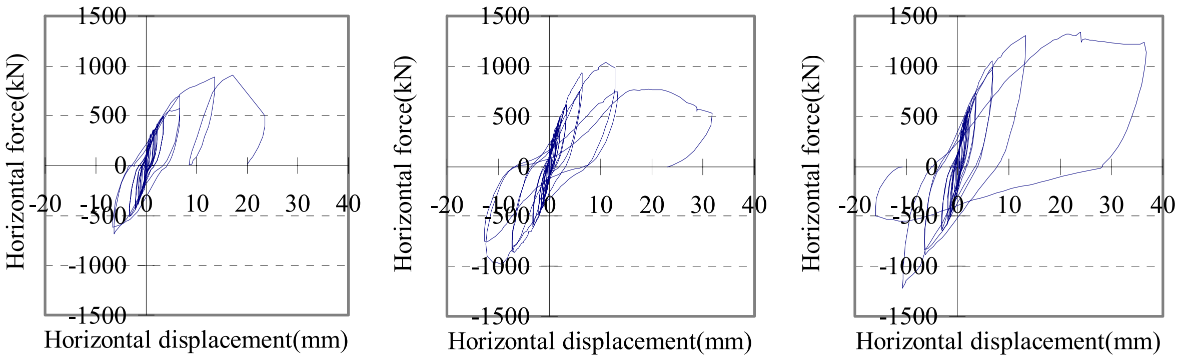

(1)Specimen Flret-0m (2)Specimen Flret-1m (3)Specimen Flret-2m

Fig.4 Horizontal force – displacement Relationship

6. Conclusions

(1) These specimens make clear that the shear force transfer property between the strengthening frame and the outside frame increases by the set up of the retrofit slab and the length of the retrofit slab.

(2) .It is possible to cast the retrofit slab underneath the existing slab with the enough filling property.

(3) By the anchors and the half-precast slabs, it is possible to use the building continuously during retrofit works.

[Reference]

[1] "Research Report about the Development of Retrofit Techniques for Apartment Houses", Housing and Urban Development Corporation, etc., March 1999, pp.184-226. (in Japanese)

[2] "Damage Classification Method for Damaged Buildings Post-Earthquake and Seismic Retrofit Guideline", The Japan Building Disaster Prevention Association, Sept.2001. (in Japanese)

Appendix 4

Section 4 *Posterior Time-Step Adjustment Technique in Substructuring Pseudo-Dynamic Test*

presented by K. Kusunoki

Fifth International Congress on Advances in Civil Engineering, 25-27 September 2002
Istanbul Technical University, Istanbul, Turkey

POSTERIOR TIME-STEP ADJUSTMENT TECHNIQUE IN SUBSTRUCTURING PSEUDO-DYNAMIC TEST
- Numerical simulation and loading test-

K. KUSUNOKI
Building Research Institute, Department of Structural Engineering, Tsukuba, Japan

Waon-Ho Yi
Kwang Woon University, Department of Architectural Engineering, Seoul, Korea

Abstract

The pseudo-dynamic test is a hybrid testing method consisting of a numerical simulation of the earthquake response by using a numerical model and a loading test of a specimen. The pseudo-dynamic testing technique has been applied to various seismic experiments since it has advantages over the shaking table test, i.e. enables us to study dynamic behaviors of relatively large-scale structures. However, experimental errors are inevitable in the pseudo-dynamic test. Some of these errors cannot be eliminated due to limitations in control system. It is often reported that dynamic responses of testing structures are much affected by cumulative control errors. To minimize the control errors in the pseudo-dynamic test, two numerical integration techniques, PTA (Posterior Timestep Adjustment technique) and MPTA (Modified PTA) are proposed herein. A posterior adjustment of the time increment from a fixed value of Δt to an adjusted value was performed to minimize the effect of the control errors in PTA and MPTA techniques. In this paper, the testing procedures and the proposed numerical technique are reviewed. First, a numerical simulation of a linear and non-linear response analyses with Multi-Degree-of-Freedom (MDF) model by considering an undershooting control error at the first story (the first story was supposed as a testing story) was carried out. Then a pseudo-dynamic loading tests with a second-degree-of-freedom system of which the first story was experimentally loaded were conducted. In the above two series, both the PTA and the MPTA were performed, and their validity to minimize the control error is discussed

Introduction

The substructuring pseudo-dynamic test (referred to as SPT test subsequently) is a hybrid method. The restoring force vectors calculated in a computer with numerical hysteresis models and measured from a loading test are combined into a global restoring force vector for the whole structure at each numerical integration step. It has advantages over the shaking table test by studying the dynamic response of relatively large-scale structures.

Computer-controlled actuators are usually applied to the loading system of SPT tests. It is well accepted that random error appears at measuring and controlling instruments. Furthermore, control error can also occur in an actuator control system. These errors are significantly affecting the accuracy of SPT test [Kabayama, 1995]. New integration techniques in which time-step is adjusted to reduce the effects of the control error, PTA and MPTA are proposed herein. The purpose of this paper is to estimate the stability and the accuracy of these techniques for an SPT test.

Control error

Actuators are usually controlled with analogue voltage. On the other hand, computers are digitally controlled. Signals of the loading system therefore must be controlled through the Analogue-Digital and Digital-Analogue transfer (referred to as A/D and D/A transfer subsequently). A minimum controllable displacement $\delta_{\min}$ depends on the precision of the A/D and D/A transfer, and it can be given as follows.

$$\delta_{\min} = \frac{2\ell}{2^n} \tag{1}$$

In this Equation, $\pm\ell$ represents an actuator stroke length and 2^n represents the precision of the A/D and D/A transfer board in a computer. It is impossible to control an actuator closer to a target displacement if the distance from a target displacement is less than $\delta_{\min}$ (Fig. 1(a)). Usually the undershooting error is applied to define the target displacement in order to avoid the damage to a specimen caused by the overshooting displacement. If the undershooting error is applied, the measured displacement does not reach the exact target displacement at each step. Thus, the hysteresis characteristic used in a numerical integration becomes different from that of a real specimen. Especially when the response displacement is relatively small in linear domain. For the latter, the hysteresis curve shows an anti-clockwise loop (Fig. 1 (b)). Although the value of the control error is very small, the calculated response is much amplified compared with the real response leading to an additional energy input caused by the anti-clockwise loop [Kabayama, 1995].

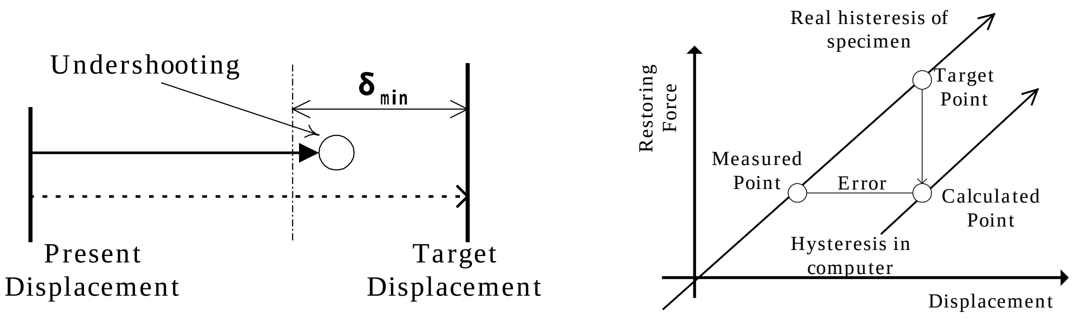

(a) Undershooting control error

(b) The effect of undershooting control error

Fig. 1: Undershooting control error and its effects

Posterior time-step adjustment technique (PTA)

It can be said that an appropriate response cannot be calculated with the SPT test using the Operator-Splitting (OS) integration technique [Nakashima et. al., 1990], which does not consider the effect of the control error. In this section, procedures of the PTA technique based on the OS technique, which reduces the effect of control error, are introduced [Yi and Peek, 1993]. The value of the control error displacement measured in an SPT test is calculated from the difference between the predictor displacement $\{y^*_{n+1}\}$ (Eq. (2)) and the measured displacement $\{\tilde{y}^*_{n+1}\}$ of the experimental portion in the SPT test. The new predictor displacement vector $\{\tilde{y}^{**}_{n+1}\}$ with variable time-step Δt_n is then defined by Eq. (3);

$$\{y^*_{n+1}\} = \{y_n\} + \{\dot{y}_n\}\Delta t + \frac{1}{4}\{\ddot{y}_n\}\Delta t^2 \tag{2}$$

$$\{\tilde{y}^{**}_{n+1}\} = \{y_n\} + \{\dot{y}_n\}\Delta t_n + \frac{1}{4}\{\ddot{y}_n\}\Delta t_n{}^2 \tag{3}$$

And the value of the variable time-step Δt_n, which minimizes the norm $\|\{\tilde{y}^*_{n+1}\} - \{\tilde{y}^{**}_{n+1}\}\|$, can be found through the Newton-Raphson convergent technique. The effect of the control error on the response displacement at n-th step obtained from Eq. (4) can be reduced using Δt_n instead of Δt and $\{\tilde{y}^{**}_{n+1}\}$ instead of $\{y^*_{n+1}\}$. In other words, Δt_n is the appropriate time-step, which minimizes the difference between the predictor and the measured displacement of a specimen.

$$[M]\{\ddot{y}_{n+1}\} + [C]\{\dot{y}_{n+1}\} + \{Q^*_{n+1}\} + [K^I](\{y_{n+1}\} - \{y^*_{n+1}\}) = -[M]\{\ddot{y}^0_{n+1}\} \tag{4}$$

In order to reduce the control error of both experimental and numerical portion, the whole displacement data is used to calculate the norm (Fig. 2 (a)). The norm of the whole displacement vector is generally formulated as Eq. (5). If the weight matrix [G] can be determined properly, an appropriate Δt_n can be obtained. However, it can be accepted that it is difficult to define [G] properly. A time range parameter θ needs to be determined in order to avoid a negative or relatively large Δt_n value as shown in Eq. (6).

$$\|\{\tilde{y}^*_{n+1}\} - \{\tilde{y}^{**}_{n+1}\}\| = \sqrt{(\{\tilde{y}^*_{n+1}\} - \{\tilde{y}^{**}_{n+1}\})^t [G] (\{\tilde{y}^*_{n+1}\} - \{\tilde{y}^{**}_{n+1}\})} \tag{5}$$

$$(\Delta t_{n\min}, \Delta t_{n\max}) = [(1-\theta)\Delta t, (1+\theta)\Delta t] \tag{6}$$

Modified posterior time-step adjustment technique (MPTA)

As mentioned in the previous section, it is difficult to determine the appropriate weight matrix [G] in the PTA technique. As a result, an appropriate Δt_n can not be found by the PTA technique. To overcome this disadvantage of this technique, a new method, MPTA is considered. In the latter, the whole structure is divided into a numerical and experimental portions. The value of Δt_n is calculated from only the displacement data of the experiment portion, which contains the control error. In this section, the procedures of the MPTA technique are introduced. In these procedures, force and displacement vectors of the whole structure $\{\ \}$ need to be divided into an experimental portion $\{\ \}_E$ and a numerical portion $\{\ \}_A$ through re-assembling nodal numbers appropriately so that $\{\ \}^t$ can form $\left\{\{\ \}_E^t, \{\ \}_A^t\right\}$.

Firstly, the predictor displacement value of the testing portion $\left\{ y_{n+1}^* \right\}_E$ is calculated with a fixed time-step Δt. Then $\left\{ y_{n+1}^* \right\}_E$ is imposed to the actuator as a target displacement. The restoring force vector $\left\{ Q_{n+1}^* \right\}_E$ and the displacement vector $\left\{ \tilde{y}_{n+1}^* \right\}_E$ of the experimental portion are measured when the distance between the target displacement and the measured displacement of a specimen is less than $\delta_{\min}$ (Fig. 2 (c)). The variable time-step Δt_n, which minimizes the norm $\left\| \left\{ \tilde{y}_{n+1}^* \right\}_E - \left\{ \tilde{y}_{n+1}^{**} \right\}_E \right\|$, can be found with the Newton-Raphson convergent technique. The equation of this norm is defined by Eqs. (7) and (8), where [I] represents the unit matrix.

$$\left\{ \tilde{y}_{n+1}^{**} \right\}_E = \left\{ y_n \right\}_E + \left\{ \dot{y}_n \right\}_E \Delta t_n + \frac{1}{4} \left\{ \ddot{y}_n \right\}_E \Delta t_n^{\ 2} \tag{7}$$

$$\left\| \left\{ \tilde{y}_{n+1}^* \right\}_E - \left\{ \tilde{y}_{n+1}^{**} \right\}_E \right\| = \sqrt{\left(\left\{ \tilde{y}_{n+1}^* \right\}_E - \left\{ \tilde{y}_{n+1}^{**} \right\}_E \right)^t [I] \left(\left\{ \tilde{y}_{n+1}^* \right\}_E - \left\{ \tilde{y}_{n+1}^{**} \right\}_E \right)} \tag{8}$$

The predictor displacement vector of the numerical portion $\left\{ y_{n+1}^* \right\}_A$ can be calculated with Δt_n as Eq. (9) (Fig. 2 (c)). The restoring force vector of the numerical portion $\left\{ Q_{n+1}^* \right\}_A$ at $\left\{ y_{n+1}^* \right\}_A$ can be calculated with the numerical model.

$$\left\{ y_{n+1}^* \right\}_A = \left\{ y_n \right\}_A + \left\{ \dot{y}_n \right\}_A \Delta t_n + \frac{1}{4} \left\{ \ddot{y}_n \right\}_A \Delta t_n^{\ 2} \tag{9}$$

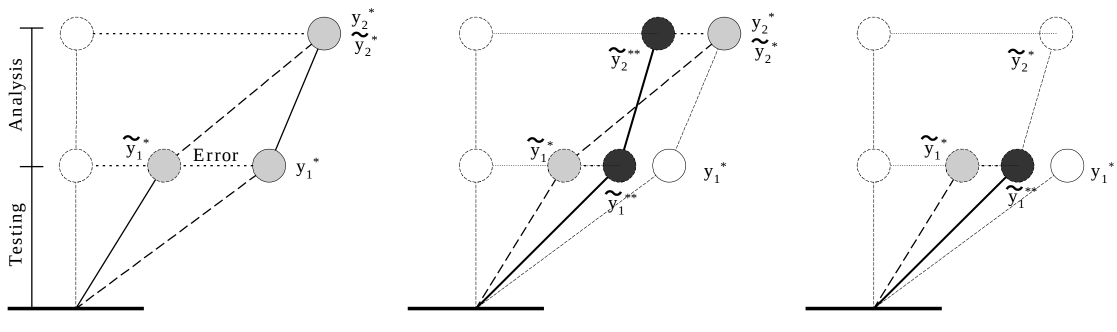

(a) SPT test (b) PTA Technique (C) MPTA Technique

Fig. 2: SPT test with the PTA and the MPTA techniques for a two-degree-of-freedom system

The restoring force vector of the whole structure $\left\{ Q_{n+1}^* \right\}$ can be calculated by combining $\left\{ Q_{n+1}^* \right\}_E$ and $\left\{ Q_{n+1}^* \right\}_A$. Finally the response displacement vector at (n+1)-th step $\left\{ y_{n+1} \right\}$ can be obtained from Eq. (4) and Δt_n. The range of Δt_n is defined by Eq. (6) in order to avoid a negative or relatively large Δt_n value as mentioned earlier.

If the increment of the predictor displacement of the experimental portion at n-th step $\left\{ \Delta y_n^* \right\}_E$ is less than $\delta_{\min}$, the actuator maintains the present position (Fig. 3 (a)). If the increment of the measured displacement is zero, Δt_n always becomes negative or zero. Then Δt is used in Eq. (4) instead of Δt_n, and the restoring force of the experimental portion is calculated numerically with a linear extrapolation technique (Fig. 3 (b)).

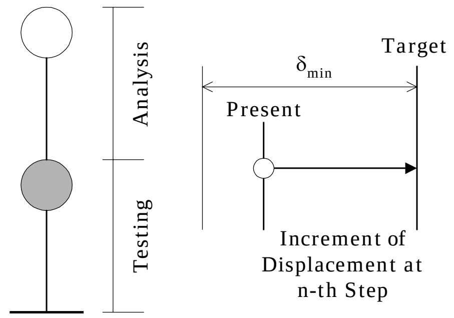

(a) Increment displacement becomes zero

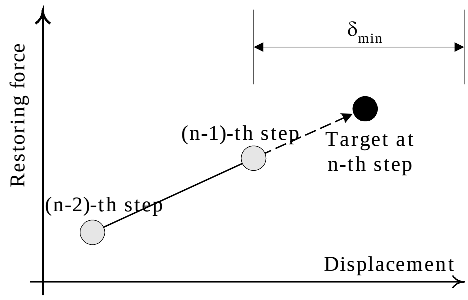

(b) Linear extrapolation method

Fig. 3: Linear extrapolation method

Numerical examination with PTA and MPTA

Linear and non-linear dynamic response analyses were carried out with a six-degree-of-freedom shear mode vibration system (referred to as MDF subsequently) by considering the effect of the control error numerically to estimate the basic characteristics of the PTA and the MPTA. The first story was assumed as an experimental portion. The unit matrix [I] was used as the weight matrix of the PTA in this paper.

The weight of each floor was 172.80 tonf and the height of each story was 4.0m. The damping coefficient was assumed 0.0%, since the main purpose of this paper is to investigate the effect of the control error. Takeda Tri-Linear Model was used as a hysteresis model of each story [Takeda et. al., 1970]. The restoring forces and the displacements at each stiffness degradation point were calculated and each parameter of the MDF is listed in Table. 1.

Table. 1: Parameters list for SDF and MDF (tonf, cm) [AIJ, 1992]

System	Story	Fc	Dc	Fy	Dy	Fu	Du
MDF	1	108.00	0.36	324.00	2.67	327.24	13.33
	2	98.74	0.36	296.23	2.67	325.85	13.33
	3	88.87	0.36	266.61	2.67	293.27	13.33
	4	80.23	0.36	240.69	2.67	264.75	13.33
	5	63.36	0.36	190.08	2.67	209.09	13.33
	6	37.03	0.36	111.09	2.67	122.19	13.33

1. Fy ; Ultimate lateral resistance in each story (base shear coefficient is assumed 0.3).
2. Dy = Story height/150.
3. Fc = Fy / 3.0.
4. Dc ; Calculated with Fc, elastic stiffness and stiffness degrading ratio (0.4).
5. Fu, Du ; Calculated so that post yielding stiffness $Fu - Fy/Du - Dy$ is Fc/Dc times 1/1000.

The input acceleration records for the pseudo-dynamic test conducted by Kabayama et al. was used as the input earthquake data by scaling its peak acceleration to 500 gal (Fig.

4).
The Max/Min stroke length of the actuator was assumed $\pm 15cm$ and the precision of the A/D and D/A transfer board were adjusted 11 bits. As a result, δ_{min} was 0.0146 cm. The undershooting control error was applied and the value of the undershooting control error was calculated to simulate the SPT test with δ_{min} in each step. The parameter θ and the weight matrix were assumed 0.5 and unit matrix [I], respectively. It should be noted that the PTA and the MPTA techniques proposed in this paper can be applied to both the undershooting and the overshooting control errors.

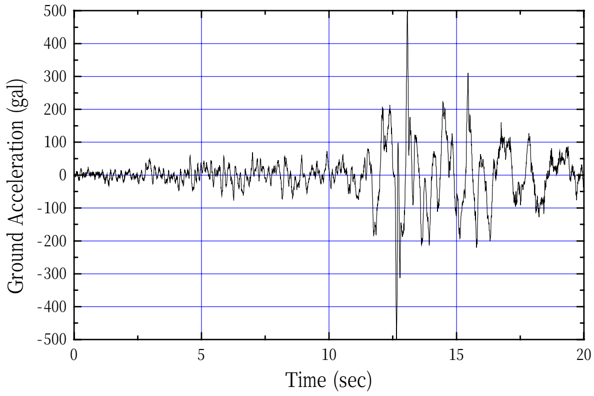

Fig. 4: The input earthquake data

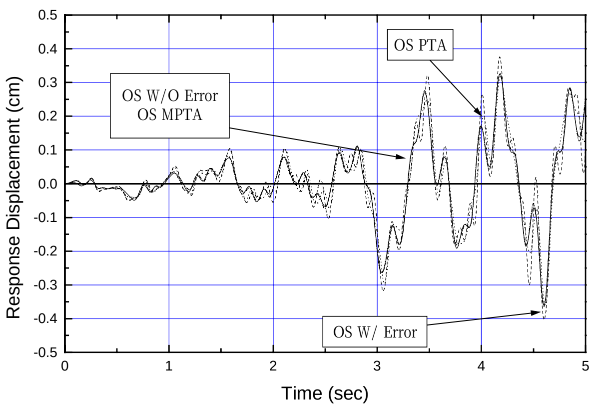

(a) Response displacements at the first story
(Linear:6DF:0~10 sec)

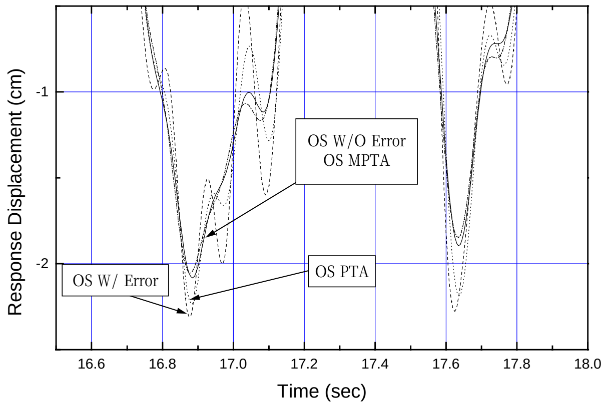

(b) Response displacements at the first story
(Linear:6DF:16.5~18 sec)

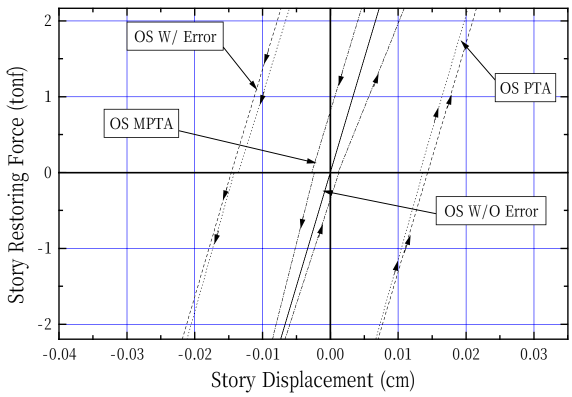

(c) Enveloped curves of the story restoring force- story displacement relationship
(Linear:6DF)

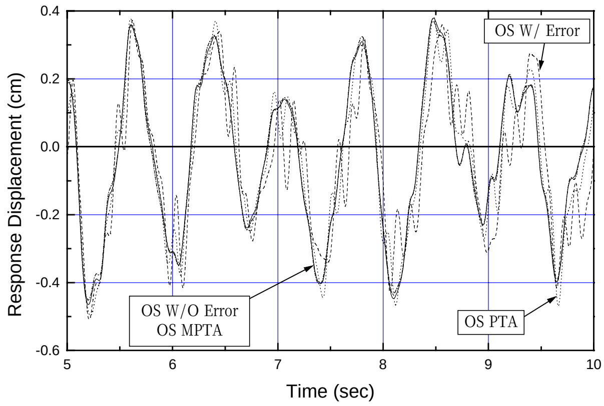

(d) Response displacements
(Non-linear:6DF:5~10 sec)

(W/: with, W/O: without)

Fig. 5: Linear and non-linear responses of MDF system

MDF SYSTEM

Fig. 5 (a) and (b) show the time histories of linear response displacement at the first story. It can be said that the response displacement of the OS /W Error was amplified compared with that of the OS W/O Error. The spurious high mode effect of the OS W/ Error was predominant because of the undershooting control error [Nakashima et. al., 1982 and 1983]. Furthermore, the PTA could not reduce the effect of the control error, and the spurious high mode effect of the PTA was also predominant as a result of the OS W/ Error. One of the reasons that the PTA cannot reduce the effect of the undershooting control error is the assumption of [G]=[I]. One can easily imagine that it is difficult to define the weight matrix [G] properly. On the other hand, the MPTA reduced the effect of the undershooting control error sufficiently. Thus the response of the MPTA was almost the same as the OS W/O Error. As shown in Fig. 5 (c), structural responses calculated using OS W/ Error, PTA and MPTA techniques showed anti-clockwise hysteresis loops. However, the area of the MPTA was smaller than that of the OS W/ Error and the PTA. Hence its response was successfully improved.

Fig. 5 (d) shows the time histories of a non-linear response displacement. The responses of the OS W/ Error and the PTA were amplified by the effect of the undershooting control error. Therefore, the spurious high mode effect of these responses was predominant as was found in the linear analysis results. As a result, the MPTA reduced the effect of control error sufficiently and the response of the MPTA agreed very well with the OS W/O Error.

Pseudo-dynamic test with Second-degree-of-freedom system

In order to confirm the validity of the MPTA technique, substructuring pseudo-dynamic test with a second-degree-of-freedom system were conducted. The structure was modeled so as to represent a shear vibration mode system. The first story was the test story that was experimentally loaded, and the responses of the second story were calculated within a computer. Since the purpose of this test was not to simulate the actual response of the structure but to confirm the validity of the MPTA technique, the hysteretic characteristics of each story were assumed as listed in Table 1, and the damping coefficient was assumed as 0.0%. The fixed time-step Δt of 0.01 sec was applied.

Outline of specimen and loading system

The dimension of the specimen is shown in Fig. 6. The hysteretic characteristics of the

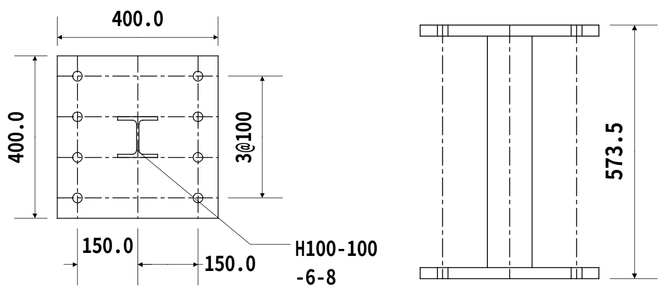

Fig. 6: Dimension of the specimen

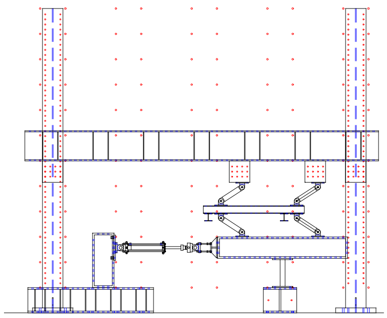

Fig. 7: The Loading system

specimen are listed on Table 1. The H-shaped steel of 100*100*6*8 was used to represent the response characteristics of the first story.

The loading system is shown in Fig.7. One actuator was used to apply a lateral force to the specimen. A pantograph system was attached on the loading beam to hold the reflection point of the specimen at mid-height of the specimen. The total weight of the loading beam, actuator, and pantograph was canceled by the counter weight.

Table 1: Hysteretic characteristics of the specimen

Direction	My (N・cm)	Qy (N)	Ke(N/cm)	Dy (cm)
X	2.893×10^{6}	3.998×10^{4}	6.352×10^{5}	1.740×10^{-1}
Y	1.929×10^{6}	1.105×10^{4}	2.2985×10^{5}	1.740×10^{-1}

Input earthquake data

The NS component of 1987 Chiba-Ken-Toho-Oki earthquake data recorded at Chiba Experimental Station of Institute of Industrial Science, University of Tokyo, was used as the input earthquake data. Twenty seconds record including the peak ground acceleration was used. Fig. 8 shows the input earthquake data.

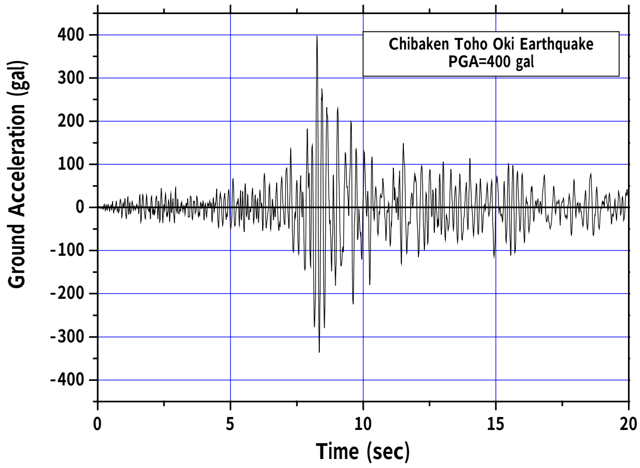

Fig. 8: Input earthquake data (Chibaken-Toho-Oki earthquake)

Test parameter

The test parameter was the actuator control precision, the precisions of the D/A transfer were 8-bit and 12-bit. It was found from the preliminary test results that the precision of 12-bit was the upper bound to control the actuator. The tests with and without the MPTA technique at the precision of 8-bit were conducted. Furthermore, a precision of 12-bit was applied to the test of which the first and second floors were loaded. The different test cases are listed on Table 2. The minimum controllable displacements for

Table 2: Details of the test case

Test case	First story	Second story	MPTA Technique
Case 1	Loaded (8Bit)	Numerical Simulation	Not used
Case 2	Loaded (8Bit)	Numerical Simulation	Used
Case 3	Loaded (12Bit)	Numerical Simulation	Not used
Case 4	Loaded (12Bit)	Loaded (12Bit)	Not used

each precision of the D/A board can be calculated as follows;

for 8-bit; $\frac{5\times 2}{2^8} = 0.0390625\,(\mathrm{cm})$, and for 12-bit; $\frac{5\times 2}{2^{12}} = 0.0024414(\mathrm{cm})$

Test results

The test durations are listed on Table 3. Since the undershooting error was applied to control the actuator, the test with the MPTA technique (case 2) needed 759 steps more than the test with fixed time-step. The test durations of case 1 and case 2, of which the D/A precision were 8-bit, were approximately 3 and 4 hours, respectively. They are allowably short to conduct the substructuring pseudo-dynamic test. It can be said that the MPTA technique does not extend the test duration too much. On the other hand, the test durations of case 3 and case 4, of which D/A precision were 12-bit, were approximately 12 and 22 hours, respectively. They were almost 4 to 8 times as long as case 1 and case 2.

Table 3: Test durations

Case	Steps	Duration	Date
Case 1	2000	3:18	9/18
Case 2	2759	4:11	9/18
Case 3	2000	11:01	9/14～15
Case 4	2000	22:02	9/4～5

The time history of the response displacement on the second floor is shown in Fig. 9. It can be seen, especially, among the middle response region that the response displacement of case 1 was amplified due to the control error. On the contrary, the responses with the precision of 12bit (case 3) were slightly reduced compared with the numerical analysis result. Moreover, the responses with the precision of 12bit were observed to shift in the large response region. The response with the MPTA technique (case 2), however, agreed very well with the numerical analysis result.

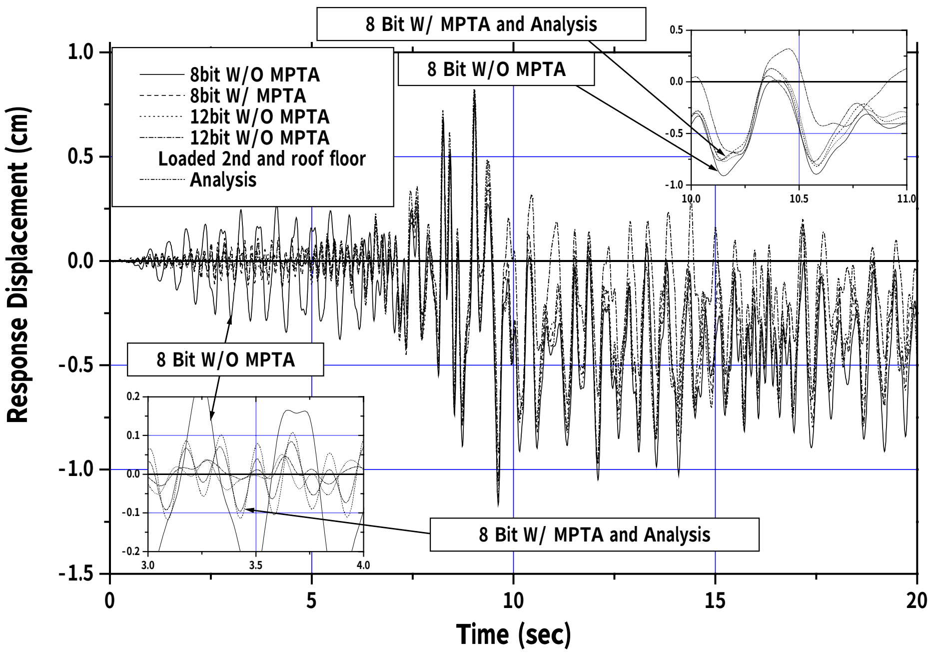

Fig. 9: Time history of the response displacement at the second floor

Concluding remarks

The Posterior Time-step Adjustment technique and the Modified PTA technique were proposed in order to reduce the effect of the control error. Linear and non-linear dynamic response analyses of the MDF shear vibration mode system considering the undershooting actuator control error at the first story was carried out. In addition, the substructuring pseudo-dynamic tests with a second-degree-of-freedom system were conducted. Results obtained from the investigation can be summarized as follows;

1) Dynamic responses are amplified by the effect of undershooting control error, and the spurious high mode effect of the MDF responses is predominant.
2) The Modified PTA technique can reduce the effect of the control error successfully for both linear and non-linear responses of the MDF systems, while the PTA technique cannot reduce it if the weight matrix of the PTA is not provided properly.
3) The modified PTA technique is a useful technique to achieve the higher accuracy of the substructuring pseudo-dynamic test with relatively low actuator control precision.
4) The modified PTA technique does not extend the test duration too much.

References

AIJ/Architectural Institute of Japan (1992), “Design Guidelines for Earthquake Resistant Reinforced Concrete Buildings Based on Ultimate Strength Concept”

KABAYAMA, K. (1995), “Study on High Accurate On-line Test”, Doctoral Thesis of Univ. of Tokyo

NAKASHIMA, M., KATO, H. and KAMINOSONO, T. (1982 and 1983), “Simulation of Earthquake Response by Pseudo-dynamic Test Technique Part 1, 2,3 and 4”, Summaries of technical papers of annual meeting, AIJ, pp.951-954(1982), pp.445-448 (1983), Oct.

NAKASHIMA, M., ISHIDA, M. and ANDO, K. (1990), ”Integration Techniques for Substructure Pseudo-dynamic Test (Pseudo-dynamic test using substructuring techniques)”, Journal of Struct. Constr. Engng, AIJ, No417, Nov.

Plesha, M. E. and Belytschko (1985), T., ”A Constitutive Operator Splitting Method for Nonlinear Transient Analysis”, Computers & Structures, Vol.20, No.4

Takeda, T., Mete A. Sozen, N. Norby Nielsen (1970), ”Reinforced Concrete Response to Simulated Earthquake”, Journal of Structural Division, Vol. 96, ST 12

Yi, W. H. and Peek, R. (1993), ”Posterior Time-Step Adjustment in Pseudo-dynamic Testing”, Journal of Engineering Mechanics, Vol.119, No. 7, July

KUSUNOKI, K., Nakano, Y., Yi, W. H., Lee, L. H. (2000), “Posterior Time-Step Adjustment Technique in Substructuring Pseudo-dynamic Test”, 12th world conference on earthquake engineering, Feb.

Appendix 5

Section 5 *Mass-eccentric Effect on response of Base Isolation System for Houses*

presented by M. Iiba

Mass-eccentric Effect on Response of Base Isolation System for Houses

Iiba Masanori[1], Myslimaj Bujar[2], Midorikawa Mitsumasa[1]
and Ishizaki Yohji[3]
[1]*Building Research Institute, Tsukuba, Japan*
[2]*McMaster University, Hamilton, Ontario, Canada*
[3]*Nitta Corporation, Nara, Japan*

ABSTRACT

In this paper, the effect of mass eccentricity on the response of recently developed base isolation systems for houses is discussed. Shaking table tests on base isolated models were carried out. Three patterns of weight distribution into the system were used to create three different scenarios: no mass-eccentricity, moderate mass-eccentricity and excessive mass-eccentricity. The torsional responses of two representative types for rolling and sliding systems are compared. A remarkable difference between peak torsional angle responses of the two systems was observed, with the rolling system showing a clear tendency to respond with larger torsional angle amplitudes as compared to the sliding system.

1. INTRODUCTION

Many structures were severely damaged during the 1995 Hyogoken-Nanbu Earthquake. Some of the buildings collapsed either at the 1st story or at their intermediate stories. There were also many people that were found dead or injured inside their houses. The seismic response records obtained at several base isolated structures during the 1994 Northridge earthquake and 1995 Hyogoken-Nanbu earthquake demonstrated clearly the efficiency of base isolation in increasing the building safety and in the same time contributed to the sudden increase in the demand for seismically isolated buildings right after these earthquakes.

There are some signs of a start-up for the expansion of base-isolated structures into private housing sector, but still far from what has been reported from the multi-unit housing sector. This is related to the following factors that need to be considered:

a) Cost performance
b) Relatively small weight of residential houses
c) Habitability and safety during strong winds or typhoons

In order to achieve the required performance for the isolators and base-isolated residences, the development of new types of isolators, which can be grouped in three systems: (a) Rubber bearing system, (b) Rolling system and (c) Sliding system, were focused. The main objective of this study is the investigation of the effect of mass eccentricity on the response of the base isolation systems. Special attention is paid to the torsional response of two representative isolators belonging to the group (b) and (c).

2. EXPERIMENTAL MODELS

The experimental setup is shown in Fig. 1. It was used for testing the base-isolation system under one- and three-directional earthquake excitations, providing thus the experimental database necessary for the investigation of the effect of mass eccentricity on the response of the system. Three patterns of weight distribution into the system were used to create three mass-eccentricity scenarios: (1) no mass-eccentricity (ECC0); (2) moderate mass-eccentricity (ECC1) and (3) excessive mass-eccentricity (ECC2). Table 1 shows the location of center of gravity (CG) for each mass-eccentricity scenario in reference to the heavy side edge. Schematic drawings and fundamental characteristics of two representatives are shown in Fig. 2. The rolling system is a combination of ball bearings in the center with high damping laminated rubber in the perimeter. As for the sliding system, it is principally designed to absorb the energy through the friction between two spherical surfaces and a sliding cylinder, which are coated with a low-friction composite material. Tests were performed on a large-scale three-dimensional shaking table installed at Public Works Research Institute, Japan.

Table 1. CG location for each mass-eccentricity scenario

Mass-Eccentricity Scenario	CG location in reference to the heavy side edge (*m*)	CG - heavy side edge distance normalized by the isolators' spacing
ECC0	2.82	1.000
ECC1	2.55	0.905
ECC2	2.29	0.812

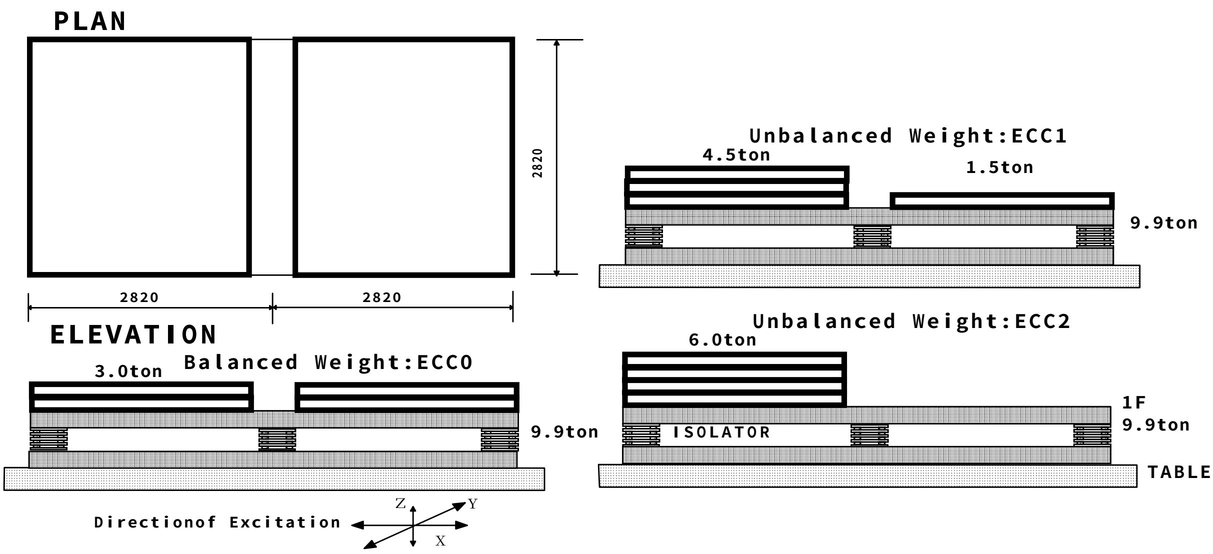

Figure 1. Base isolated model with mass eccentricity

Table 2. Adjusted PGV values for each component of the input motion

EQ Name	1940 El Centro			1995 JMA Kobe		
Direction	X	Y	Z	X	Y	Z
Actual PGV (cm/s)	24.8	20.4	6.32	23.1	23.9	12.4
	49.1	39.7	12.2	44.6	48.3	23.1

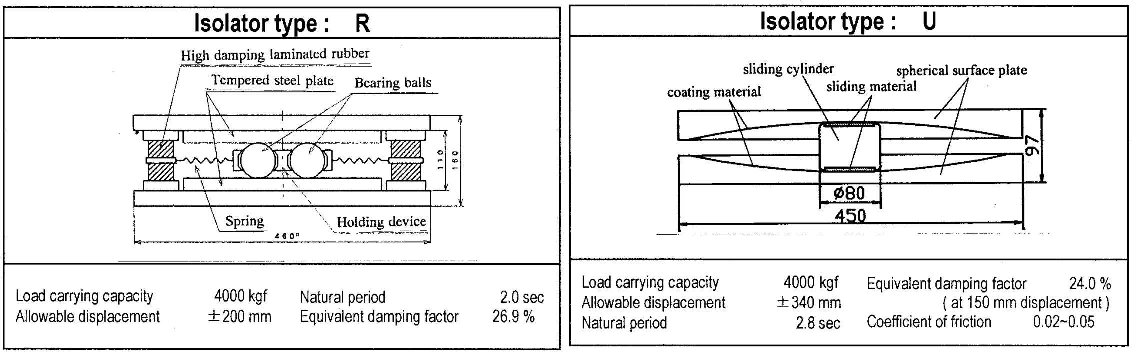

a) Rolling system **b)** Sliding system

Figure 2. An outline of fundamental characteristics of two representative isolators

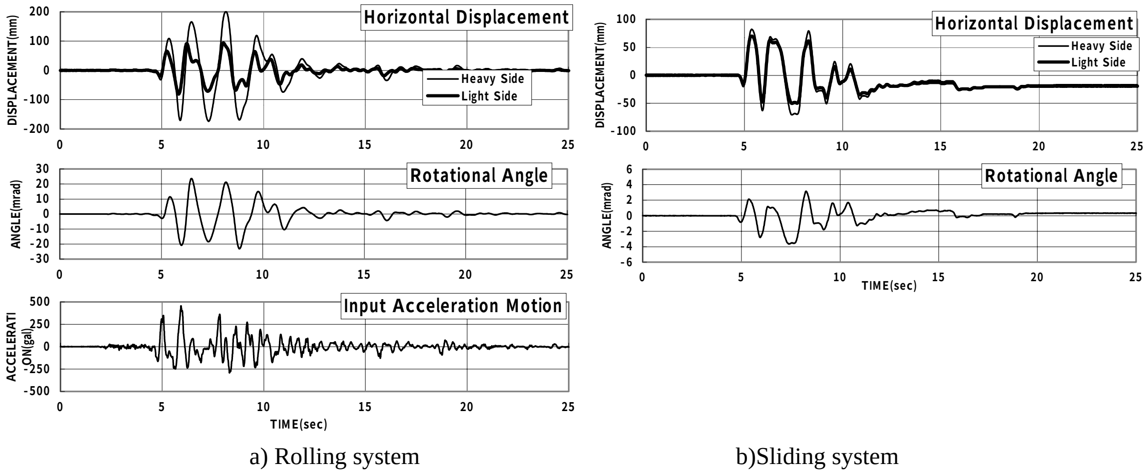

a) Rolling system b)Sliding system

Figure 3. Response time histories of rolling and sliding systems for ECC2 mass-eccentricity case

Strong ground motions recorded during the El Centro Earthquake of 1940 and Kobe Earthquake of January 17, 1995 (JMA Kobe Station record) were used as input motions at the shaking table. Based on the peak ground velocity (PGV) value observed in each record, the input earthquake waves were proportionally adjusted to the intensity levels of 25 and 50cm/s. The actual PGV values for each component of input motion are shown in Table 2.

3. SHAKING TABLE TEST RESULTS

In Fig. 3 are shown response time histories for rolling and sliding systems. They correspond to the ECC2 mass-eccentricity scenario, using only the NS component of 1995 JMA Kobe earthquake motion as seismic excitation in the Y direction. For both systems, it can be noticed that the displacement response of the heavy side is larger than that of the light side. The variation of peak displacement response at both edges with respect to mass-eccentricity ratio is shown in Fig. 4. As the mass-eccentricity increases the peak displacement response of the heavy side increases, while that one of the light side decreases. In addition, it can be noticed that the torsional effect on the displacement response of the rolling system is larger than that of the sliding system.

As shown in Fig. 5, it can be also noticed that the rolling system tends to rotate easily due to the mass-eccentricity. Figure 6 shows the relationship between shear force and horizontal displacement for the ECC0 case, using the NS component of 1995 JMA Kobe earthquake motion as seismic excitation in the Y direction. As it can be noticed from these two plots, the rolling type system delivers less hysteretic damping compared to the sliding system that shows a larger capacity in energy absorption for quite a wide range of displacement response.

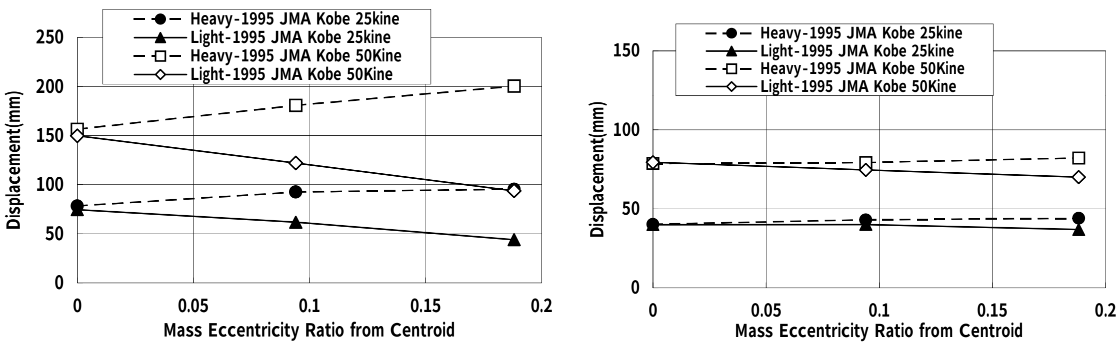

a) Rolling system b)Sliding system

Figure 4. Variation of peak edge displacement responses with mass-eccentricity ratio.

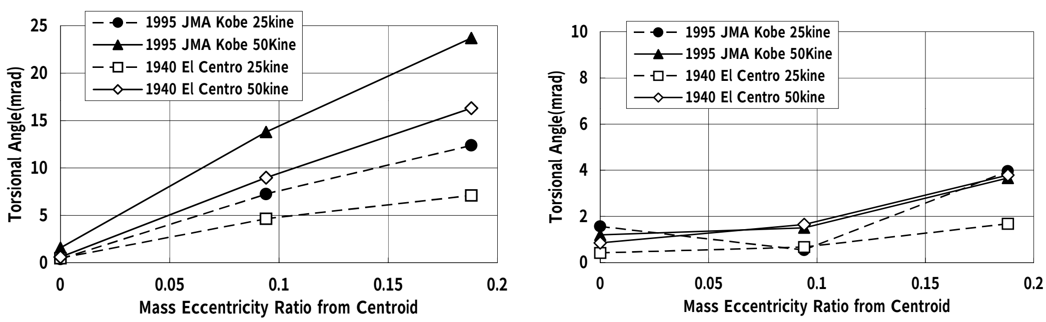

a) Rolling system b)Sliding system

Figure 5. Variation of peak torsional angle response with mass-eccentricity ratio

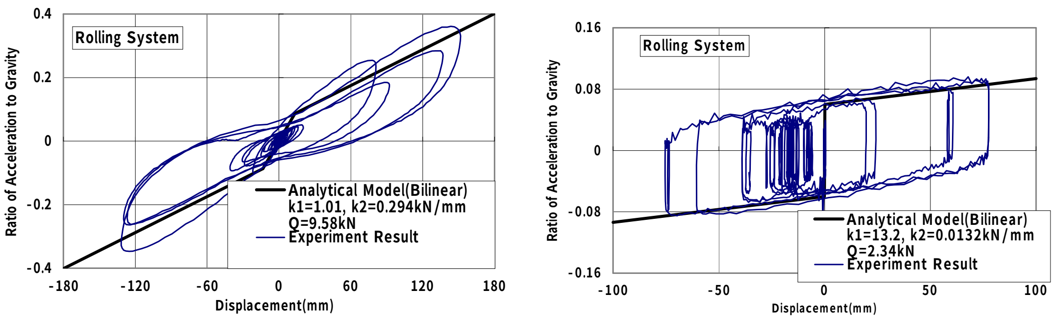

a) Rolling system b)Sliding system

Figure 6. Shear force – displacement relationship from analytical modeling and experimental data

4. ESTIMATION OF TORSIONAL RESPONSE BY STATIC PROCEDURE

An attempt is made in this section to estimate the torsional response by making use of static equilibrium. The analytical model conceived for this purpose is illustrated in Fig. 7. The displacement due to torsion is determined as follows:

a) Center of gravity: $x_g = \sum (W_i x_i) / \sum W_i$, $y_g = 0$

b) Isolator's stiffness: $K_i = K(u_{yi})$ (secant modulus, displacement dependency in Fig. 6)

c) Center of stiffness: $x_k = \sum (K_i x_i) / \sum K_i$

d) Stiffness eccentricity: $e_y = x_k - x_g$

e) Torsional angle: $\theta = M_K / K_t$, where $M_k = \left\{ \sum (K_i u_{yi}) \right\} \cdot e_y$, $K_t = \sum K_i \left\{ (x_i - x_k)^2 + y_i^{\,2} \right\}$

f) Displacement: $u_{yi} = u_{yk} + \theta (x_k - x_i)$, where u_{yk} is displacement at the center of stiffness

The maximum response for the ECC0 mass-eccentricity case, u_{y0} , is used as an initial value for the horizontal displacement response. Since nonlinear characteristics of the isolators are taken into account, steps b) to f) are cyclically repeated until the displacement convergence is reached.

In Fig. 8 is shown the relationship between peak torsional angle response and the mass-eccentricity for the case when the NS component of JMA Kobe earthquake motion is used as seismic excitation in the Y direction. For comparison, two solid lines are also drawn in the graph representing the results obtained by the static procedure. In case of the sliding system, a good agreement is observed. It doesn't appear to be the same for the rolling system.

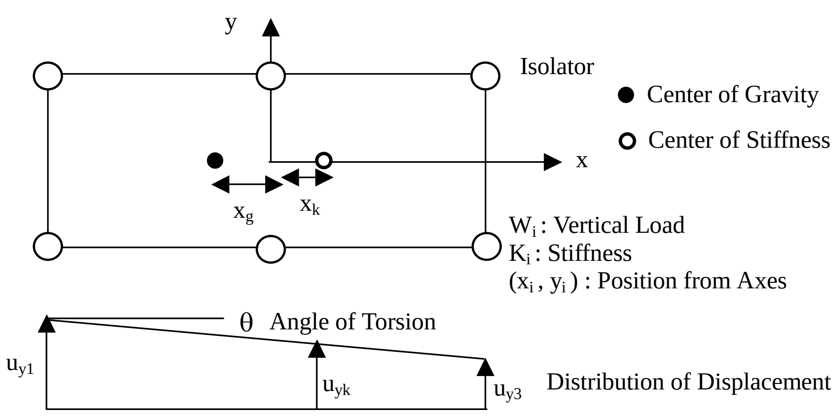

Figure 7. Simplified model used for the estimation of torsional angle response

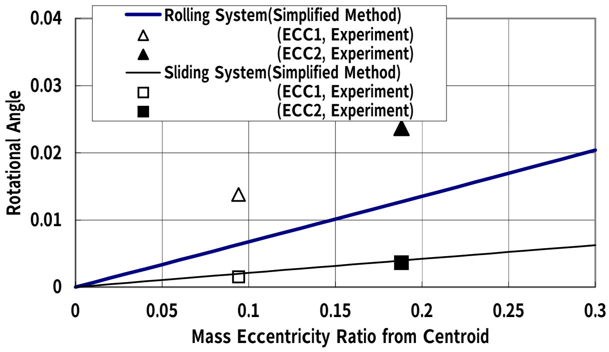

Figure 8. Comparison of peak torsional angle responses

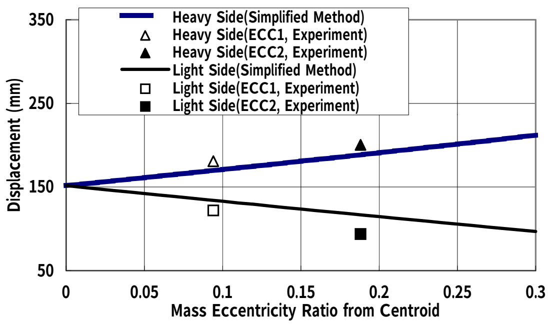

a) Rolling system

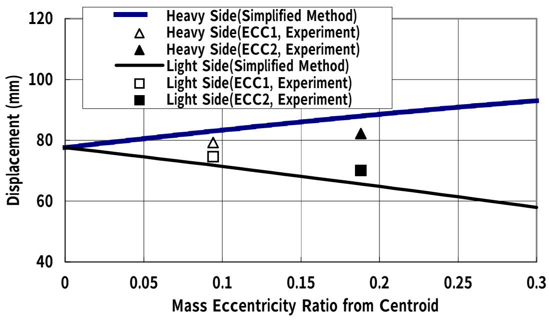

b)Sliding system

Figure 9. Comparison of peak edge displacement responses

Similarly to Fig. 8, in Fig. 9 is shown the relationship between peak edge displacement response and the mass-eccentricity. As compared to the peak torsional angle, a much better agreement is observed here between the experimental results and those obtained by the analytical simulation for the rolling system. Most likely, this is related to the fact that peak torsional angle and peak edge displacements do not occur at the same instants.

5. CONCLUDING REMARKS

The effect of mass-eccentricity on the torsional response of base isolation systems for houses was investigated. Results indicate that torsional response of base isolated systems is not only a function of mass-eccentricity and earthquake ground motion characteristics, but is also very much dependent on the mechanical characteristics of the isolation systems. A remarkable difference between peak torsional angle responses of the rolling and sliding systems was observed. It appears that the sliding system is less sensitive to mass-eccentricity as compared to the rolling system.

ACKNOWLEDGEMENTS

The authors would like to express their sincere thanks to all the members of the committee on "Development of new technologies for seismic isolators for houses", the chairman of which is Mr. Shoichi Yamaguchi, president of Tokyo Kenchiku Structural Engineers, for providing data and valuable suggestions related to this study. The kind assistance of Dr. Keiichi Tamura, Public Works Research Institute in operating the shaking table is greatly appreciated.

REFERENCES

Iiba, M., Yamanouchi, H., Midorikawa, M., et al. (1998) "Research on Performance of Base Isolated House", *Proc. of the Second World Conference on Structural Control*, Kyoto, Japan, 2, pp1119-1126.

Iiba, M., Midorikawa, M., Kawai, M., et al. (1988) "Shaking Table Tests on Seismic Behavior of Isolators for Houses", *Proc. of the 10th Japan Earthquake Engineering Symposium*, Yokohama, Japan, pp2653-2658

Iiba, M., Midorikawa, M., Yamanouchi, H., et al. (2000) "Shaking Table Tests on Performance of Isolators for Houses Subjected to Three Dimensional Earthquake Motions", *Proc. of the 12 World Conference of Earthquake Engineering*, No.1765

Appendix 6

Section 6 *Sub-Structure Pseudo Dynamic Testing on 12 story Reinforced Concrete Frame with Soft First Story*

presented by H. Kuramoto

Sub-Structure Pseudo Dynamic Testing
on
12 Story Reinforced Concrete Frame
with
Soft First Story

ICCEED, Toyohashi University of Technology

Hiroshi KURAMOTO

Motivation

The 1995 Kobe Earthquake damaged to many RC buildings with soft first story.

MOC revised some of the Notifications relating to RC buildings with SFS as action in an emergency.

More detailed examination is required to establish a rational evaluation method of seismic performance of the building.

Objectives

- To investigate causes of the collapse of the building and its mechanisms.
- To examine systems for preventing the collapse.
- To develop a rational evaluation method for the seismic performance of RC buildings with soft first story.

Method of Study

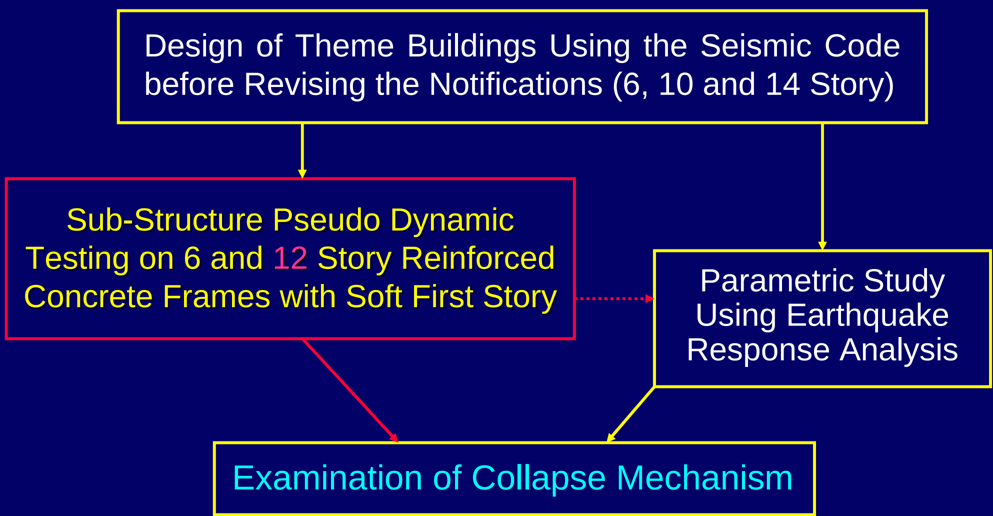

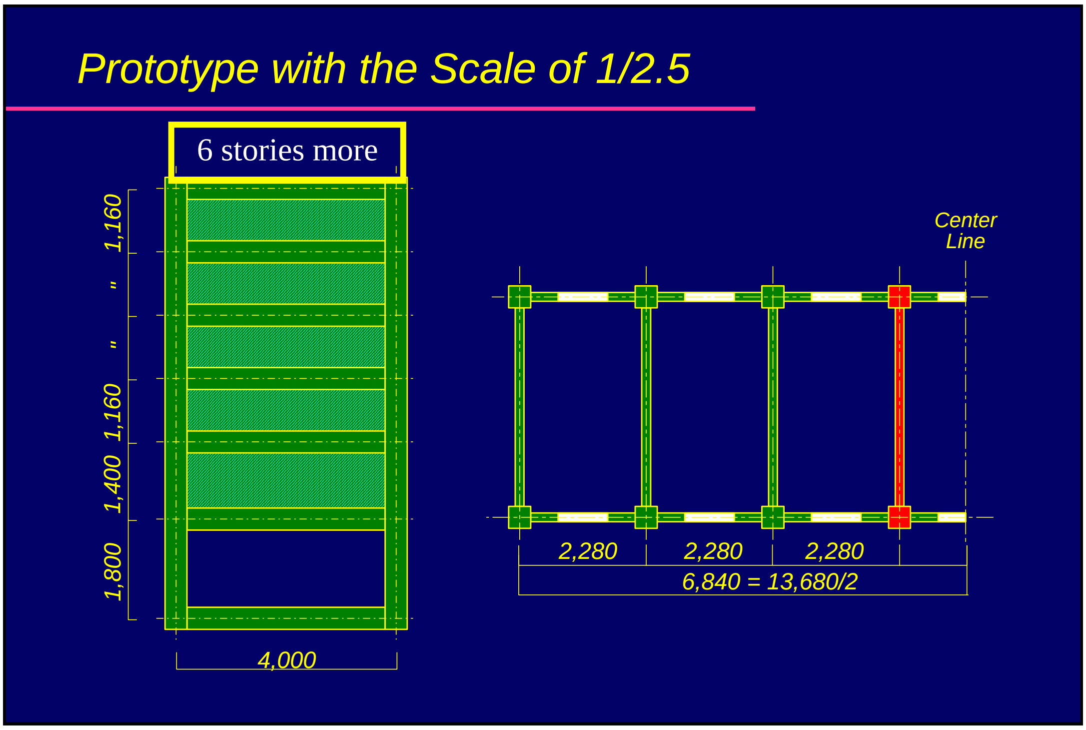
Prototype with the Scale of 1/2.5
6 stories more
1,160
"
"
1,160
1,400
1,800
4,000
Center
Line
2,280
2,280
2,280
6,840 = 13,680/2

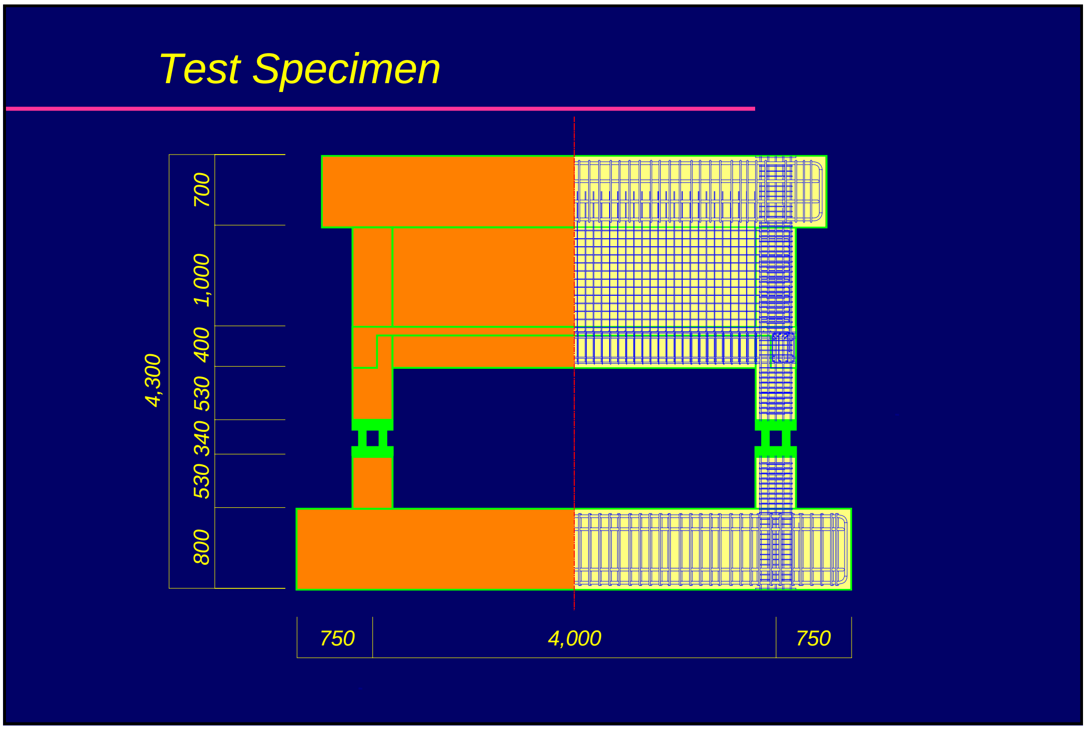
Test Specimen
700
1,000
400
530
340
530
800
4,300
750
4,000
750

Load Cell to Measure the Shear and Axial Forces in Columns at the First Story

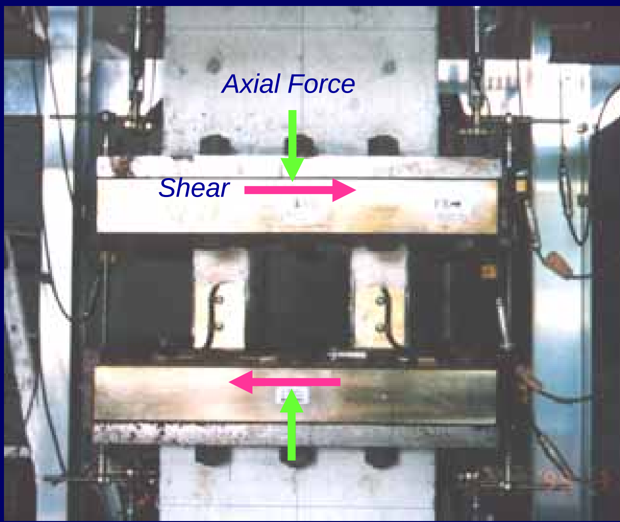

Loading Apparatus

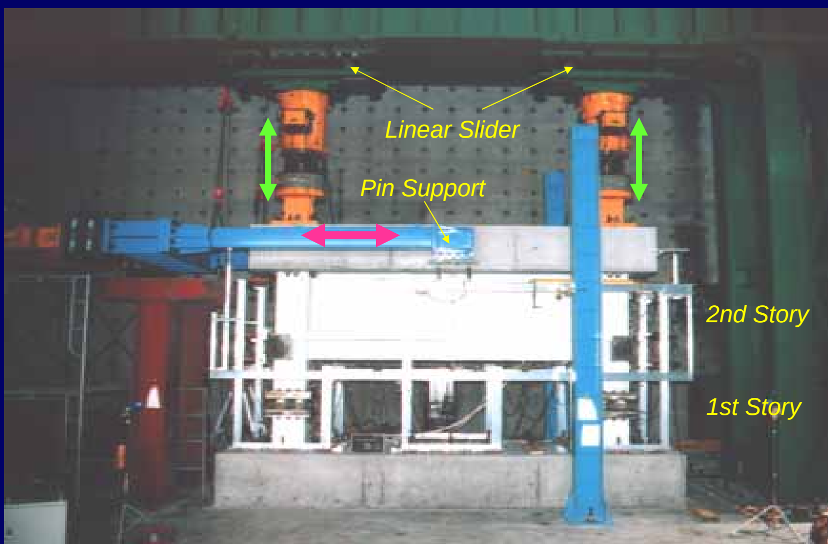

Input Ground Motions

- *El Centro NS (1940) : 10 kine, 25 kine, 50 kine*
- *JMA-Kobe NS (1995) : original (90 kine)*

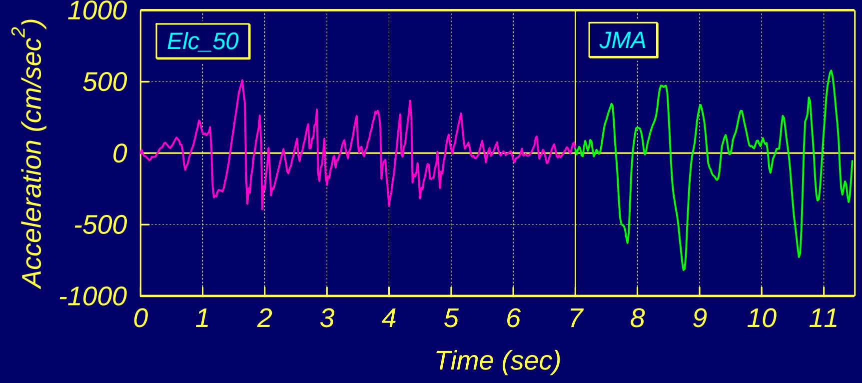

Failure of Columns at 1st Story

West Side

East Side

Failure of Columns at 1st Story

West Side East Side

Failure of a Shear Wall at 2nd Story

West Side East Side

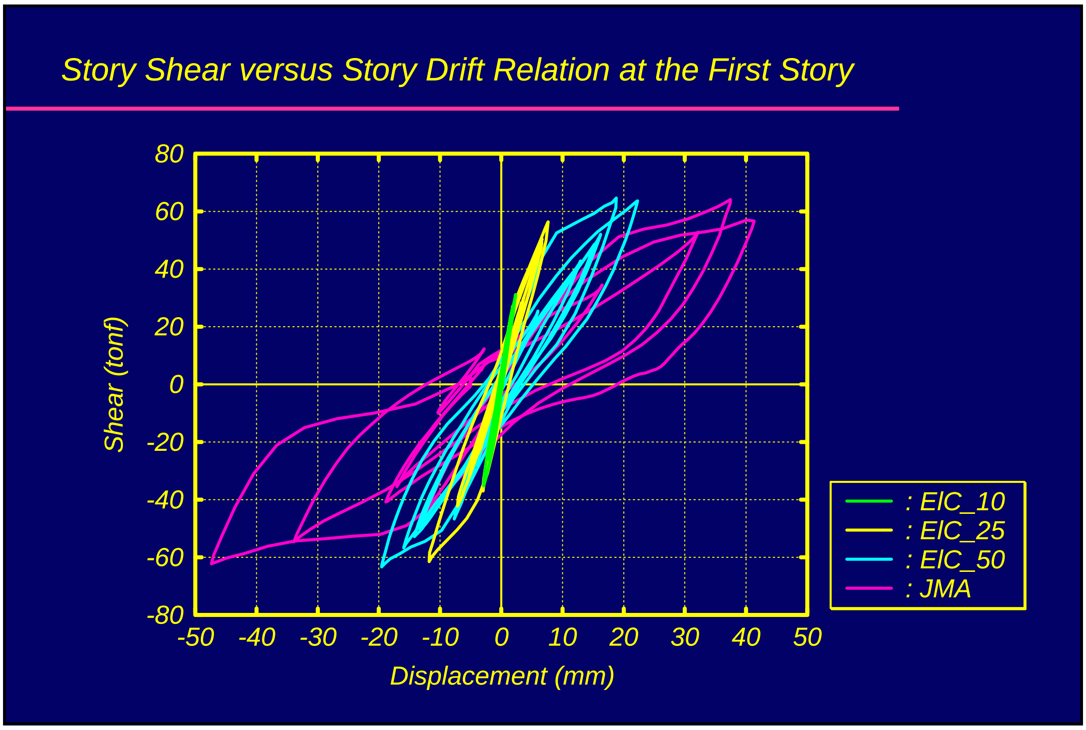
Story Shear versus Story Drift Relation at the First Story
Shear (tonf)
Displacement (mm)
: ElC_10
: ElC_25
: ElC_50
: JMA

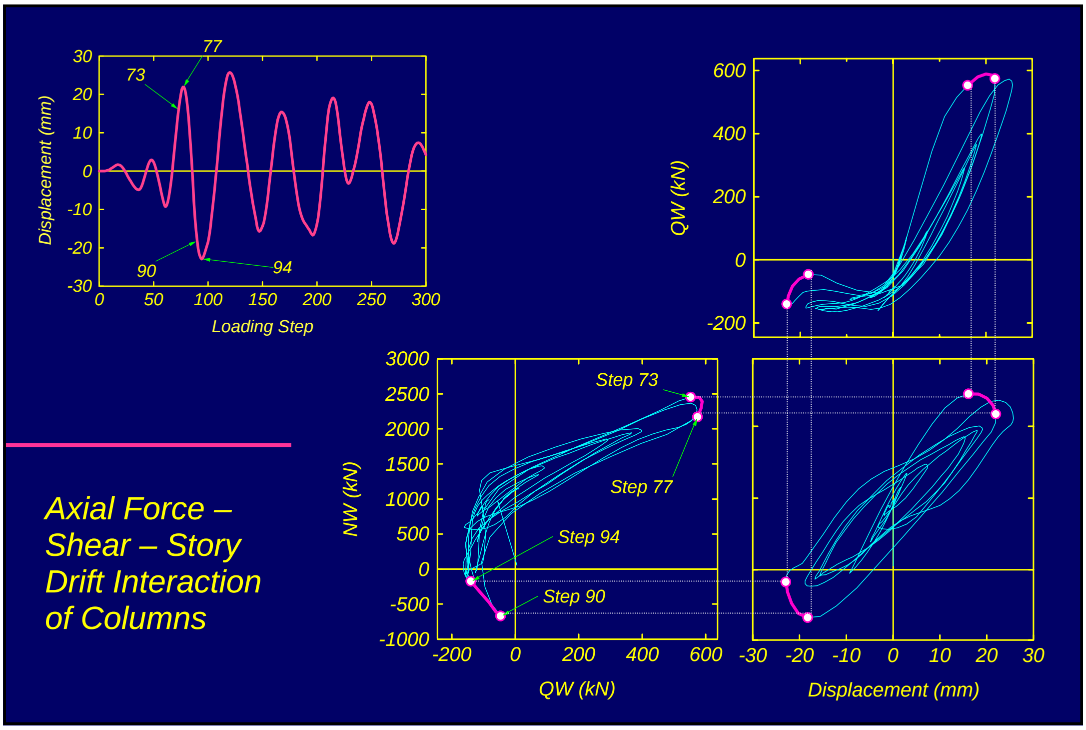
Axial Force – Shear – Story Drift Interaction of Columns
Displacement (mm)
Loading Step
73
77
90
94
QW (kN)
NW (kN)
Step 73
Step 77
Step 94
Step 90
Displacement (mm)

External Force Distribution and Displacement Distribution along Building Height

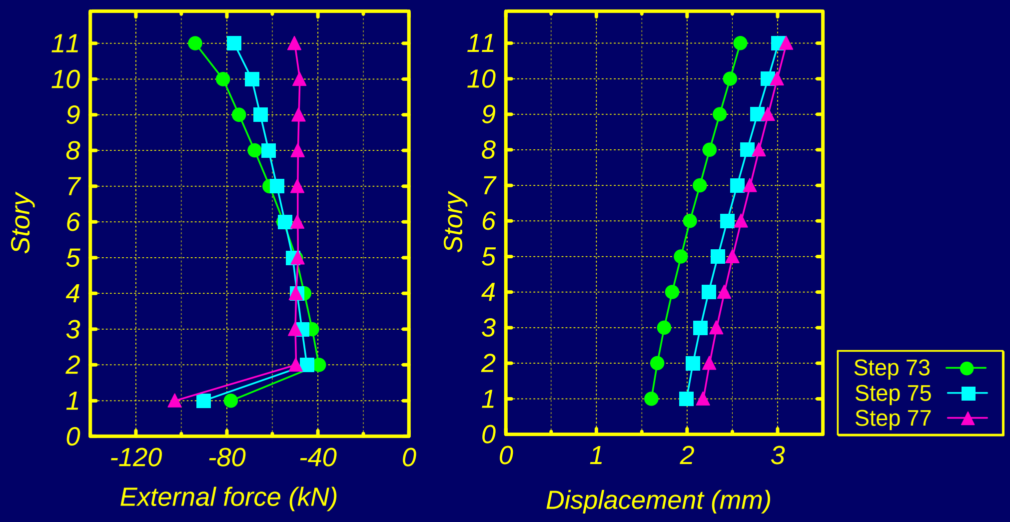

Conclusion

Sub-Structure Pseudo Dynamic Testing
on 12 Story Reinforced Concrete Frame with Soft First Story

- Collapse Mechanism:
  Story collapse mechanism in the 1st story with the flexural yielding of columns
- Maximum Story Drift Angle at the 1st story:
  1/63 for El Centro NS 50kine input and 1/29 for JMA-Kobe NS original input
- Axial Force Ratio of Columns at Maximum Response: -0.15〜0.52
- External Force Distribution along the building height at Maximum Response:
  Uniform shape
- Higher mode effects are observed before reaching the maximum displacement response.

Appendix 7

Section 7 *European Laboratory For Structural Assessment (ELSA) by F. Taucer*

presented by F. Taucer

European Laboratory For Structural Assessment (ELSA)

Safety in Structural Mechanics Unit

Mission of ELSA Unit

**To provide research
and contribute to European Standards
for risk mitigation
in construction, transport, and industrial installations
through integrated use of
experimental testing and numerical modeling
in Structural Mechanics**

Safety in Structural Mechanics Unit

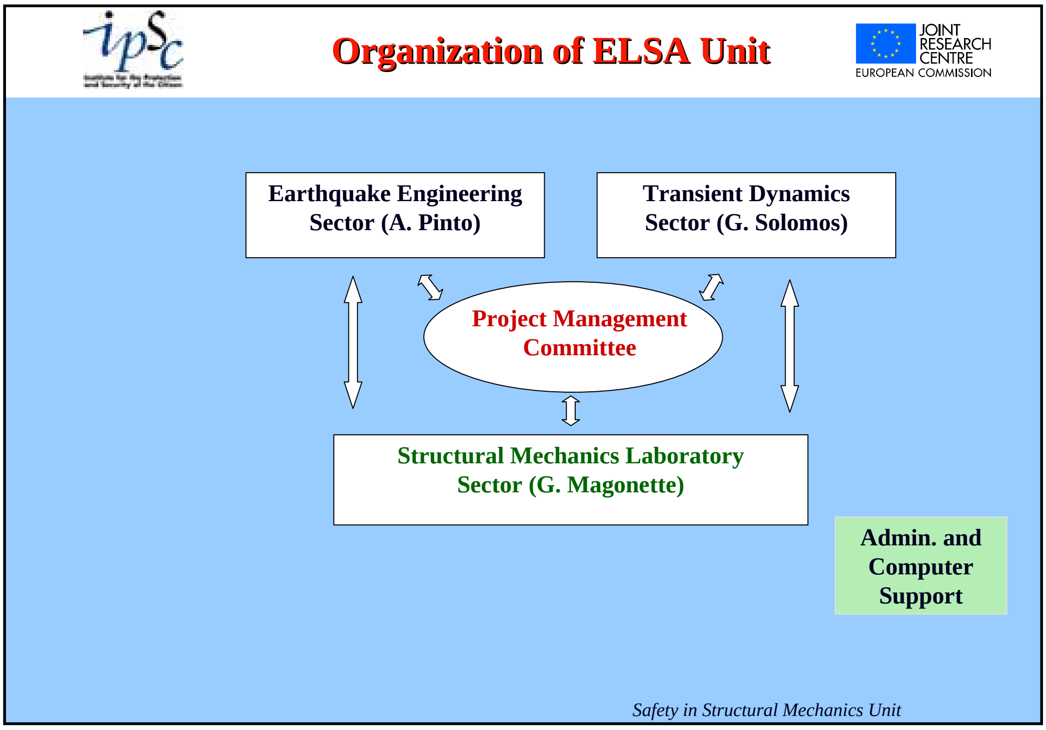
Organization of ELSA Unit
JOINT RESEARCH CENTRE
EUROPEAN COMMISSION
Earthquake Engineering Sector (A. Pinto)
Transient Dynamics Sector (G. Solomos)
Project Management Committee
Structural Mechanics Laboratory Sector (G. Magonette)
Admin. and Computer Support
Safety in Structural Mechanics Unit

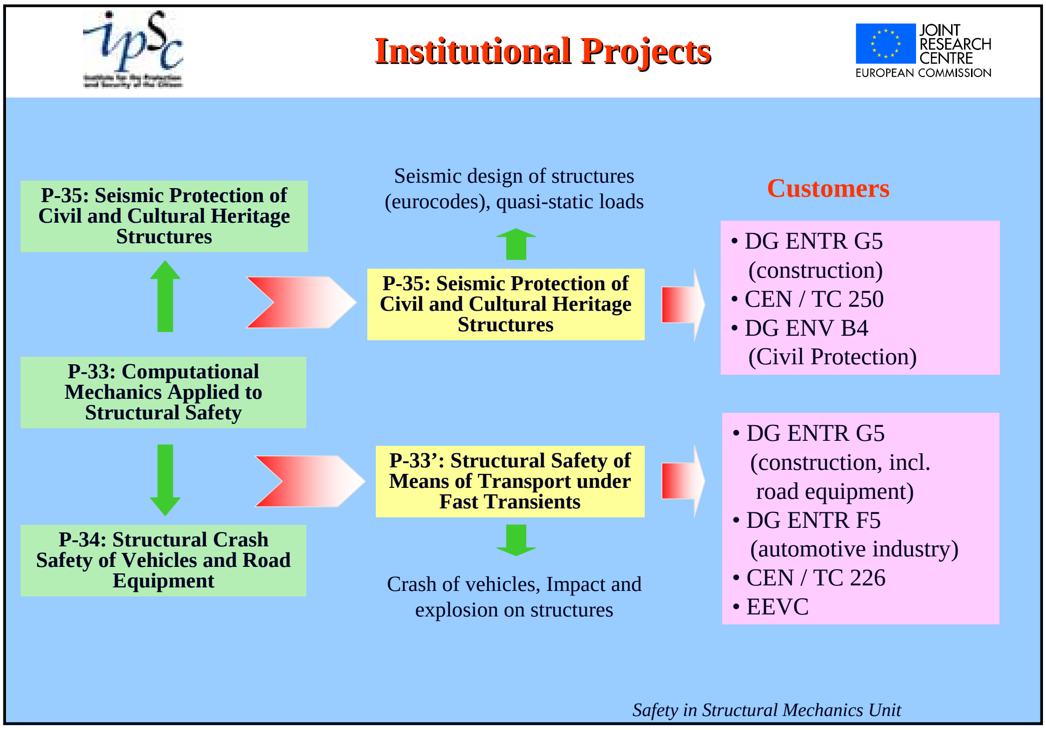
Institutional Projects
JOINT RESEARCH CENTRE
EUROPEAN COMMISSION
P-35: Seismic Protection of Civil and Cultural Heritage Structures
P-33: Computational Mechanics Applied to Structural Safety
P-34: Structural Crash Safety of Vehicles and Road Equipment
Seismic design of structures (eurocodes), quasi-static loads
P-35: Seismic Protection of Civil and Cultural Heritage Structures
P-33’: Structural Safety of Means of Transport under Fast Transients
Crash of vehicles, Impact and explosion on structures
Customers
• DG ENTR G5 (construction)
• CEN / TC 250
• DG ENV B4 (Civil Protection)
• DG ENTR G5 (construction, incl. road equipment)
• DG ENTR F5 (automotive industry)
• CEN / TC 226
• EEVC
Safety in Structural Mechanics Unit

ipSc

Human resources (01.2002)

JOINT RESEARCH CENTRE
EUROPEAN COMMISSION

ELSA Personnel	A	B	C	D	GH	Aux.	END	Vis. Sc.	Total
Unit Management									
Earthquake engineering									
Transient Dynamics									
Structural mech. Lab.									
Admin. And Info. Support									
Total									

Safety in Structural Mechanics Unit

ipSc

Financial Resources in FP5

JOINT RESEARCH CENTRE
EUROPEAN COMMISSION

Earthquake Engineering

INSTITUTIONAL FP5	
SCA (15)	
TMR (4)	
TPW (2)	
TOTAL (22)	

Transient Dynamics

INSTITUTIONAL FP5	
SCA (10)	
TPW (3)	
TMR (0)	
TOTAL (14)	

Safety in Structural Mechanics Unit

The main ELSA Tools

Earthquake Engineering

- ELSA reaction wall
- Hardware implementation of the PsD method
- CASTEM 2000 FEM software (CEA)

Transient Dynamics

- LDTF large Hopkinson bar
- Laboratory on Dynamics of materials
- EUROPLEXUS code (collaboration agreement with CEA)

- Electronics and Strain Gage laboratories
- Computer network and web site

Safety in Structural Mechanics Unit

Why Structural/Earthquake Engineering Research?

- Citizen protection: exponential increase of human and economic losses in modern society (increased complexity of infrastructures and networks), growth of population and land occupation, …)
- Role of the States and Authorities: Only 10% of the capital insured. In spite of this, re-insurance proposes Risk Sharing (between industry, insurance, re-ins., State, Regions)
- Industry development / competitiveness: New materials, new technologies for both new and existing (retrofit) constructions
- The need for harmonized and advanced norms and standards (e.g.: Eurocodes): Open market, Acceptable safety levels, …

Safety in Structural Mechanics Unit

Wordwide Great Natural Disasters 1950 - 1999
Far exceeding 100 deaths
and/or US$ 100 bns in claims

JOINT RESEARCH CENTRE
EUROPEAN COMMISSION

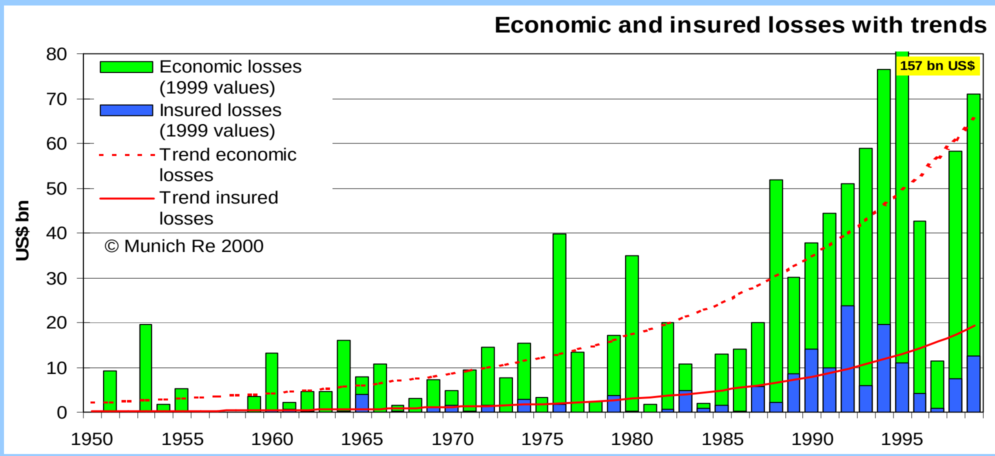

Safety in Structural Mechanics Unit

European Context

JOINT RESEARCH CENTRE
EUROPEAN COMMISSION

Kocaeli Earthquake (Turkey, 1999)

Deads: 17,000
homeless: 600,000
Reconstruction cost:
10-20 Billion Euros
35% of industry affected

Assisi, IT, 1997

Azores, PT, 1998

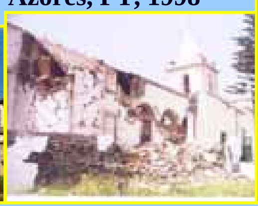

Athens, GR, 1999

Safety in Structural Mechanics Unit

The Role of the Design Code in Building Performance

JOINT RESEARCH CENTRE
EUROPEAN COMMISSION

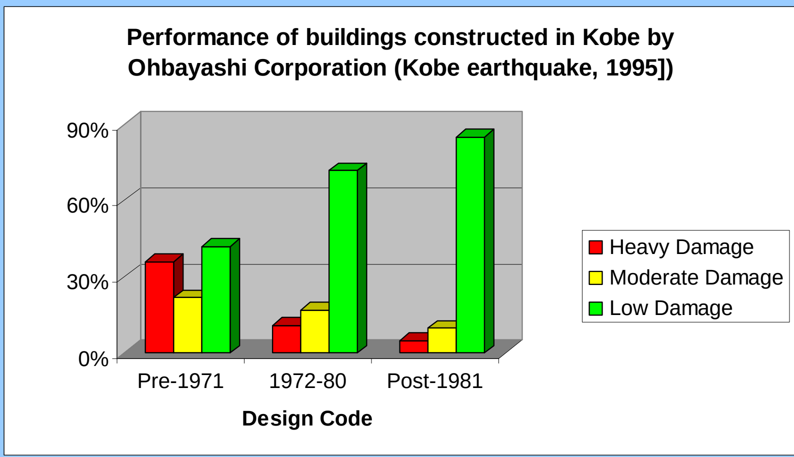

Safety in Structural Mechanics Unit

Earthquake Simulation in Laboratory

JOINT RESEARCH CENTRE
EUROPEAN COMMISSION

2 complementary approaches

Shaking Table

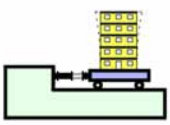

- dynamic test
- reduced scale
- open loop

Reaction Wall

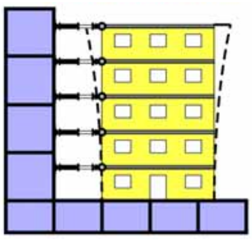

- pseudo-dynamic test
- full scale
- closed loop

Safety in Structural Mechanics Unit

ELSA reaction wall

JOINT RESEARCH CENTRE
EUROPEAN COMMISSION

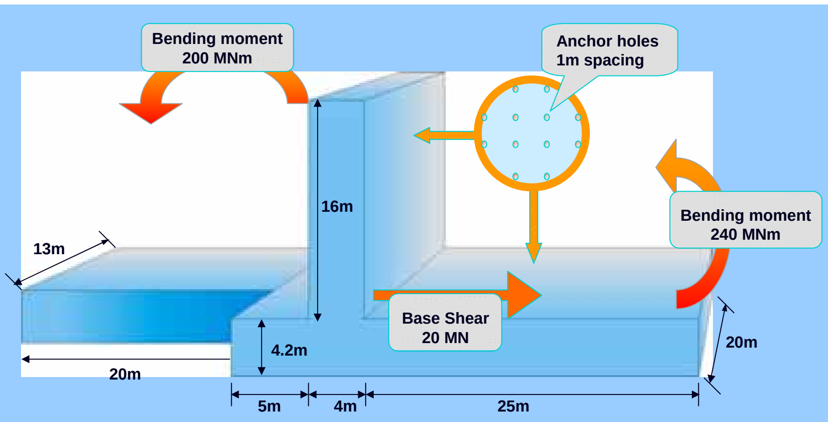

- 16 actuators 0.5 - 1 MN
- 2 testing platforms

- Unique test installation in Europe
- Allows pseudo-dynamic tests at full scale
- Integrated in European network of shaking tables

Safety in Structural Mechanics Unit

Pseudo-dynamic Testing Method

JOINT RESEARCH CENTRE
EUROPEAN COMMISSION

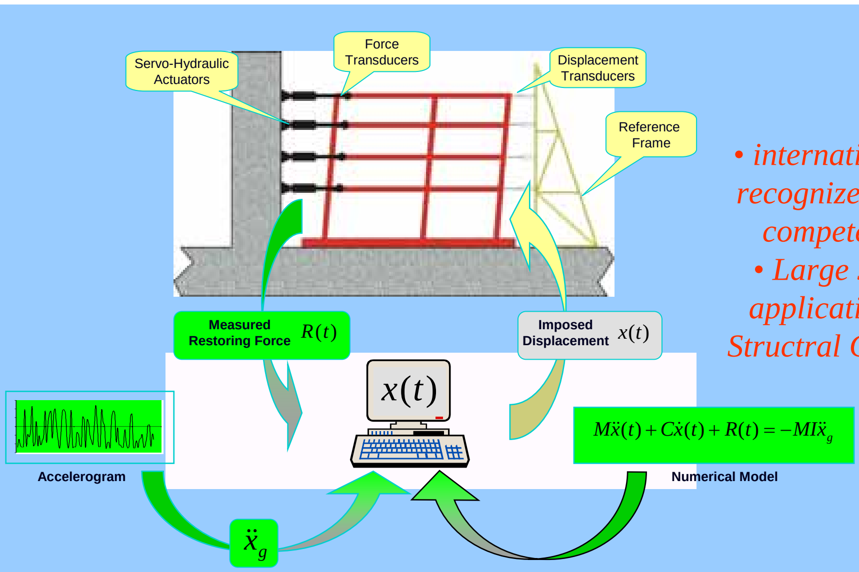

- *internationally recognized JRC competence*
- *Large scale application of Structral Control*

Safety in Structural Mechanics Unit

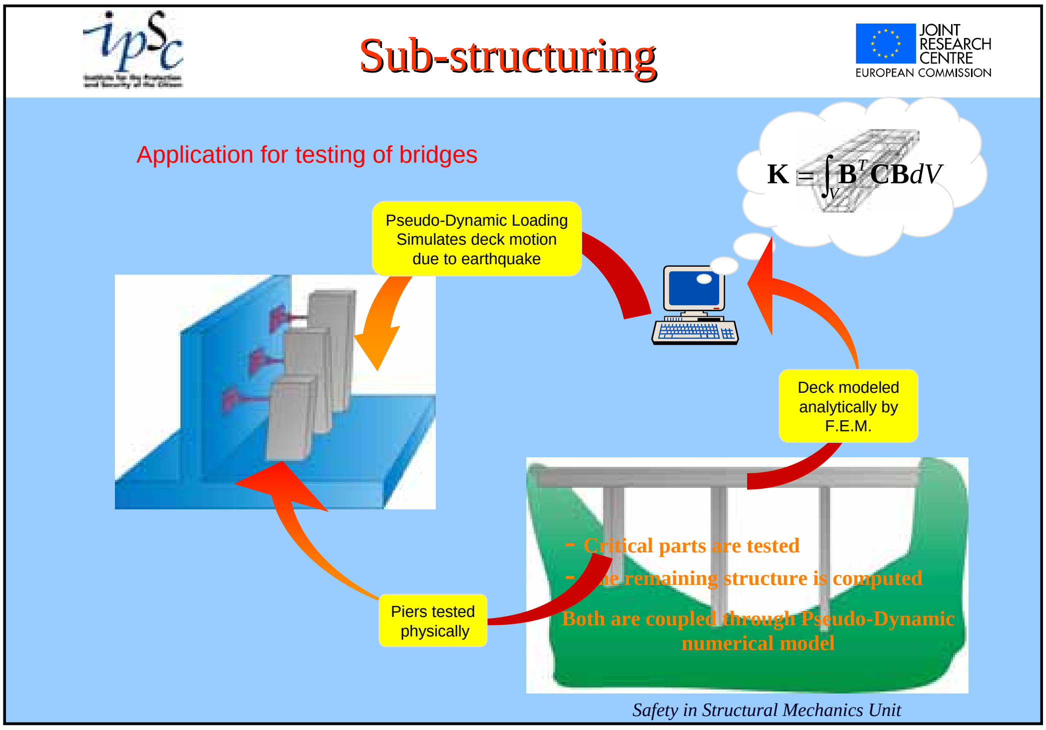
Sub-structuring
JOINT RESEARCH CENTRE
EUROPEAN COMMISSION
Application for testing of bridges
Pseudo-Dynamic Loading Simulates deck motion due to earthquake
$K = \int_V B^T C B dV$
Deck modeled analytically by F.E.M.
- Critical parts are tested
- remaining structure is computed
Both are coupled through Pseudo-Dynamic numerical model
Piers tested physically
Safety in Structural Mechanics Unit

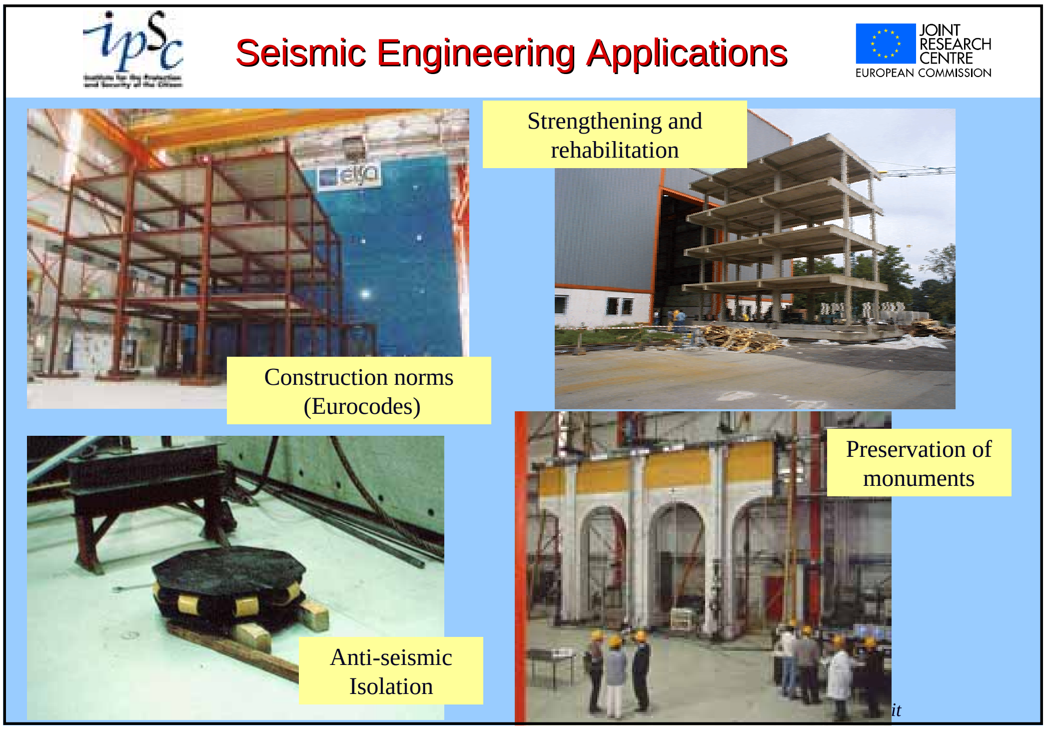
Seismic Engineering Applications
JOINT RESEARCH CENTRE
EUROPEAN COMMISSION
Strengthening and rehabilitation
Construction norms (Eurocodes)
Preservation of monuments
Anti-seismic Isolation

Earthquake Engineering European network

JOINT RESEARCH CENTRE
EUROPEAN COMMISSION

ECOEST
European Consortium of Shaking tables
Panel selection Committee

Marie Curie
Training sites
JRC, Bristol

Users
• ECOLEADER projects
•TMR networks

NTU
Athens

EERC
Bristol

JRC
Ispra

Reaction Wall

ISMES
Bergamo

LNEC
Lisbon

CEA
Saclay

Shaking tables

International Cooperation
Japan, US, others

Safety in Structural Mechanics Unit

Test on building model in « real time »

JOINT RESEARCH CENTRE
EUROPEAN COMMISSION

Safety in Structural Mechanics Unit

COSISMO Project
(Seismic Behaviour of Monuments)

JOINT RESEARCH CENTRE
EUROPEAN COMMISSION

Partners:

- DGEMN
- LNEC
- JRC

OBJECTIVES

- *Mitigation of Seismic Risk of Monumental Structures*
- Development of Methods and Tools for Seismic Vulnerability Assessment of Monuments
- Development of Retrofitting Techniques
- Application to the S. Vicente Monastery in Lisbon

Safety in Structural Mechanics Unit

Test on monument model

JOINT RESEARCH CENTRE
EUROPEAN COMMISSION

Safety in Structural Mechanics Unit

Numerical Modeling of stone-Block Structure

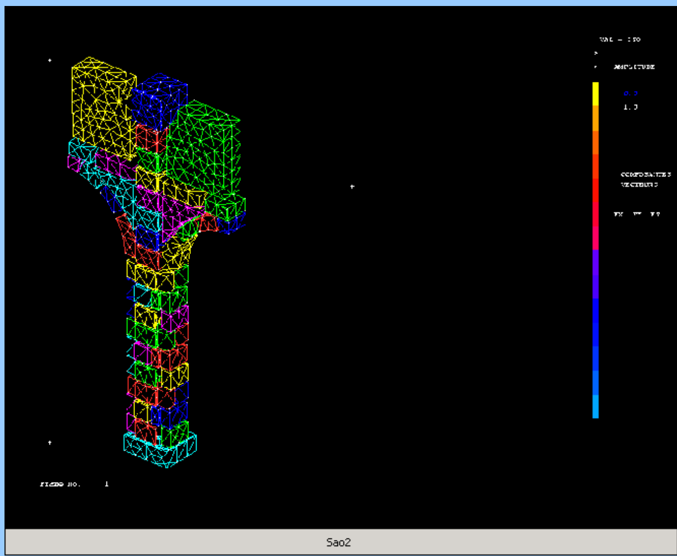

Vulnerability Assessment of Bridges

Construction of the large-scale bridge piers outside of the ELSA Laboratory

Pseudodynamic testing with substructuring: Application to the Warth Bridge, Austria

Physical piers in the lab

Numerical models for the substructured piers A20, A30

Numerical models for the substructured piers A50, A60

Numerical model for the deck and PSD master

Master experimental process and data acquisition

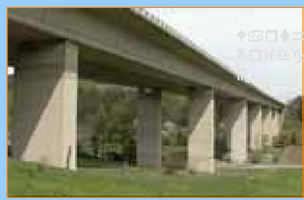

Safety in Structural Mechanics Unit

Application of composites to seismic resistance of reinforced concrete buildings

Wet lay-up application of a quasi-isotropic carbon FRP on the shear walls of a reinforced concrete dual frame

Safety in Structural Mechanics Unit

Active control in civil engineering (ACE)

Context: Brite-EuRam III (1997 - 2000)
General objective:
To control wind, rain and traffic vibrations of long span cable-stayed bridges
Partners:

- Bouygues (F) - Coordinator
- DERA (GB)
- Newlands Technology (GB)
- Johs.Holt (N)
- Joint Research Centre (EU)
- Tech. Universität Dresden (D)
- Université Libre de Bxl (B)
- VSL (F)

Active control in civil engineering (ACE)

Aims of testing campaign at ELSA

- to improve understanding of induced vibrations
- to validate the numerical tools for prediction of cable dynamic behavior
- to verify the capability of the active system to mitigate induced vibrations
- to evaluate performance and reliability of the whole implementation.

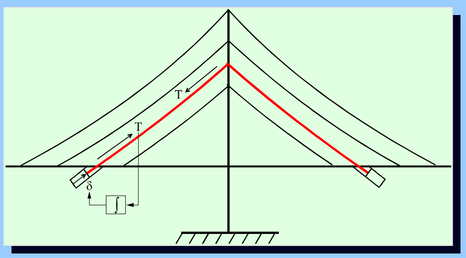

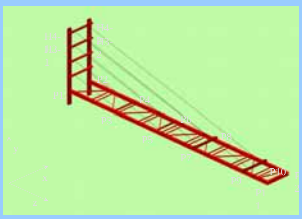

Active control in civil engineering (ACE)

JOINT RESEARCH CENTRE
EUROPEAN COMMISSION

Safety in Structural Mechanics Unit

ELSA - Achievements/Recognition

JOINT RESEARCH CENTRE
EUROPEAN COMMISSION

- Key contributions to Eurocode 8 through Reference tests allowing for approval by national standardization bodies
- Worldwide leading position on Pseudo-dynamic testing of large/full-scale structures.
- Internationally recognized expertise in numerical modeling of civil structures.
- Contribution to the position of the European Research in the International scene (Europeans are today preferential partners)

Safety in Structural Mechanics Unit

ELSA - Achievements/Recognition

JOINT RESEARCH CENTRE
EUROPEAN COMMISSION

- Large-scale Facility (HCM, TMR, IHP)
- Marie Curie Training Site (IHP)
- Research Training Networks (HCM, TMR, IHP)
- 19 SCAs during FP5 (≅ 18% of the total budget)
- More than 140 refereed publications (1999-2001)
- Referees in high-level research evaluation panels (e.g.: NSF-projects/infrastructures)

Safety in Structural Mechanics Unit

Future of EE Research at ELSA

JOINT RESEARCH CENTRE
EUROPEAN COMMISSION

- Eurocodes approval and maintenance (JRC/ELSA and DG ENTR)
- A key role in ERA
  - Training through research
  - Integrated projects
  - Networking of European experimental facilities
- Enlargement
  - Most of Candidate Countries are earthquake sensitive ý Training, Adoption of Eurocodes, Participation in Integrated projects, …

Safety in Structural Mechanics Unit

ELSA – A key role in ERA

JOINT RESEARCH CENTRE
EUROPEAN COMMISSION

- A ‘Reference Training Site’
- Integrated project for Earthquake risk mitigation in Europe (Belgirate, 2000 Workshop recommendations)
- ERA and information technologies (through networking)
  - Provide EE Facilities and Community with advanced platform/s for data storage, documentation and exchange and analytical developments *(essential for perenniality of data and tools)*
  - Enhance experimental techniques and procedures by full exploitation of the electronic communication facilities
  - Establish appropriate collaboration with NSF - NEES (e.g.: JRC the European node of NEESgrid)

Safety in Structural Mechanics Unit

ELSA / Transient Dynamics Research

JOINT RESEARCH CENTRE
EUROPEAN COMMISSION

- **Objective** Citizen protection through validation of the safety of various structural systems under fast transients, such as ***crash, impact, blast*** and ***explosion***
- **Rationale** Structural safety under fast transients (including biomechanical aspects) is a major concern of the modern society since it concerns:

  industry and energy production infrastructures; automotive, aeronautical and water transportation systems, civil structures under accidental or perpetrated attacks, etc.
- **Underlying physical principles** Under severe dynamic conditions, materials and structures exhibit very specific behaviour (*strain rate effect, fluid-structure interaction*)

Safety in Structural Mechanics Unit

ELSA / Transient Dynamics Research

JOINT RESEARCH CENTRE
EUROPEAN COMMISSION

- Existence of the unique experimental facility **LDTF** (impact testing)
- FEM simulation code **EUROPLEXUS** (jointly developed with CEA)

validated code simulations via precision impact testing

⬇

- Long experience and numerous collaborations with EU research institutions (CEA, FZK, FRAMATOME, MPA, EDF, SIEMENS, ENEA, ENSA, ENEL, SNECMA, CRF…)
- Small but high-yield group, well recognized in Europe and internationally

Safety in Structural Mechanics Unit

Transient Dynamics Activity Areas

JOINT RESEARCH CENTRE
EUROPEAN COMMISSION

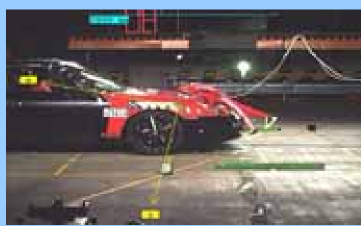

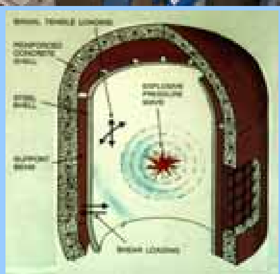

Safety in Structural Mechanics Unit

Transient Dynamics Activity Areas (origin)

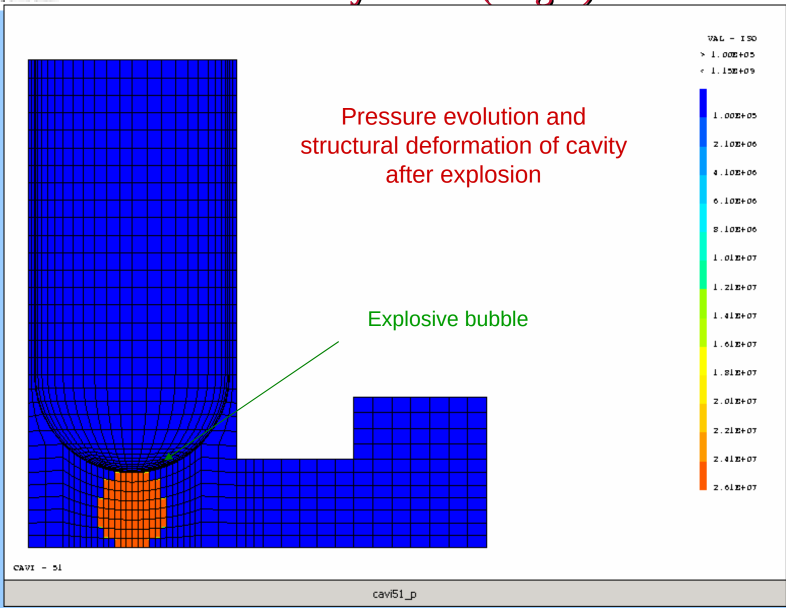

Safety in Structural Mechanics Unit

Principle of LDTF Installation

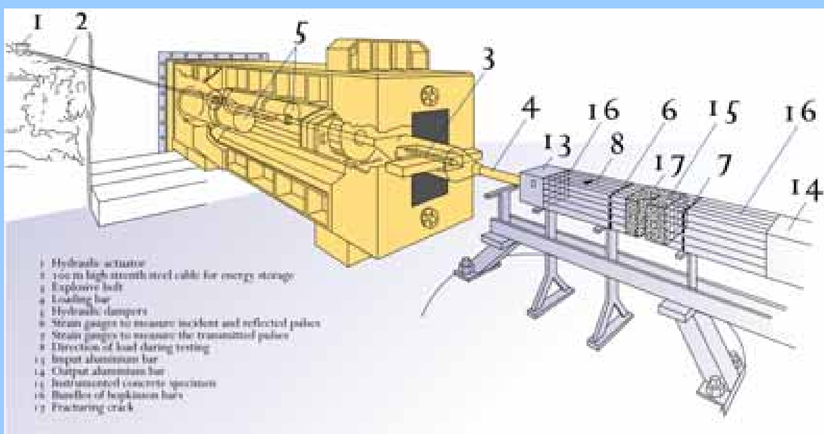

Large Dynamic Test Facility (LDTF)

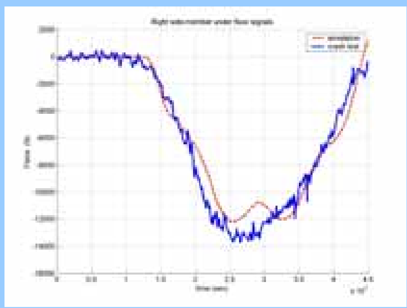

force transmitted to the right side-member under floor

Role and contribution / Prospects

- Independent expertise in support of the Commission policies (DG ENTR):
  - directives EC 96/27 and 96/79 on crashworthiness of vehicles
  - standards EN1317 1,2 on road safety barriers (CEN/TC226)
  - ongoing normative action on pedestrian safety
  - concrete and anchors construction standards
- European networking of users for EUROPLEXUS code (collaboration with CEA and SAMTECH)
- Reference measurements in crash / impact testing and modeling techniques; materials dynamic characterization
- Suitable to play a leading role in ERA/FP6; training and networking with European impact laboratories

Safety in Structural Mechanics Unit

Appendix 8

Section 8　Smart Structural System Large Scale Shaking Test

presented by M.Teshigawara

Smart Structural System

Large Scale Shaking Test

1. Introduction
2. Objectives
3. Specimen
4. Shaking Tests
5. Summary

Masaomi Teshigawara

Dept. of Structural Engineering Chief Research Engineer

Building Research Institute

What is S.S.S.?

1. Function of Sensing、Processing、Actuating
2. Auto Adaptive to Provide Safety and Function Effectively

1. Improvement of Structural Performance
2. Performance Based Maintenance and Sustainable Structure

Building Research Institute

Objectives of Large Scale Shaking Test

- Verification of Structural Control
  - Rocking system
  - Semi-Active Base Isolation System with M/R Damper
  - Semi-Active Structural Control with M/R Damper

- Verification of Smart Sensors and Damage Identification
  - System Identification for Damage detection
  - Smart sensors

BUILDING RESEARCH INSTITUTE

Shakeing Table and Schedule

- **Shaking Table**
  - National Research Institute for Earth Science and Disaster Prevention (NIED), Science and Technology Agency, Tsukuba, Japan

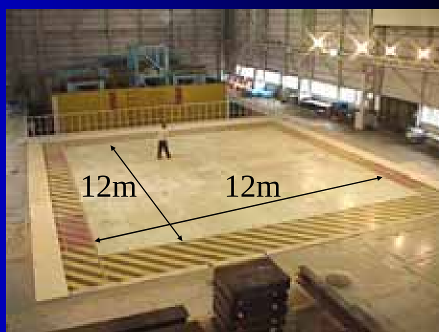

Schedule

February-April, 2002
July-August, 2002 (if necessary)

BUILDING RESEARCH INSTITUTE

Frame

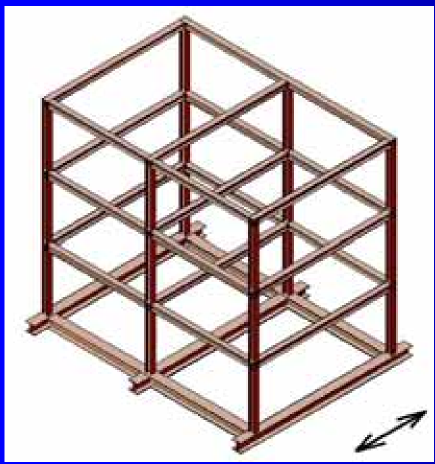

Shaking

- **Members**
  - C：H148✕100✕6✕9
  - B：H150✕150✕7✕10
- **Mass**
  - W3=4.65(t)
  - W2=4.76(t)
  - W1=4.76(t)
- **Span**
  - 3m✕1span (Loading Di.)
  - 2m✕2spans (Trans. Di.)
- **Story Height**
  - 1.8(m) each story
- **Natural Period**
  - 0.490(s)
- **Elastic Limit**
  - Story Drift=26.9(mm)
  - Base Shear=111.7 (kN)

Building Research Institute

Test Specimen

Appearance Photo of Test Specimen

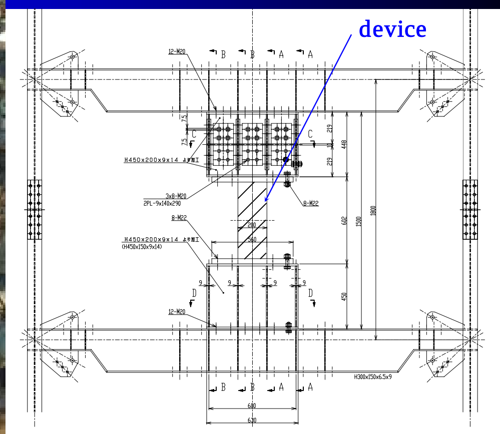

Installation Figure of Damage Device

Building Research Institute

Column for Damage

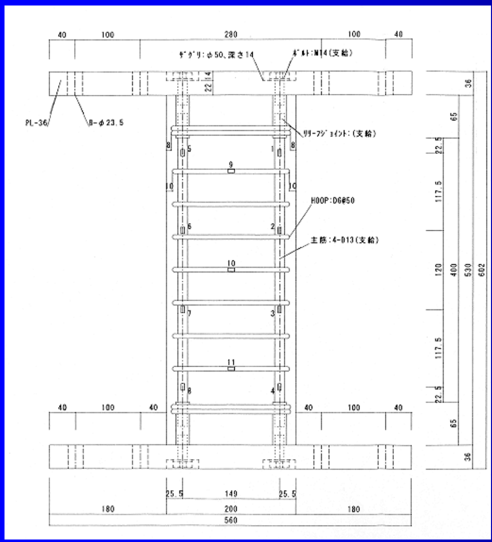

Size of Cross Section	100×200(mm)
Height	400(mm)
Specified Design Strength	50(N/mm2)
Main Reinforcement	4−D13 (SD245)
HOOP	□−D6@50
Material of Cement System	Polyethylene Fiber + Steel Cord

Building Research Institute

Measurement of load

- Q (RC Column) =Q (Total) −Q (Frame)
- Shear force of Frame from strain of steel columns

  → Calibration test of simple beam

- Verification by shaking Test

  → Shaking test of Open Frame

Building Research Institute

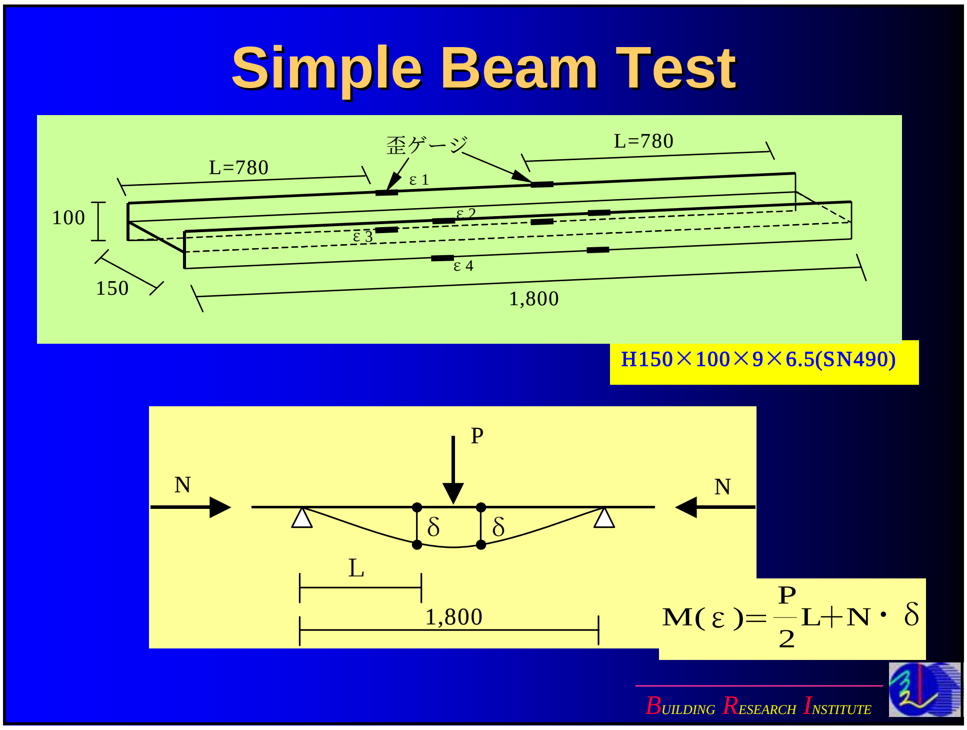
Simple Beam Test
歪ゲージ
L=780
L=780
ε1
ε2
ε3
ε4
100
150
1,800
H150×100×9×6.5(SN490)
P
N
N
δ
δ
L
1,800
M(ε)=P/2 L+N・δ
Building Research Institute

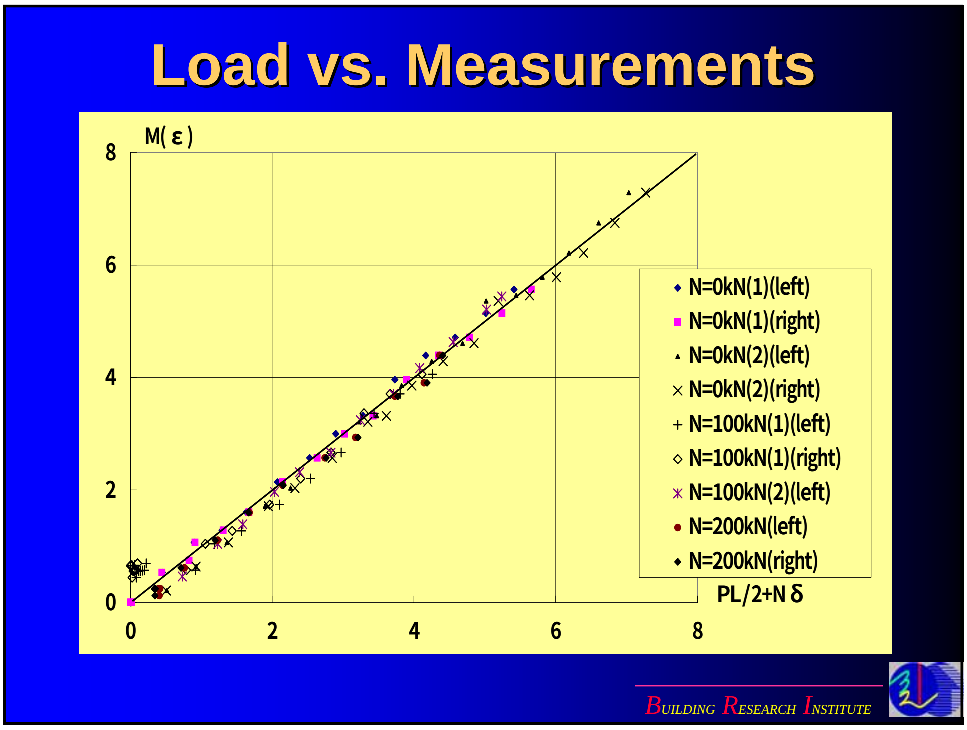
Load vs. Measurements
M(ε)
8
6
4
2
0
0
2
4
6
8
PL/2+Nδ
N=0kN(1)(left)
N=0kN(1)(right)
N=0kN(2)(left)
N=0kN(2)(right)
N=100kN(1)(left)
N=100kN(1)(right)
N=100kN(2)(left)
N=200kN(left)
N=200kN(right)
Building Research Institute

Results from Open Frame Test

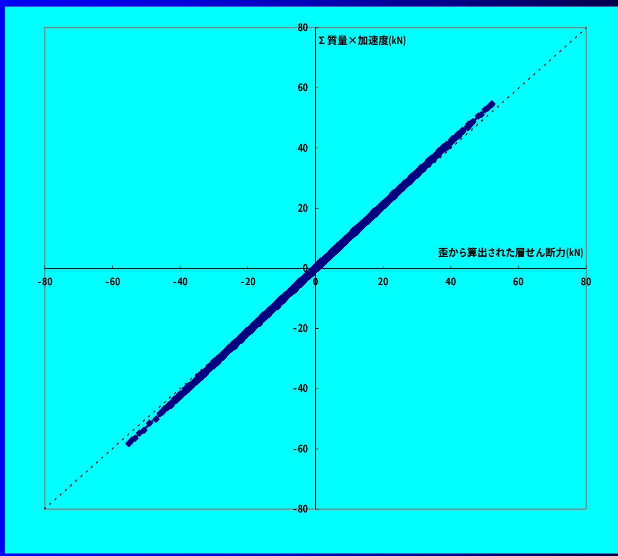

BUILDING RESEARCH INSTITUTE

Damage Detection

Input Motion

No.	Input wave	Target Level
1	BCJ wave	2.5cm/sec
2	El Centro 1940 NS	5cm/sec
3	El Centro 1940 NS	10cm/sec
4	El Centro 1940 NS	15cm/sec
5	BCJ wave	20cm/sec
6	El Centro 1940 NS	30cm/sec
7	El Centro 1940 NS	40cm/sec
8	El Centro 1940 NS	50cm/sec
9	El Centro 1940 NS	60cm/sec

BUILDING RESEARCH INSTITUTE

Instrumentation

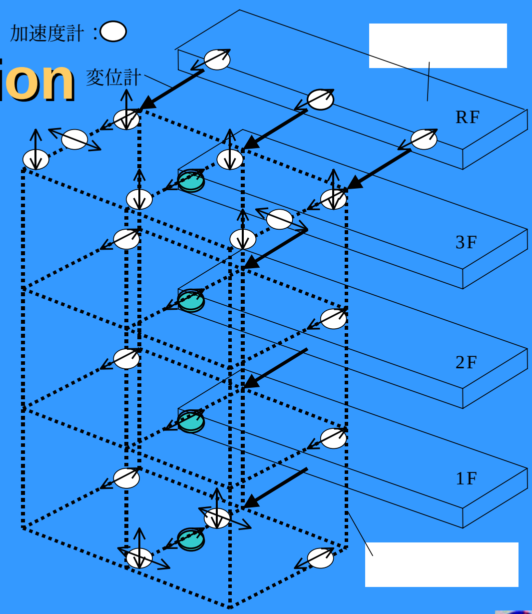

BUILDING RESEARCH INSTITUTE

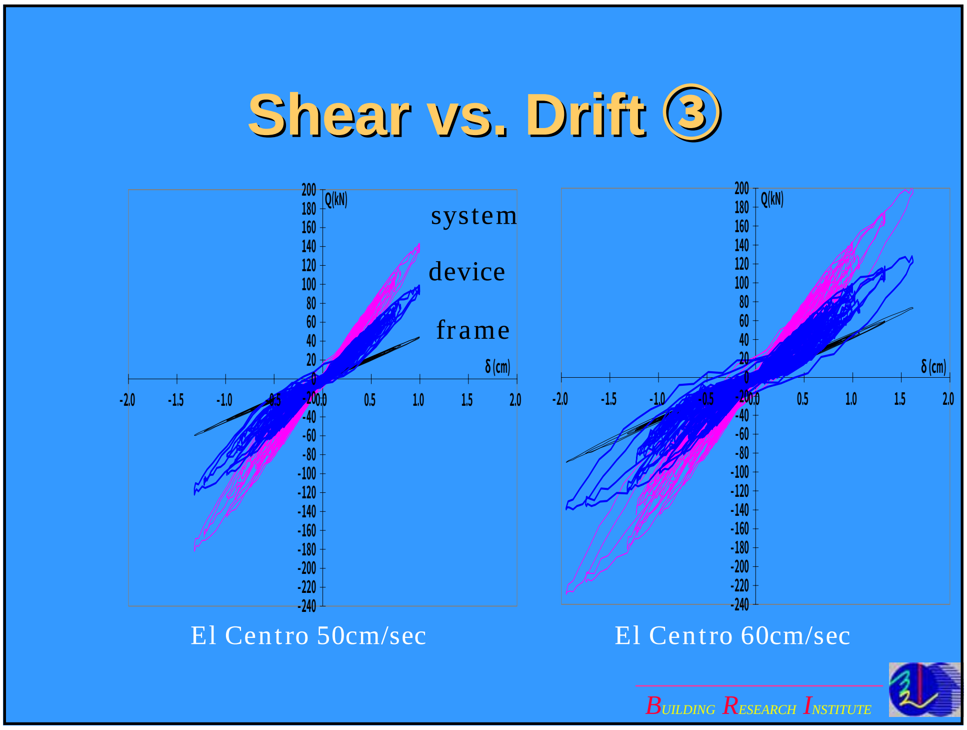
Shear vs. Drift ③
Q(kN)
system
device
frame
δ(cm)
El Centro 50cm/sec
El Centro 60cm/sec
Building Research Institute

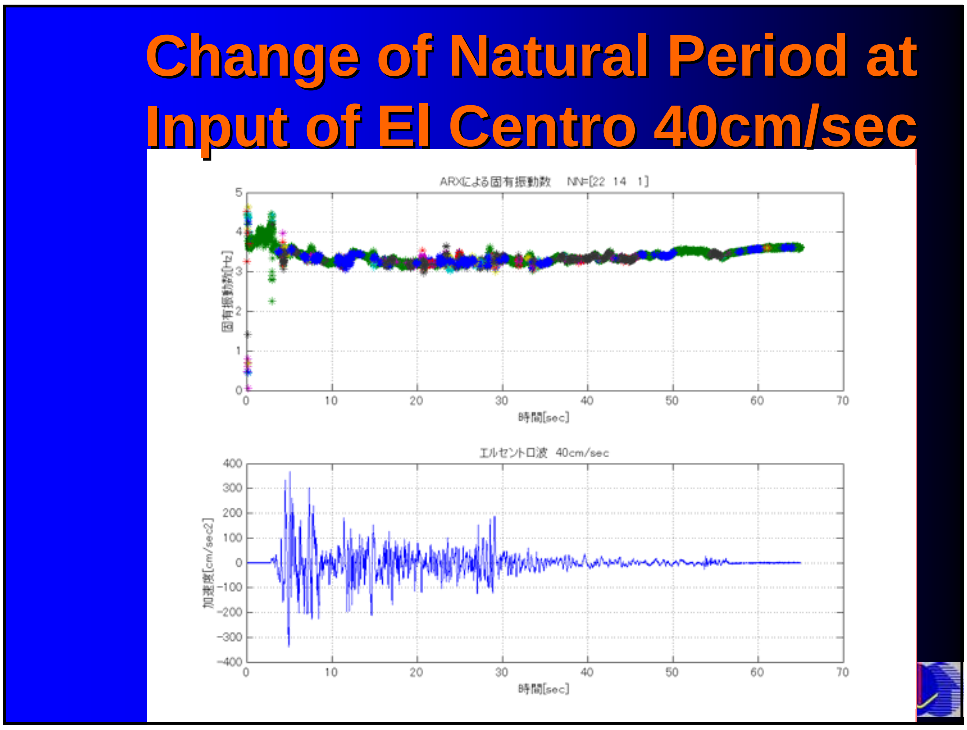
Change of Natural Period at Input of El Centro 40cm/sec
ARXによる固有振動数 NN=[22 14 1]
固有振動数[Hz]
時間[sec]
エルセントロ波 40cm/sec
加速度[cm/sec2]
時間[sec]

Change of Damping Coefficient at Input of El Centro 40cm/sec

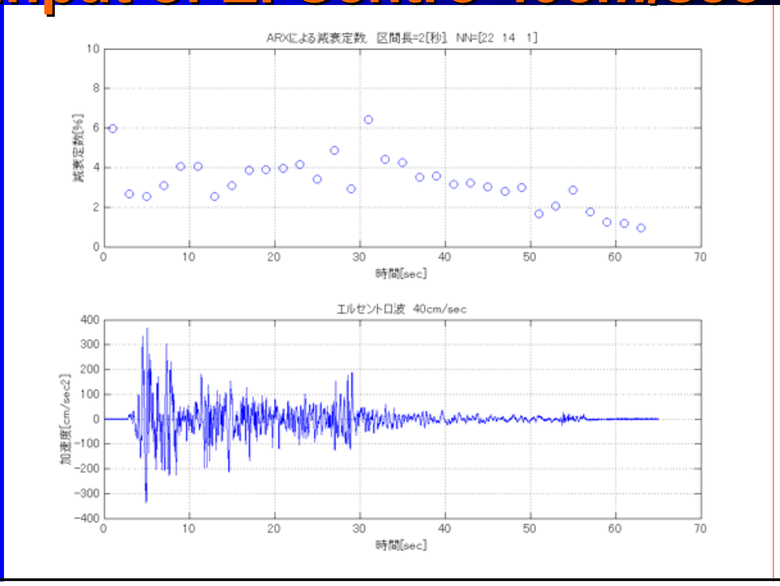

Change of Transfer Function due to Damage

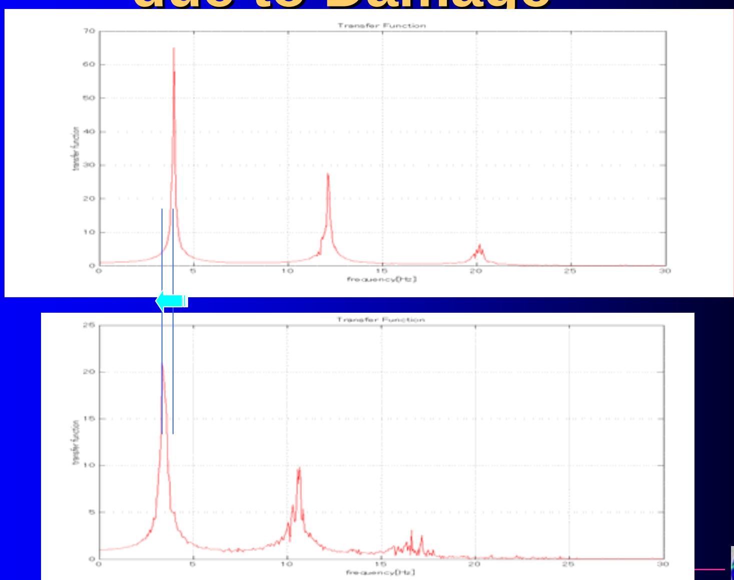

BUILDING RESEARCH INSTITUTE

Damage Identification by Flexibility Method (after El Centro 40cm/sec)

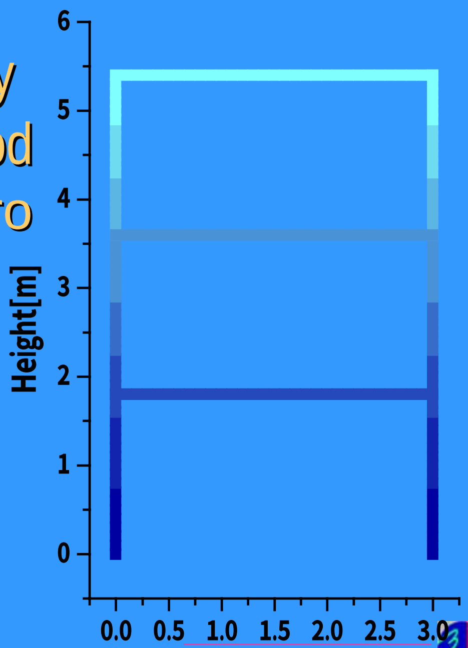

Dark color indicates damage parts

BUILDING RESEARCH INSTITUTE

Structural Control by M/R Damper

BUILDING RESEARCH INSTITUTE

Design of Magneto-Rheological damper

Structure

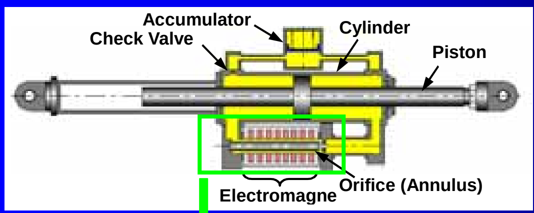

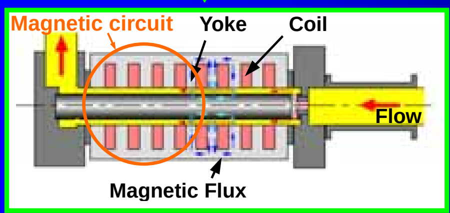

Design Specifications

Max.Force		40kN
Stroke		±295mm
Cylinder Bore		φ90mm
Orifice	Section	Outer diameter φ48mm
		Gap 3.0mm
	Length	420mm
Electromagnet	Inductance	37.4mH×3
	Resistance	12Ω×3
	Max.Current	3A
MR fluid		Bando: #230

Conceptualism of MR fluid

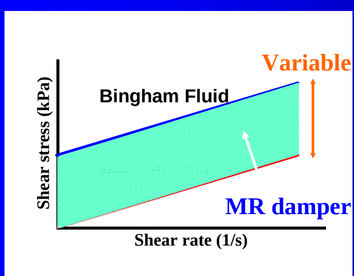

[Characteristic of Bingham Fluid]

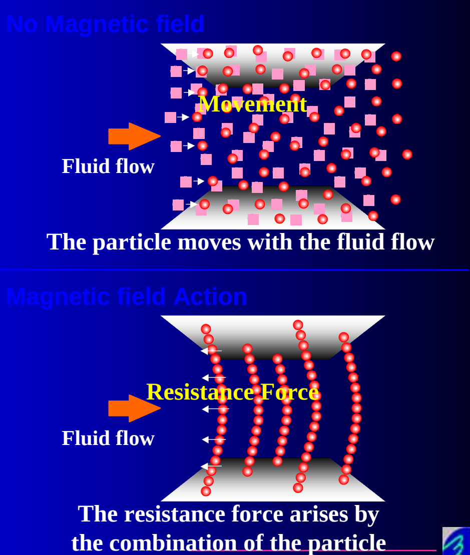

Building Research Institute

Experimental Setup for MR damper

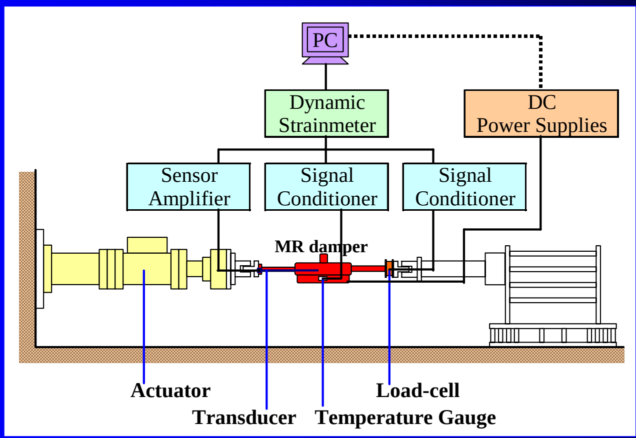

Dynamic loading test

Building Research Institute

Dynamic loading test (Sinusoidal wave)

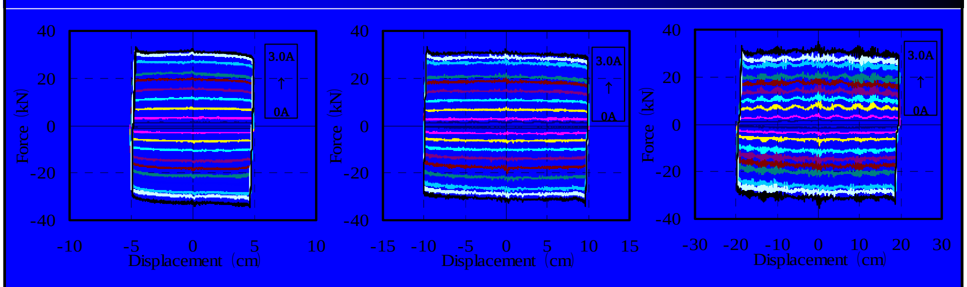

0.1Hz, 5cm, 3.14cm/s   0.1Hz, 10cm, 6.28cm/s   0.1Hz, 20cm, 12.56cm/s

Experimental Results

Building Research Institute

Force – Piston velocity Relationship

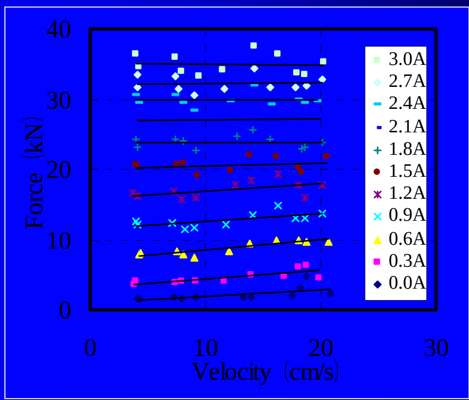

BUILDING RESEARCH INSTITUTE

Control algorithm

$$F = \begin{cases} \mathrm{sgn}(\dot{u})k\left(\sqrt{\left(\dfrac{\lambda_{opt}\dot{u}}{\omega}\right)^2 + u^2} - |u|\right) & (u\dot{u} \geq 0) \\ k\dfrac{\lambda_{opt}\dot{u}}{\omega} & (u\dot{u} < 0) \end{cases}$$

F :MRダンパーの制御力
k :免震層の剛性
$u,\dot{u}$:免震層の変位,速度
$\mathrm{sgn}(\dot{u})$:免震層速度の符号
ω ：免震構造物を１質点とした場合の円振動数
λ_{opt} :制御定数(今回は 0.7)

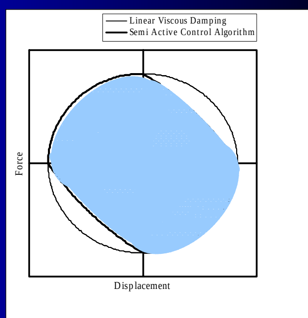

制御の履歴ループ

BUILDING RESEARCH INSTITUTE

Control system

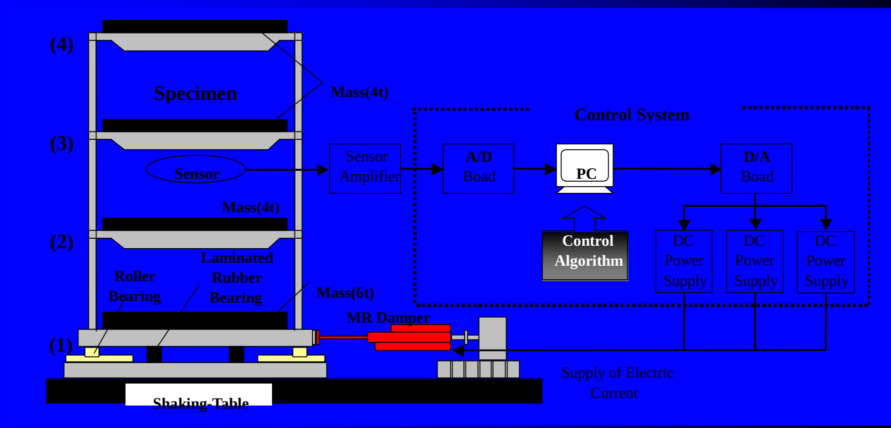

Outline of base-isolated test frame

Input Wave

- Sweep sinusoidal wave
- White noise
- Elcentro (1940) NS
- Hachinohe (1968) NS
- JMA Kobe (1995) NS
- Taft (1952) EW

} 50cm/s

↑ base-isolated test frame

Parameters test frame →

Member	Column	H150×100×6×9
	Beam	H150×150×7×10 (H300×150×6.5×9)
Material		SM490
Mass (ton)	3rd story	4.67
	2nd story	4.78
	1st story	4.78
	Base isolated layer	5.87
Stiffness (kN/cm)	3rd story	27.60
	2nd story	28.42
	1st story	35.37

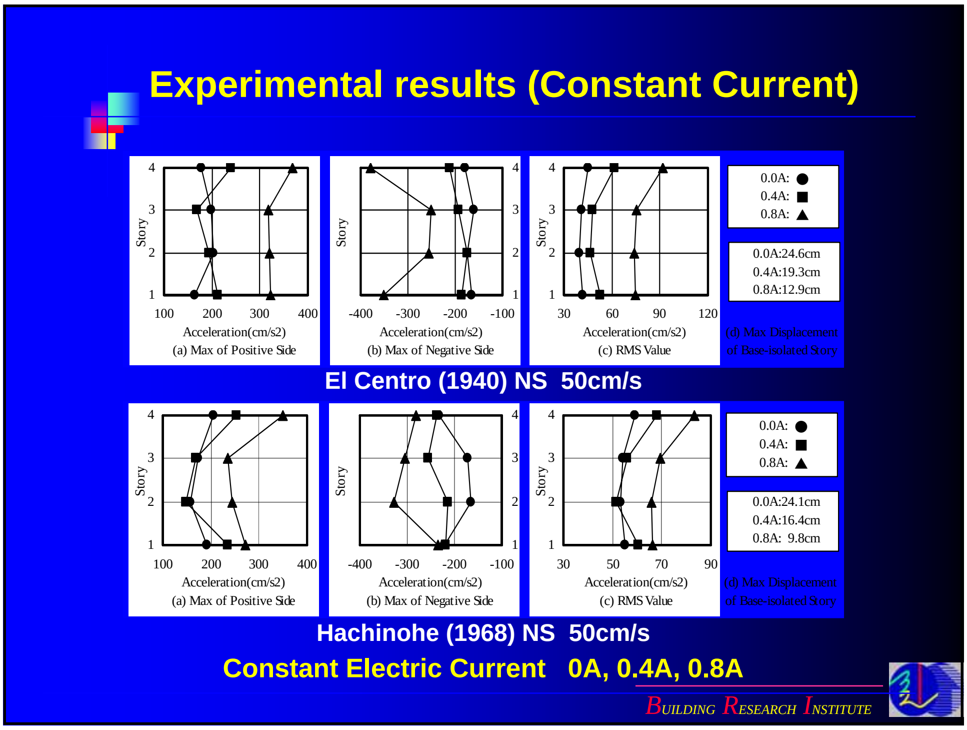
Experimental results (Constant Current)
Story
Acceleration(cm/s2)
(a) Max of Positive Side
(b) Max of Negative Side
(c) RMS Value
0.0A: ●
0.4A: ■
0.8A: ▲
0.0A:24.6cm
0.4A:19.3cm
0.8A:12.9cm
(d) Max Displacement of Base-isolated Story
El Centro (1940) NS 50cm/s
0.0A:24.1cm
0.4A:16.4cm
0.8A: 9.8cm
Hachinohe (1968) NS 50cm/s
Constant Electric Current 0A, 0.4A, 0.8A
BUILDING RESEARCH INSTITUTE

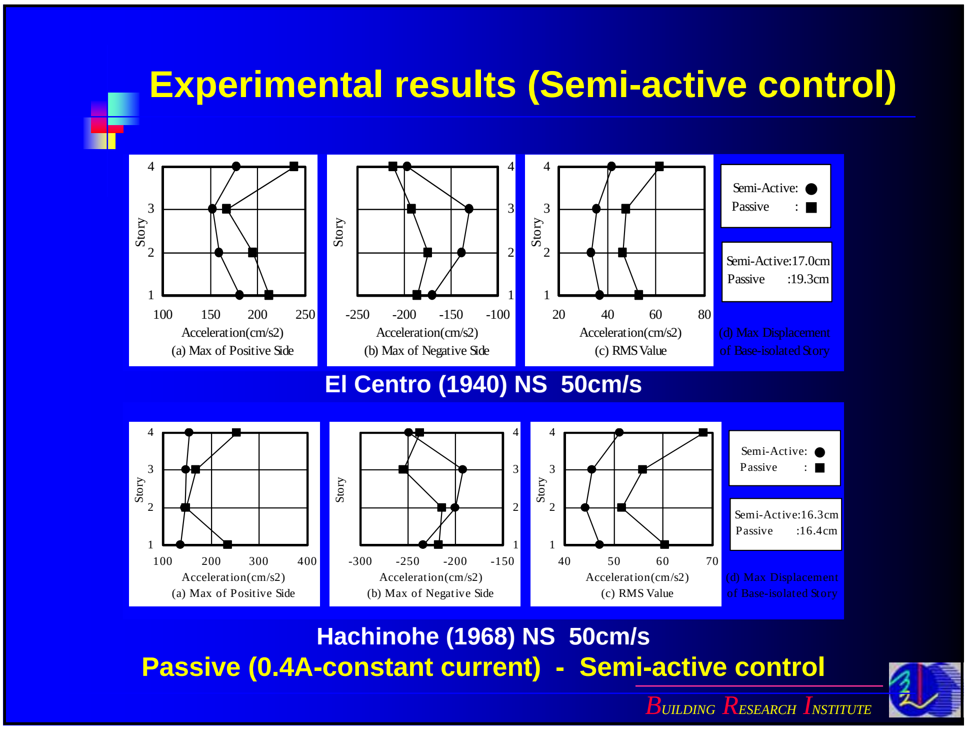
Experimental results (Semi-active control)
Story
Acceleration(cm/s2)
(a) Max of Positive Side
(b) Max of Negative Side
(c) RMS Value
Semi-Active: ●
Passive : ■
Semi-Active:17.0cm
Passive :19.3cm
(d) Max Displacement of Base-isolated Story
El Centro (1940) NS 50cm/s
Semi-Active:16.3cm
Passive :16.4cm
Hachinohe (1968) NS 50cm/s
Passive (0.4A-constant current) - Semi-active control
BUILDING RESEARCH INSTITUTE

Rocking System with Base Plate Yielding Type

System Concept

- Up-Lift with yielding of base plate before yielding of super structure

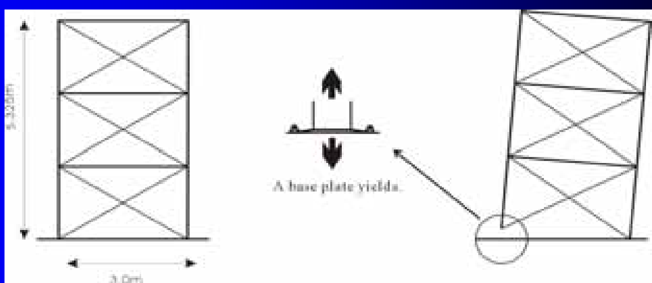

Test Specimen

- Height：5.325 m（1.725 m + 1.8 m + 1.8 m）
- Span：3.0 m
- Aspect ratio：1.775

（PC-bar Brace are installed）

Building Research Institute

Base Plate

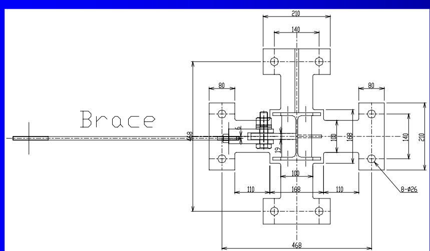

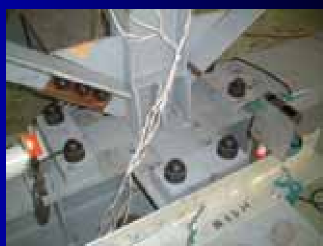

PL-6mm & 9mm。2 & 4 fins for PL-9mm

Model name	JIS	Yield Point (N/mm2)
BP6	SS400	329.85
BP9, BP9-2	SS400	292.11

Building Research Institute

Input Motion

- 1940 El Centro NS,
- Time interval is reduced by $1/\sqrt{2}$

Building Research Institute

Test Result（1）

- Up-Lift Deformation

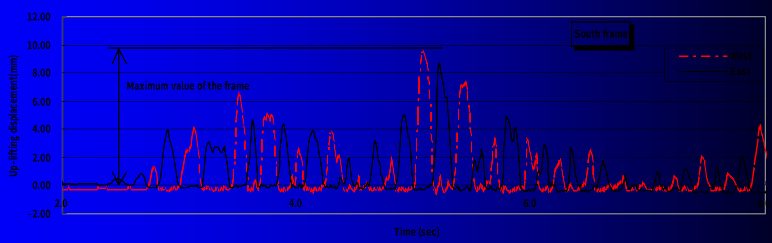

BP-2 model、MPA=5.84 m/sec^2

Building Research Institute

Test Result (2)

- Base Shear & Up-Lift Deformation

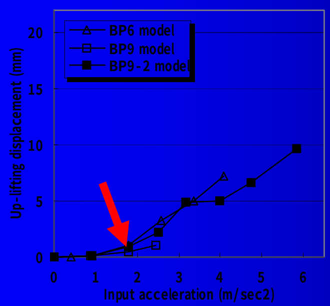

Up-Lift

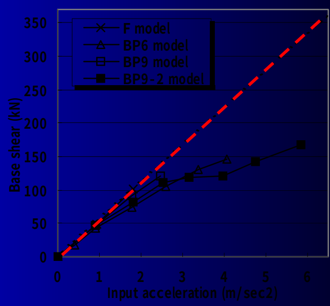

Base Shear

BUILDING RESEARCH INSTITUTE

Test Result (3)

- Up-Lift & Top Deformation

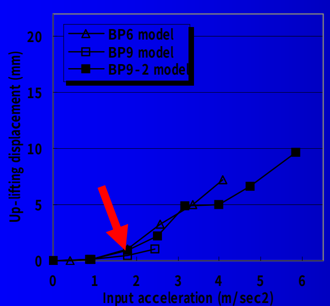

Up-Lift

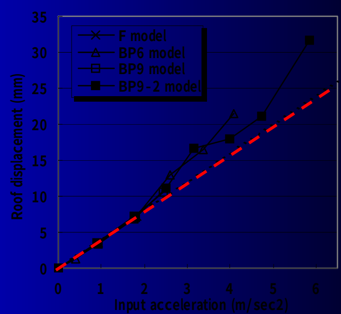

Top

BUILDING RESEARCH INSTITUTE

Test Result (4)

- Story Shear

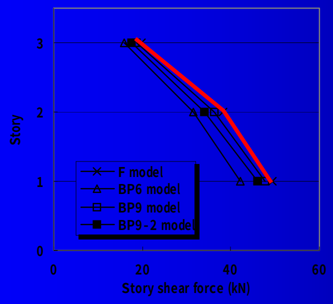

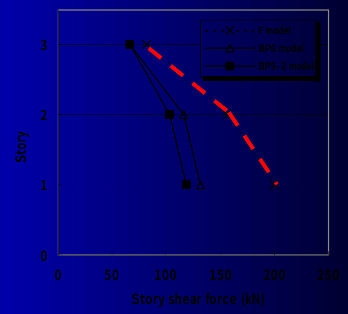

MPA=0.9 m/sec^2 MPA=3.5 m/sec^2

BUILDING RESEARCH INSTITUTE

Reference

- 2001.5.16〜6.28
- Aspect Ratio 2.5

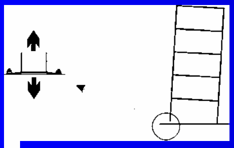

(a) Base plate yielding system

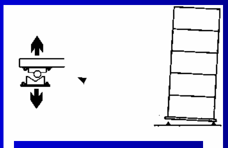

(b) Simple rocking system

BUILDING RESEARCH INSTITUTE

Appendix 9

Section 9 *Safety Assessment for Earthquake Risk Reduction: An EU Research and Training Network*

presented by F. Taucer

Safety Assessment for Earthquake Risk Reduction: An EU Research and Training Network

Mid-Term Review Meeting
24 May 2002, JRC Ispra

Overview

SAFERR

Reduction of Seismic Risk

Background | PREC8 | ICONS | SAFERR | Closure

Aims:

To mitigate seismic risk through European collaboration for:

- Training of young researchers Furthering research and development of innovative concepts
- Integration of earthquake geophysics, structural engineering, engineering seismology and geotechnical engineering
- Increasing awareness through outreach activities, training and education
- Introducing appropriate seismic provisions in traditional design and construction practices

Means:

- Research and training networks funded by the EC and national agencies
- Establishment of a permanent core European research and development group with experience in research and networking

SAFERR

International Efforts

Background PREC8 ICONS SAFERR Closure

Centralised earthquake risk mitigation networks

USA

Four centres of excellence in earthquake engineering:

- NCEER, PEER, MAE, MCEER
- Formed by consortia of universities
- Funded by NSF, industry and/or State sources

Japan

Nationally-organised networks in earthquake engineering:

- Topic-specific and of short life-span
- Funded by government
- Recently adopted US model

SAFERR

European Networks Philosophy

Background PREC8 ICONS SAFERR Closure

Topical philosophy:

Holistic approach to choice of research topics

- Consideration of Demand, Supply and their interaction
- Contribution from organisations with required expertise

Managerial philosophy:

Clear framework

- To maintain a balance between research development and training within networks
- Consideration of EC proposal requirements

Foresight and global framework

- To integrate the different networks towards the maintenance of a core European earthquake engineering community

SAFERR

Prenormative Research in Support of Eurocode 8 (PREC8) – Co-ordinators : UPAVIA

Background PREC8 ICONS SAFERR Closure

Aims:

Furthering European earthquake engineering design

- Investigation of weaknesses in the pre-standard for EC8 using both experimental and analytical techniques
- Recommendations for Code revision

Areas of research:

Task 1	Task 2	Task 3	Task 4	Task 5
Seismic Behaviour of RC Frames	Infill Models & Effects on Response	Reinforcing Steel Properties	Seismic Behaviour of RC Bridges	Foundations & Retaining Structures

SAFERR

Participation in PREC8

Background PREC8 ICONS SAFERR Closure

Institution	Responsible Scientist
1. University of Liege (B)	A.Plumier
2. Geodynamique et Structure (F)	A.Pecker
3. GRECO (F)	J.Mazars & J.M.Reynouard
4. Darmstadt University of Technology (D)	J.Woerner
5. University of Patras (GR)	M.N.Fardis
6. University of Basilicata (I)	M.Dolce
7. Politecnico di Milano (I)	E.Faccioli
8. Universita di Pavia (I) - Co-ordinator	G.M.Calvi
9. Universita di Roma "La Sapienza" (I)	P.E.Pinto
10. Universidad Politecnica de Madrid (E)	E.Alarcon
11. Imperial College (UK)	A.S.Elnashai
ECOEST I	
1. National Technical University of Athens (GR)	G.Gazetas & P.Carydis
2. ISMES, Bergamo (I)	M.Casirati
3. Joint Research Centre, Ispra (I)	A.V.Pinto
4. National Laboratory of Civil Engineering, Lisbon (PT)	E.C.Carvalho
5. University of Bristol (UK)	R.Severn

SAFERR

Deliverables of PREC8

Background PREC8 ICONS SAFERR Closure

Title	Editor
Vol. 1: Standardisation of shaking tables	A.Crewe
Vol. 2: Seismic behaviour and design of foundations and retaining structures	E.Faccioli , R.Paolucci
Vol. 3: Large scale shaking tests of geotechnical structures	R.Severn , C.Taylor
Vol. 4: Experimental and numerical investigations on the seismic response of bridges and recommendations for code provisions	G.M.Calvi , P.E.Pinto
Vol. 5: Pseudo-dynamic and shaking table tests on RC bridges	
Vol. 6: Experimental and numerical investigations on the seismic response of RC infilled frames and recommendations for code provisions	A.V.Pinto M.N.Fardis
Vol. 7: Numerical investigations on the seismic response of RC frames designed in accordance with Eurocode 8	E.Carvalho , E.Coelho
Vol. 8: Shaking table tests of RC frames	
Vol. 9: European activities for the development of Eurocode 8	P.Carydis, T.Severn, G.M.Calvi

SAFERR

Innovative Concepts in Seismic Design of New and Existing Structures (ICONS) - JRC

Background PREC8 ICONS SAFERR Closure

Aims:

- Advancement of existing knowledge and development of innovative techniques in earthquake engineering
- Provide a framework for training young researchers

Research topics and participants:

Task 1	Task 2	Task 3	Task 4	Task 5
Seismic Action	Assessment, Repair & Strengthening	Innovative Design Concepts	Composite Structures	Shear-wall Structures
GDS, POLIMI, UPAVIA, ICSTM	ULIEGE, GEO,TUD, UPATRAS,UPAVIA, UROMA, UMADRID, ICSTM	UPATRAS, GDS, POLIMI UPAVIA, GEO, UROMA	ULIEGE, TUD, UMADRID, ICSTM	GEO, UPATRAS, UROMA

ECOEST II – (LNEC, NTUA, JRC, ISMES, CEA, UBRISTOL)

SAFERR

Large-Scale Testing – Walls and Dual Frame

Background PREC8 ICONS SAFERR Closure

↑ Shake table tests on selectively repaired walls (LNEC)

→ PSD tests on dual frame-shear wall RC structure (JRC)

SAFERR

ICONS - Achievements

Background PREC8 ICONS SAFERR Closure

- Technical developments
  - Displacement-based design and assessment methodologies
  - Displacement demand spectra
  - Selective repair techniques, guidelines for composite structures
- High quality training of young researchers
  - More than 50 YRs appointed for a total of 427 training-months
  - Exchange of researchers between institutions
  - YRs participation in 11th ECEE and 12th WCEE
- Publications
  - More than 40 publications, including scientific reports, journal and conference papers
  - Report series published jointly with ECOEST II
- Industrial interest
  - Awareness of earthquake risk-related problems raised
  - Industrial involvement in experimental programme

SAFERR

ICONS - Publications

Background | PREC8 | **ICONS** | SAFERR | Closure

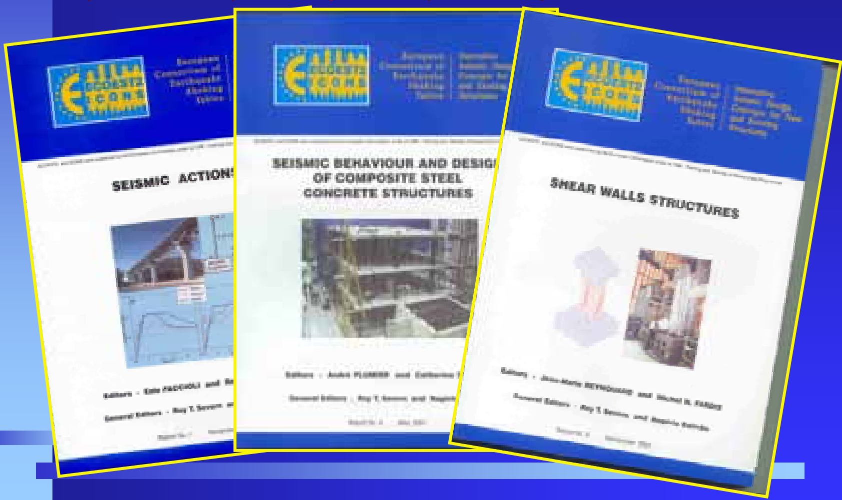

SAFERR

Safety Assessment for Earthquake Risk Reduction (SAFERR) – Coordinators ICSTM

Background | PREC8 | ICONS | **SAFERR** | Closure

Aim:

- Advancement, application & dissemination of seismic risk mitigation measures
- Combination of research with technical training of YRs
  - → Specialist equipment training
  - → Development of communication and management skills

Features:

- Greater participation
- Ambitious scope of research

SAFERR

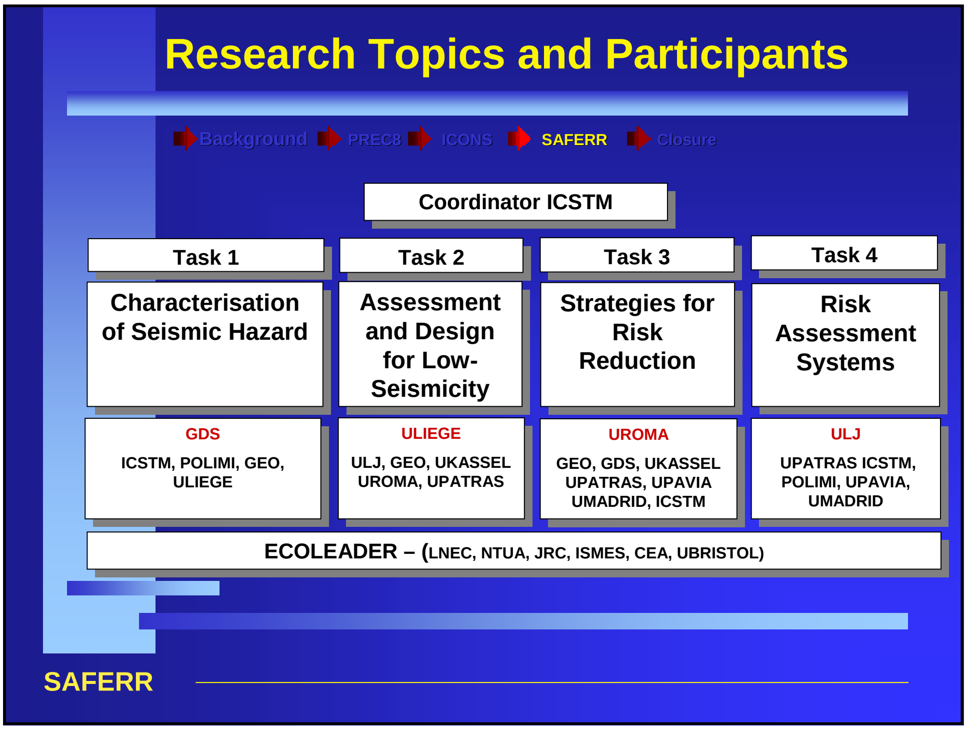
Research Topics and Participants
Background
PREC8
ICONS
SAFERR
Closure
Coordinator ICSTM
Task 1
Characterisation of Seismic Hazard
GDS
ICSTM, POLIMI, GEO, ULIEGE
Task 2
Assessment and Design for Low-Seismicity
ULIEGE
ULJ, GEO, UKASSEL UROMA, UPATRAS
Task 3
Strategies for Risk Reduction
UROMA
GEO, GDS, UKASSEL UPATRAS, UPAVIA UMADRID, ICSTM
Task 4
Risk Assessment Systems
ULJ
UPATRAS ICSTM, POLIMI, UPAVIA, UMADRID
ECOLEADER – (LNEC, NTUA, JRC, ISMES, CEA, UBRISTOL)
SAFERR


Partners
Background
PREC8
ICONS
SAFERR
Closure
SAFERR

Training of Young Researchers

Background PREC8 ICONS SAFERR Closure

Partner	Pre-Doc	Post-Doc	Total	To Date
1. ICSTM	26	4	30	20
2. POLIMI	24	3	27	17
3. LNEC	18	8	26	15
4. JRC	18	4	22	12
5. UROMA	24	12	36	24
6. UPATRAS	17	11	28	17
7. UPAVIA	20	10	30	18
8. GEO	0	24	24	16
9. UMADRID	25	3	28	12
10. ULIEGE	28	4	32	20
11. UKASSEL	30	0	30	0
12. GDS	19	8	27	15
13. ULJ	21	6	27	23
Total	270	97	367	209

SAFERR

Non-SAFERR Researchers

Background PREC8 ICONS SAFERR Closure

Partner	Other Sources - Contract	Other Sources – To Date	No. of Researchers - Contract	No. of Researchers – To Date
1. ICSTM	36	22	7	8
2. POLIMI	27	12	6	6
3. LNEC	14	5	6	6
4. JRC	14	6	7	4
5. UROMA	46	22	7	7
6. UPATRAS	29	14	5	5
7. UPAVIA	30	5	6	6
8. GEO	18	8	5	5
9. UMADRID	34	15	8	5
10.ULIEGE	14	7	2	2
11.UKASSEL	38	0	7	0
12.GDS	13	4	4	3
13.ULJ	27	25	8	10
Total	340	145	78	67

SAFERR

Training of Young Researchers

Background PREC8 ICONS SAFERR Closure

- Technical training
- Training in communications skills
- Management skills
- Training on specialist equipment
- Training through visits and secondments

SAFERR

Technical Achievements

Background PREC8 ICONS SAFERR Closure

Achievements (T1):

- A simple procedure has been developed to account for vertical earthquake ground motion in seismic design codes. It is under consideration by the EC8 drafting panels and US guidelines committees. (T1 – S2)
- A robust formulation for extending available design spectra from three seconds to ten seconds has been developed and verified. The displacement spectra in the newest draft of EC8 are based on this work. (T1-S3)
- Important advancements on modelling the effect of geological features on the definition of hazard. The work is pioneering and will be further developed to derive simple and accurate methods to account for the effect of surface geology on ground motion and design spectra. (T1-S4)

SAFERR

Technical Achievements

Background PREC8 ICONS **SAFERR** Closure

Achievements (T2):

- Non-seismically designed reinforced concrete and masonry structures have been extensively studied to establish quantitatively unintentional seismic resistance. This will lead to possibly exempting populations of structure in Europe from seismic design and great economies whilst retaining an acceptable level of safety. (T2-S1,2)
- Extensive experimental and analytical work has lead to new and verified guidance on the seismic resistance of large lightly reinforced concrete walls. This has had a direct effect on code provisions in France as well as the EC8 RC design chapters. (T2-S3)

SAFERR

Technical Achievements

Background PREC8 ICONS **SAFERR** Closure

Achievements (T3):

- Isolation-dissipation systems for bridges have been comprehensively assessed leading to new insight into the conditions under which isolation-dissipation may not mitigate the expected damage. This work is most significant to the protection and development of the Pan-European road network. (T3-S1)
- The largest database of experimental observations on non-seismically detailed RC members available worldwide has been assembled. This provides a unique opportunity to accurately assess the seismic resistance of RC buildings not designed for seismic loading, which constitutes the majority of structures in Europe. (T3-S2)
- Novel analytical approaches have been developed to model repaired structures while taking into account the existing damage state and the specific behaviour of new repair member/material response, such as FRP and added RC walls. These developments lead to quantitatively-supported decisions on repair and strengthening of the existing built infrastructure. (T3-S3)

SAFERR

Technical Achievements

Achievements (T3):

- Detailed modelling and analysis of a number of flat stab RC structures lead to the quantification of the level of seismic resistance of this important structural form. Noting that flat slab structures are widespread and are indeed the preferred form in many southern European countries, this is a most significant development. (T3-S4)
- Studies on long and short bridges subjected to coherent and incoherent motion have broken new ground and have yielded valuable information on the risk level to which these structures are subjected. Guidance on the additional risk to which bridges are subjected on short span (high speed train-type) has been derived. (T3-S5)
- Advances have been achieved in understanding the dynamic behaviour of inclined piles and pile groups. The extensive analytical results, obtained at this level of detail for the first time, are being simplified to arrive at code-type design expressions taking into account the inelastic structure and soil behaviour, as well as interaction effects. (T3-S6)

Technical Achievements

Achievements (T4):

- A new method of mapping seismic risk using displacements has been developed, using a dual probabilistic-deterministic approach for intermediate and long periods. This is of great significance for the derivation of European hazard maps applicable to deformation-based seismic design. (T4-S1)
- Major advances in characterising fragility of RC buildings based on a very large observational database and experiments on full-scale structures have been made. Also, analytical fragility relationships for bridges have been derived. This allows the assessment of seismic damage before and after earthquakes and aid in decision-making and disaster mitigation planning. (T4-S2)
- A recently-developed integration procedure for hazard and vulnerability is being implemented and applied to a number of cities in Greece, including advanced fragility formulations and hazard definition. The potential significance of this work lies in its ability to make direct use of dynamic demand prediction whilst retaining practical applicability. (T4-S3)

Publications

Background PREC8 ICONS SAFERR Closure

- Six papers authored by researchers from more than one SAFERR partner institution
- Thirteen papers from SAFERR work authored by researchers from one SFAERR partner institution
- Plans for ten papers in journals and international conferences from SAFERR work

SAFERR

Dissemination and Publicity

Background PREC8 ICONS SAFERR Closure

- Publications – Papers and Reports
- Web Sites – SAFERR and Partners'
- Industrial Contacts
- International Contacts

SAFERR

International Collaboration

Background | PREC8 | ICONS | SAFERR | Closure

- Joint MSc and PhD programmes for YRs with a number of international institutions
- Joint Workshop with MAE and GNDT – 23 May 2002
- Joint Coordination Group and Web Site
- Joint Research and Development
- Joint Conference in June 2003 – Erice, Italy
- Workshop with Japanese Researchers, May 2002

SAFERR

Closure

Background | PREC8 | ICONS | SAFERR | Closure

- A coherent group of researchers with long experience and track record in seismic risk assessment and mitigation
- Established a system for delivery of both high quality training of young researchers and significant technical advancements towards earthquake risk reduction
- Training undertaken on a wide range of transferable skills in a multi-disciplinary environment combining engineering seismology, geotechnical and earthquake structural engineering
- SAFERR expertise recognised by European industry and academia

SAFERR

Appendix 10

Section 10 *Seismic Performance Assessment & Rehabilitation: SPEAR*

presented by F. Taucer

European Laboratory for Structural Assessment (ELSA)

JOINT RESEARCH CENTRE
EUROPEAN COMMISSION

Seismic Performance Assessment & Rehabilitation: SPEAR

Competitive and Sustainable Growth (Growth 2001, dedicated call)

Contract G6RD-CT-2001-00525

P. Negro
Joint Research Centre, Ispra, Italy

WORKING MEETING WITH DG ENTR UNIT G5

European Laboratory for Structural Assessment (ELSA)

JOINT RESEARCH CENTRE
EUROPEAN COMMISSION

The history

- Collaboration agreements were established with Japanese and US research organizations.
- The problem of the seismic assessment and rehabilitation of existing buildings was jointly identified as the most socially and economically relevant.
- An Expression of Interest was submitted to the Programme Growth.
- The EoI was selected as deserving specific research work. A dedicated Growth call was issued.
- The proposal prepared by the SPEAR consortium was selected for funding among other proposals.

Facts

- Earthquakes pose a large threat to the life and property in Europe. Average annual casualties due to earthquakes in the EU and candidate stated exceeds 20,000. Direct economic losses in Izmit (TR) were estimated as 20 billion Euro, and in Athens 2 billion Euro.
- Casualties and losses are mainly due to deficient R/C buildings, and, to a lesser extent, to old URM buildings.
- The same problem is being addressed in other countries. Research efforts have been or are being undertaken. A harmonized approach should possibly be sought.
- A method for the identification of hazardous buildings and their cost-effective seismic upgrading should be developed. The work will contribute to the revision of EC8 Part 1-4, during its conversion from ENV to EV by 2003.

The consortium

- University of Patras (Administrative coordination) (GR)
- JRC (Scientific and technical coordination)
- LNEC (P)
- University of Rome (I)
- University of Pavia (I)
- Imperial College (UK)
- University of Ljubljana (SL)
- EQE Europe (UK)

The overseas partners

- Building Research Institute, Ministry of Construction, Japan.
- University of Tokyo.
- The three US Earthquake Engineering Research Centres funded by NSF:
MAE, MCEER, PEER.
- Earthquake Engineering Research Centre, University of Ankara, Turkey.

Workpackages

- WP1: Conceptual framework and background of seismic assessment and rehabilitation
- WP2: Practical seismic assessment and rehabilitation
- WP3: Tests of RC members and small structures
- WP4: PsD testing of large RC structure
- WP5: Proposals for seismic assessment and rehabilitation
- WP6: International cooperation
- WP7: Project management

JOINT RESEARCH CENTRE
EUROPEAN COMMISSION

Workplan

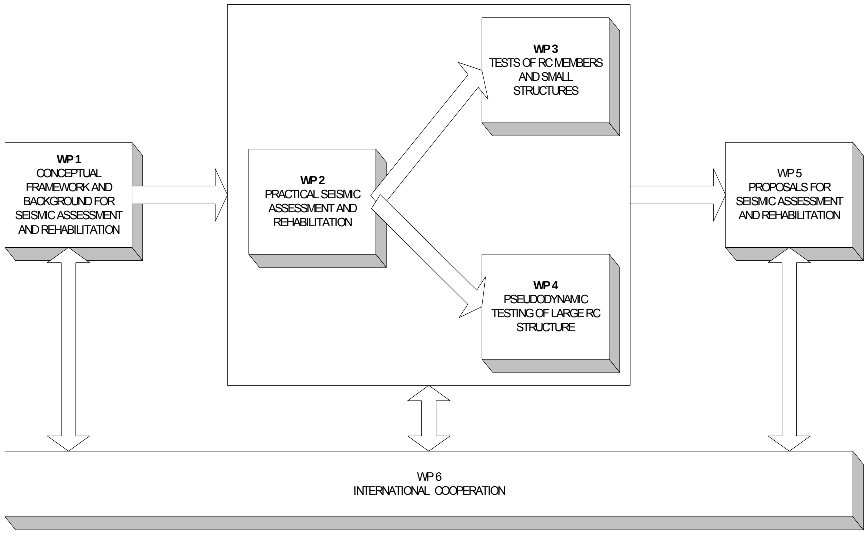

JOINT RESEARCH CENTRE
EUROPEAN COMMISSION

Workpackages

WP1: Conceptual framework

- Internationally harmonised definition of performance parameters and criteria. Emphasis on cyclic damage, local to global relations, effects on load bearing capacity.
- Review of common rehabilitation strategies for RC and masonry buildings
- Review and inventory of common and new (advanced composites) rehabilitation techniques

Workpackages

WP2: Practical assessment & rehabilitation

- Comparative evaluation of existing methods (ICONS, NODISASTR, ECOEST - Japan Building Disaster Prevention Agency, NZ Association of EE, FEMA)
- Development/modification of simple methods.
- Development of models for strength and deformation of retrofitted elements.
- Development of rules for proportioning of the retrofitted elements (focus on deformation capacity).

Benchmark structures

Workpackages

WP3: Tests on elements & substructures

- Definition, design and assessment. Elements will be selected so that they are representative, they supplement other tests other than duplicating. High axial load and irregularity included.
- Numerical simulations and assessment with existing and new methods.
- Cyclic tests on columns and joints, before and after retrofitting.
- Tests on subassemblages: cyclic tests on a 1:1.5, 3-storey plane frame; on a 1:1.5, 2-storey, 1-bay-by-1-bay 3D frame; shake table test on a smaller scale 3D structure.

Tests on subassemblages

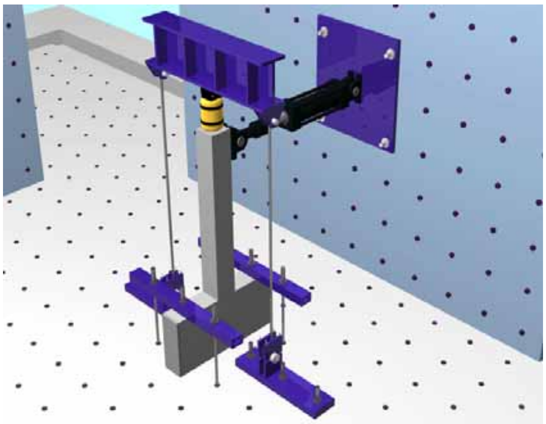

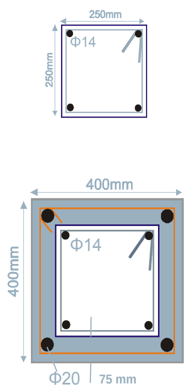

Workpackages

WP4: PsD tests

- Definition, design and construction. The mock-up will be representative of non-seismic RC construction of the 70’s. Irregularities in plan and detailing will be included.
- Pre-test assessment & numerical simulations.
- Tests on the un-retrofitted structure.
- Repair and local member upgrading with advanced composites. Re-testing.
- Repair and global upgrading. Jacketing to correct plan-wise irregularities.
- Re-test to failure.

The test structure

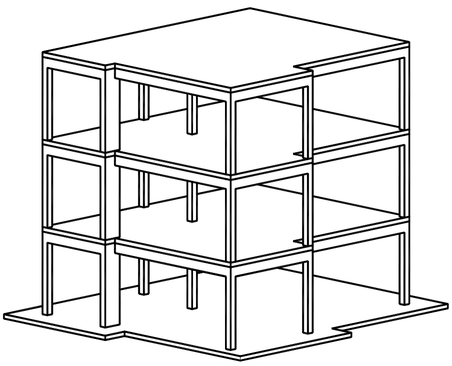

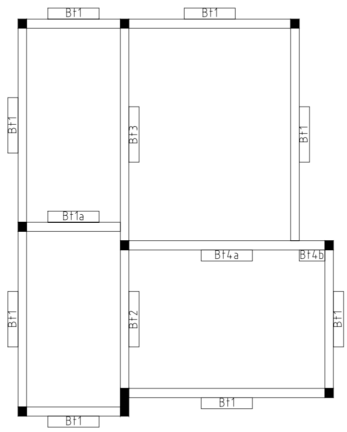

JOINT RESEARCH CENTRE
EUROPEAN COMMISSION

Non-seismic detailing

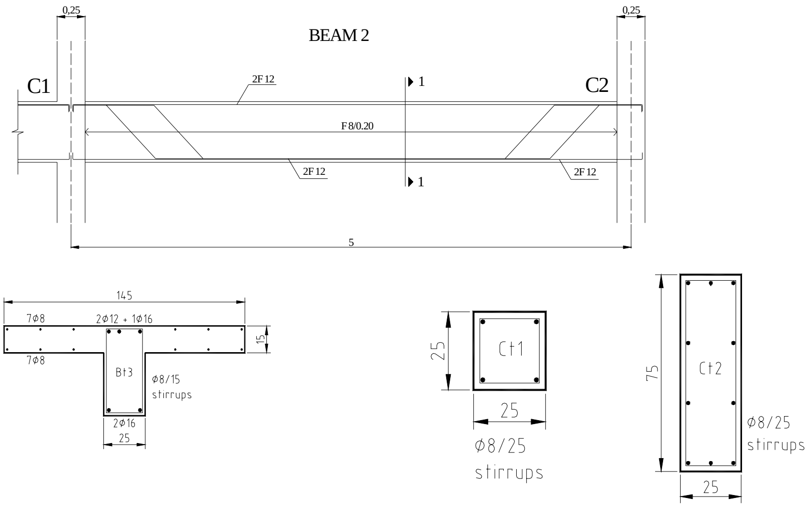

JOINT RESEARCH CENTRE
EUROPEAN COMMISSION

Workpackages

WP5: Guidelines for assessment & rehabilitation

- Post-test assessment of performance parameters and criteria, existing and new methods, schemes and techniques.
- Drafting of guidelines.
- Proposals for EC8, Part 1-4. The final draft of part 1-4 is expected by February 2003.

A new NAS partner

- By means of a recently approved NAS proposal, the Higher Technology Institute in Nicosia, Cyprus, will join the SPEAR consortium.
- The additional research work will address the possibility of adopting existing and new EC8 provisions in NAS.

Appendix 11

Section 11 *Japanese Design And Construction Guidelines For Seismic Retrofit Of Building Structures With Frp CompositesFRP sheet retrofit guideline*

presented by H. Fukuyama

JAPANESE DESIGN AND CONSTRUCTION GUIDELINES FOR SEISMIC RETROFIT OF BUILDING STRUCTURES WITH FRP COMPOSITES

Hiroshi Fukuyama [1]
Gustavo Tumialan [2]
Antonio Nanni [3]

[1] Department of Structural Engineering, Building Research Institute
1 Tatehara, Tsukuba, Ibaraki 305-0802, JAPAN
[2, 3] Department of Civil Engineering, University of Missouri-Rolla
224 Engineering Research Lab, 1870 Miner Circle, Rolla, MO 65409-0710, USA

ABSTRACT

The increasing uses of FRP materials for the strengthening and upgrade of buildings has motivated the international engineering community to produce guidelines for the proper design, handling and installation of the externally bonded FRP systems. Thus, independent efforts coordinated by different organizations such as the Japan Building Disaster Prevention Association (JBDPA) and the American Concrete Institute (ACI) have led to implementing appropriate provisions. The JBDPA guidelines mainly focus on seismic retrofitting of structural elements, which implies the strengthening for shear of deficient structural elements. This paper describes and comments on some of the design approaches provided by the JBDPA guidelines for the strengthening of reinforced concrete (RC) columns. This was one of the main targets of the Japanese experience on infrastructure strengthening, which became an imperative task after the post-earthquake observations of the damage caused by the Kobe earthquake in 1995. Finally, comparisons with the ACI guidelines for the strengthening of RC members with FRP systems are also formulated.

KEYWORDS
Construction, Design, Ductility, FRP Sheets, Flexural Capacity, Guidelines, RC Beams, RC Columns, Seismic Capacity Evaluation, Seismic Retrofit, Shear Capacity

INTRODUCTION

In 1995, the Hyogoken-Nanbu Earthquake caused to the city of Kobe the greatest disaster of the postwar era in Japan. As a result of the inflicted damage and to reduce the impact of potential seismic events in other parts of the country, the Building Research Institute of Japan promoted a program for the development of effective strategies for seismic retrofitting of buildings. One of the areas targeted by this program was the use of Fiber Reinforced Polymer (FRP) materials. In September 1999, the Japan Building Disaster Prevention Association (JBDPA) published the "Seismic Retrofitting Design and Construction Guidelines for Existing Reinforced Concrete (RC) and Steel-encased Reinforced Concrete (SRC) Buildings with FRP Materials". These guidelines were developed based on the results of investigations conducted in Japan, mainly after 1995, and reflect the combined efforts of the Japanese academy, industry, and governmental agencies. This paper describes and comments on some of the design approaches provided by the JBDPA guidelines for the strengthening of RC elements.

SEISMIC CAPACITY EVALUATION

The "Seismic Capacity Evaluation Standards" (JPDPA, 1977 revised in 1990) and "Guidelines for Seismic Rehabilitation of RC Buildings" (JPDPA, 1977 revised in 1990) are used in conjunction with the guidelines for seismic retrofitting of RC buildings. These guidelines have been used since 1977 as an instrument to evaluate the seismic performance of existing RC buildings. Since these provisions represent the first step in the retrofitting process, their basic concepts are briefly described in this section. The seismic capacity of a building is quantified by the seismic index I_s, which should be estimated for every story and frame direction. It is defined as follows:

$$I_s = E_o\, S_D\, T \qquad (1)$$

where E_o expresses the basic seismic index, S_D is the structural design index, which accounts for plan or story-height irregularities, gravitational and stiffness centroid eccentricities. T represents the time index to account for the degree of deterioration of the building, manifested by cracks and permanent deformations.

The basic seismic index is a function of the strength index C, and the ductility index F. The basic seismic index E_o is expressed as:

$$E_o = \frac{n+1}{n+i}\, f(C, F) \qquad (2)$$

where 'n' is the number of stories and 'i' is the story being analyzed. The seismic index intends to represent the capability of the building story being analyzed to absorb energy. Thus, if a story is assumed to consist of a series of vertical members, such as those illustrated in Figure 1a, the load deflection curves for this story subject to a monotonic load can be represented by the curve shown in Figures 1b. The variable α represents the ratio between the lateral force acting in the element and the capacity of the element. For the computation of E_o, predetermined values for α and F are provided by the "Seismic Capacity Evaluation Standards". The largest value obtained by using the equations illustrated in Figure 1c and 1d is used for the computation of I_s.

Three procedures are recommended to estimate I_s, which are dependable on the characteristics of the story to be analyzed. These procedures can be described as:

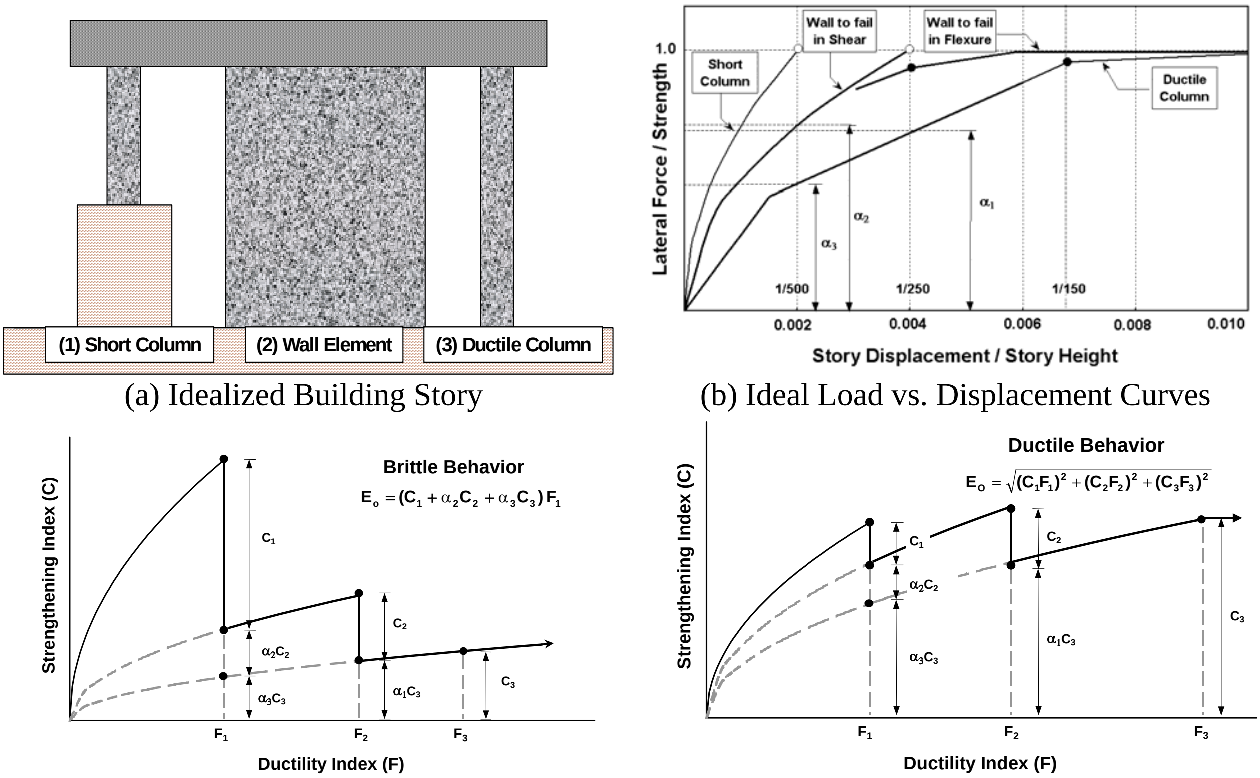

(a) Idealized Building Story (b) Ideal Load vs. Displacement Curves

(c) Brittle Behavior (d) Ductile Behavior

Figure 1: Seismic Capacity Evaluation

- The first procedure is the simplest, which is used for stories with a large density of walls. The ultimate strength is estimated based on the concrete shear strength and cross section area of columns and walls.
- The second procedure requires the calculation of the ultimate capacity and ductility of columns and walls. The beams are usually assumed to be rigid. This procedure is used for “weak column-strong beam” frames.
- The third procedure implies to calculate the ultimate capacity and ductility of the vertical members as well as beams. All the possible mechanisms of failure are taken into account.

Once the seismic index I_s is estimated, this value is compared to a limit index I_{so}. If the I_s index is larger than the limit index, the building is expected to have a good performance during a seismic event. Otherwise, the structures must be retrofitted to comply with the requirements of current building standards. Evaluations conducted on damaged buildings due to earthquakes indicated that whenever the I_s indices were less than 0.3 severe damage was observed. Also, when the values of the I_s indices were larger than 0.6, the damage observed in the buildings was moderate. This was evident from the evaluations performed to the building structures after the Hyogoken-Nanbu Earthquake in 1995, where a value of 0.6 indicated the border limit between severe and moderate damage. Thereby, the “Standards for Seismic Capacity Evaluation of RC Buildings” specify a value equal to 0.6 as limit index I_{so} to prevent collapse or severe damage. When the structures is found to be structurally deficient, new values for C and/or F have to be estimated to meet the structural demand.

SCOPE OF THE JBDPA GUIDELINES FOR STRENGTHENING WITH FRP

The Japanese guidelines for seismic retrofitting of RC building with FRP materials (JPDPA, 1999) provide specifications on the characteristics of the FRP materials commonly used in Japan, their proper handling and installation. Also, pertaining design and detailing recommendations are provided, which mainly target the shear strengthening of either columns or beams. Some of the main provisions are described in the subsequent sections. The guidelines are part of the "Guidelines for Seismic Rehabilitation of RC Buildings" (JPDPA, 1977 revised 1990), a comprehensive publication that documents different retrofitting methods utilized in Japan.

MATERIALS

The JBDPA guidelines describe the properties of PAN-class high-strength carbon fiber sheets, and aramid fiber sheets. In its turn, aramid is sub-classified as aramid 1 and aramid 2. Carbon fiber sheets are labeled based on the tensile strength of the fiber; whereas, the denomination of the aramid fiber sheets is based on the tensile strength in a width of one meter. The values of tensile strength and modulus of elasticity have been estimated from laminates made of carbon or aramid fibers bound in a resin matrix. Table 1 presents the properties of fibers bound by epoxy or methacrylate resin.

TABLE 1
PROPERTIES OF FRP SHEETS

Characteristic	**Carbon Fiber**		**Aramid Fiber**	
	3400 MPa Class	2900 MPa Class	Aramid 1	Aramid 2
Type of Fiber	PAN-class High-Strength		Homopolymer	Copolymer
Tensile Strength	≥ 3400 MPa	≥ 2900 MPa	≥ 2060 MPa	≥ 2350 Mpa
Young's Modulus	230^{+45}_{-15} GPa		118 ± 20GPa	78 ± 15GPa
Fiber Density	1.80 ± 0.05		1.45 ± 0.05	1.39 ± 0.05

The viscosity of the adhesive resins influences the efficiency of the strengthening work. Thus, if sagging is likely to occur, a resin of higher viscosity is recommended. Also, if smooth impregnation in the fiber is required, a resin with lower viscosity should be used. In the case of primers, epoxy and methacrylate resin are commonly used. Due to potential alterations of the hardening process, it is not allowed to use an epoxy-based primer in combination with a methacrylate-based adhesive or vice versa. In similar way, if the putty material is not compatible with the adhesive and primer resins, imperfect adhesion may occur.

DESIGN APPROACHES FOR STRENGTHENING OF COLUMNS

In order to determine the required amount of FRP strengthening, the Japanese guidelines provide expressions to calculate the flexural and shear strengths, and ductility index of RC members. The equations are based on those presented by the "Standards for Seismic Capacity Evaluation" and the "Guidelines for Seismic Rehabilitation of RC Buildings". These equations have been widely used for the design of new construction The definitions of the variables used hereafter are presented at the end of this paper.

Ultimate Flexural Capacity of Columns

The ultimate flexural capacity of a RC column is calculated from the following expressions, which are recommended by a guide for structural design of new buildings, which must comply with the "Japanese Building Standard Law".

For $N_{max} \geq N > N_b$:

$$M_u = \left[0.5a_g\sigma_y g_1 D + 0.024(1+g_1)(3.6-g_1)bD^2F_c\right]\left(\frac{N_{max}-N}{N_{max-}N_b}\right) \quad \text{(N-mm)} \tag{3a}$$

For $N_b \geq N \geq 0$:

$$M_u = 0.5a_g\sigma_y g_1 D + 0.5ND\left(1-\frac{N}{bDF_c}\right) \quad \text{(N-mm)} \tag{3b}$$

For $0 > N \geq N_{min}$:

$$M_u = 0.5a_g\sigma_y g_1 D + 0.5Ng_1 D \text{ (N-mm)} \tag{3c}$$

N_b, N_{max} and N_{min} can be computed from:

Balanced Axial Force:

$$N_b = 0.22(1+g_1)bDF_c \quad \text{(N)} \tag{4a}$$

Ultimate Axial Force in Compression:

$$N_{max} = bDF_c + a_g\sigma_y \quad \text{(N)} \tag{4b}$$

Ultimate Axial Force in Tension:

$$N_{min} = -a_g\sigma_y \quad \text{(N)} \tag{4c}$$

The shear force associated to the flexural capacity M_u can be computed as:

$$Q_{mu} = \frac{\alpha M_u}{h_o} \quad \text{(N)} \tag{5}$$

A α value equal to two may be used to estimate the shear arm. Figure 2 shows the agreement between the experimental and predicted values when using the previous equations.

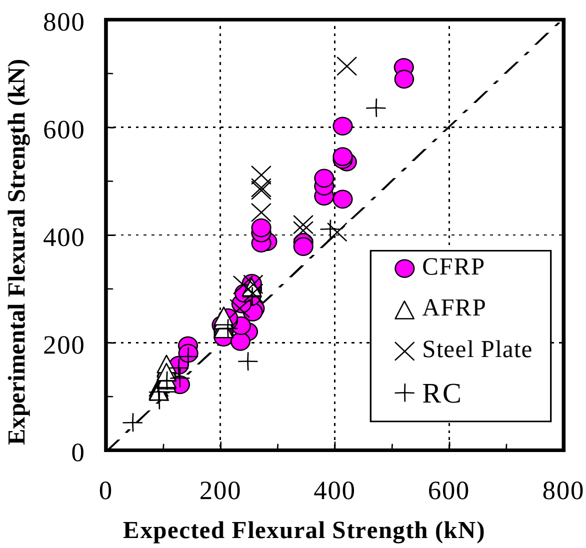

Figure 2: Validation of the Equation for Flexural Strength of Columns

Ultimate Shear Capacity of Columns

The equation used to quantify the shear capacity of an RC member strengthened with FRP composite systems is also similar to that used for structural design of new buildings. The only modification is the addition of the product $p_{wf}\sigma_{fd}$ to the summation $\Sigma p_w\sigma_{wy}$, which intends to take into account the contribution of the FRP reinforcement. Thus:

$$Q_{su} = \left[\frac{0.053 p_t^{0.23}(17.6 + F_c)}{M/Qd + 0.12} + 0.845\sqrt{\sum p_w \sigma_{wy}} + 0.1\sigma_o \right] bj \qquad (N) \qquad (6a)$$

where:

$$\sum p_w \sigma_{wy} = p_{ws}\sigma_{wys} + p_{wf}\sigma_{fd} \leq 10\text{MPa} \qquad (6b)$$

An upper limit of 10 MPa is imposed to $\Sigma p_w\sigma_{wy}$ based on the fact that a larger amount of strengthening would not significantly increase the shear capacity of the strengthened member. Equation 6a can also be applied to predict the ultimate capacity of columns failing by bond splitting, and columns having longitudinal round reinforcing bars.

Another consideration to mention is that the value of the shear span-to-depth ratio expressed as M/Qd must not be less than one nor larger than three. The tensile strength of FRP for shear design is estimated as: $\sigma_{fd} = \min\{E_{fd}\varepsilon_{fd}, 2/3\sigma_f\}$. The value of ε_{fd} equal to 0.7% is adopted based on previous investigations, which have shown that the measured strain in the FRP laminate at the final stage, was between 0.5% and 1.5%. These investigations have also shown that specimens strengthened with a large amount of external reinforcement ($p_{wf}E_{fd}$) possessed smaller strains at failure. Along with the first consideration, to avoid the rupture of the FRP laminate, a value of two-thirds of the tensile strength of the FRP laminate was adopted as a margin of safety, when designing for shear.

Figure 3 illustrates a good agreement between experimental and predicted values for shear strength of RC members strengthened with FRP material when shear failure (rupture of the laminate or compression failure of the concrete strut) and bond splitting are observed.

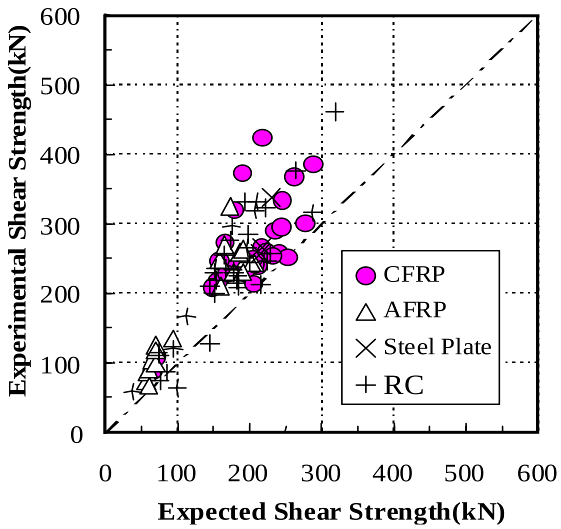

(a) Shear Failure

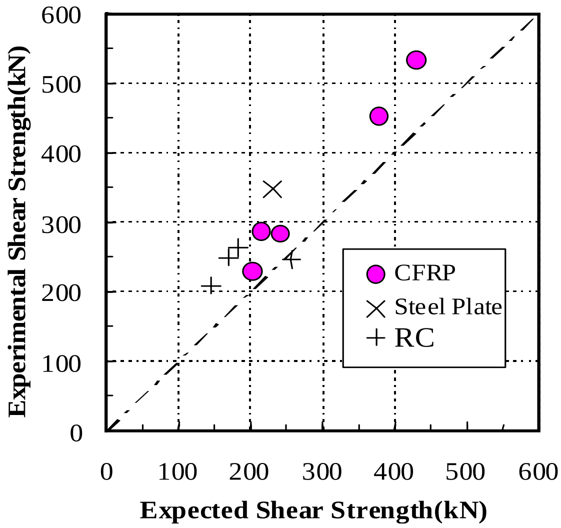

(b) Bond Splitting Failure

Figure 3. Validation of the Equation for Shear Strength of Columns

Ductility Factors and Ductility Index of Columns

The ductility index F is a function of the ductility factor μ, and can be expressed by the following relationships obtained from a degrading tri-linear hysteresis model.

$$F = \phi\sqrt{2\mu - 1} \tag{7a}$$

where:

$$\phi = \frac{1}{0.75(1 + 0.05\mu)} \tag{7b}$$

The ultimate ductility factor μ of columns strengthened with FRP materials is expressed as the margin ratio of the shear strength to the shear force associated to the flexural strength. This factor can be calculated as follows:

$$\mu = 10\left(\frac{Q_{su}}{Q_{mu}} - 0.9\right), \text{ where } 1 \le \mu \le 5 \tag{8}$$

It is known that the ultimate shear strength increases when the axial force in the column is increased. Also, the ultimate flexural strength decreases when the axial force is larger than the balanced axial force. This will cause that the associated shear force Q_{mu} decreases, leading to a larger value of ultimate ductility factor μ. Thereby, to avoid the use of larger ductility values, the code specifies to calculate Q_{mu} based on the balanced moment, whenever the axial force exceeds the balanced axial force.

DESIGN APPROACHES FOR STRENGTHENING OF BEAMS

Ultimate Flexural Capacity of Beams

The ultimate flexural capacity of RC beams is computed by using the following equation:

$$M_u = 0.9 a_t \sigma_y d \qquad \text{(N-mm)} \tag{9}$$

The flexural capacity may also be calculated with equation 3b considering a value of axial force equal to zero. The equations provided for the guidelines are for strengthening rectangular RC beams; the influence of the reinforcement of slabs is not considered. The shear force associated to the flexural capacity M_u is calculated as:

$$Q_{mu} = \frac{\alpha M_u}{L_o} \quad \text{(N)} \tag{10}$$

Ultimate Shear Capacity of Beams

To estimate the ultimate shear capacity of RC beams strengthened, the term representing the influence of the axial force in equation 6a is dropped, thus equation 11 is obtained. Similarly to the case of columns, the value of the shear span-to-depth ratio, M/Qd, must not be less than one nor larger than three. In addition the term $\Sigma p_w \sigma_{wy}$ must satisfy the relationship given by equation 6b.

$$Q_{su} = \left[\frac{0.053 p_t^{0.23} (17.6 + F_c)}{M/Qd + 0.12} + 0.845\sqrt{\sum p_w \sigma_{wy}} \right] bj \qquad (N) \tag{11}$$

Figure 4 compares the experimental and predicted values for the maximum strength of RC beams strengthened in shear with FRP materials. It is observed that the calculated values by using equation 11 are on the safe side.

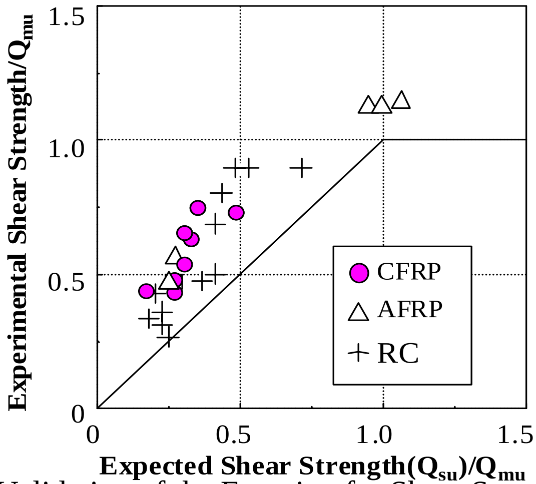

Figure 4: Validation of the Equation for Shear Strength of Beams

SPECIAL PROVISIONS

Strengthening Without Removal of Mortar Finishing

An advantage of using FRP materials for strengthening RC elements is that the disruption to the building occupants or other individuals in the nearby area is minimum. One source of disruption is that caused by noise, dust and vibration when removing the finishing mortar. Surfaces finished with mortar were very common in Japan up to the mid-1970s, when the need for mortar finishing was basically eliminated with the improvement the formworks. As a principle, the Japanese guidelines require the removal of finishing mortar for strengthening of columns. However, the guidelines present special specifications for the strengthening of RC rectangular columns without removing the finishing mortar, which can be carried out when appropriate control during the execution of the strengthening work is provided. These specifications are based on previous experimental programs, which demonstrated that the shear capacity and ductility are not reduced when columns are wrapped around with FRP materials with the presence of finishing mortar. In addition, based on those researches, in order the strengthening to be effective, any existing cracks on the finishing mortar have to be repaired prior to installing the FRP system. It is also specified that surfaces of mortar finishing painted with layers of thick painting materials may remain. The bond strength of these materials must be at least 1 MPa; in addition, they must not have any adverse chemical reaction with the epoxy adhesives. It is not recommended to attach FRP materials to surfaces constituted of plastering, finishing tiles, wallpaper, etc.

The survey of the conditions of the finishing mortar should be based on the number of years of service of the structure, the surface conditions, history of previous repair works and characteristics of finishing mortar. The strength of the mortar is estimated by means of any suitable tool such as Schmidt rebound hammers. Defining t_m as the thickness of finishing mortar and D as the largest cross sectional dimension of the column the following recommendations are provided for the design of the strengthening:

- If $t_m \leq D/15$ and the results of the survey indicate that the mortar finishing can remain, the design is conducted as the mortar finishing had been removed.
- If $t_m > D/15$, the mortar finishing needs to be removed unless a special study is conducted.

In any case, with or without removal of mortar finishing, the lap length is specified to be larger than 200 mm. The radius corner must be larger than 10 mm when AFRP is used, and larger than 20 mm for the case of CFRP wrapping. Due to concrete cover consideration, the radii should not exceed 30 mm for any case.

Anchoring Systems

FRP systems that do not completely wrap the entire section will likely peel off from the concrete surface. To develop larger tensile stresses in the laminate, mechanical anchorages can be used at the termination points. Previous investigations demonstrated the use of Schemes C, D, E and F in Figure 5, increased the shear capacity. However, these schemes may not be effective in beams having short span or when the amount of reinforcement increases. It has been observed that the beam can split from the slab along the corners, as illustrated in Scheme C. To account for this, it is advisable to check the level of shear stresses at those corners to foresee the splitting. If the splitting is likely to occur, the guidelines recommend the use of anchorage schemes as those labeled as Schemes A and B.

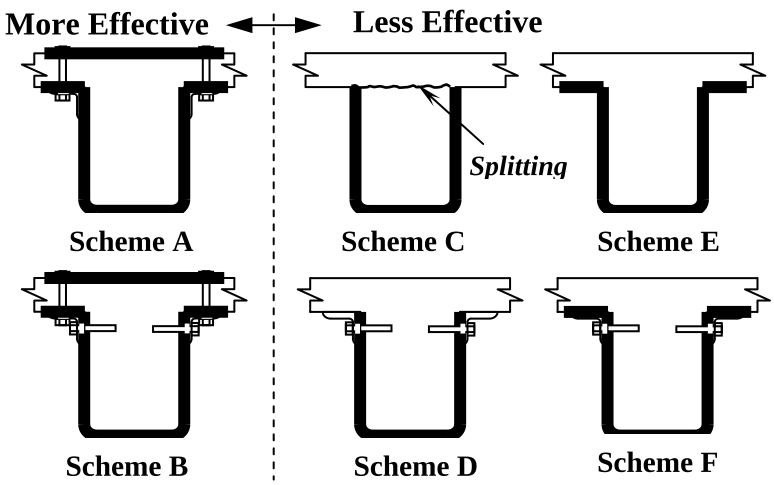

Figure 5: Anchorage Schemes

Specifications should be provided to fully guarantee the effectiveness of angles and bolts, which will ensure the increase of shear strength. The specifications should include the number and strength of bolts. Also, the "L" shapes must be designed to avoid rotation or plastic deformation caused by the tensile stresses in the laminate. Since the corners are not necessarily at 90^o degrees, the designer should also provide specifications on the corner preparation and anchorage installation procedures.

CONSTRUCTION PRACTICE

Execution of the Strengthening Work

The work activities related to the strengthening of RC building structures should comply with the Contractors Law of the Ministry of Land, Infrastructure and Transport of Japan. The JBDPA guidelines provide adequate guidance for strengthening RC members with different combinations of continuous fibers and impregnating resins. These combinations include CFRP/epoxy resin, CFRP/methacrylate, and AFRP/epoxy resin. In its turn, the resins can be one-part or two-parts. Since there are no test results available on AFRP/methacrylate, specifications about this particular combination are not provided. Depending on the fiber-resin combination to be used, the required weight by square meter and the time interval for each step of the FRP installation are specified. As an example, Table 2 presents some specifications when FRP sheets are attached by using epoxy resins or a methacrylate resins.

The strengthening work requires to be inspected after the installation of the FRP systems. This is done to ensure the absence of defects such as blisters, partial peeling and residual resin. If blisters are observed, a resin compatible with the primary resin can be injected. When partial peeling is observed, it is recommended to remove the attached area without damaging the FRP lower layers, and replace it with a new sheet. The new sheet should overlap the existing sheet at least 200 mm. If residual resin is detected, it should be removed using sandpaper without damaging the FRP sheet.

TABLE 2

SPECIFICATION FOR INSTALLATION OF FRP WITH ONE-PART RESINS

Process	FRP/Epoxy Resin		FRP/Methacrylate Resin	
	Weight of Material (kg/m^2)	Time Interval	Weight of Material (kg/m^2)	Time Interval
Primer	0.2-0.3	≥4 hrs., within 3 days	0.075-0.1	≥60 min.
First layer of resin	0.4-0.5	Immediately	0.4-0.5	≥5 min.
FRP sheet installation	1.15 m^2/m^2	≥ 2 min. (for fabric type); ≥ 20 min. (for pre-preg type), within 90 min.	1.5 m^2/m^2	Within10 min.
Second layer of resin	0.3-0.4	Immediately	0.4-0.5	Within10 min.
Air voids elimination	-----	≥4 hrs., within 3 days	-----	≥60 min.

Contractor Qualifications

The engineers and technicians, carrying out the strengthening work, must have been properly trained on the handling of the raw materials and installation of FRP systems. Manufacturers and public agencies involved with the use FRP materials provide appropriate professional training and certification.

COMPARISON WITH THE ACI-440 GUIDELINES

The ACI committee 440 (2001, document under review) has developed guidelines for the strengthening of RC structures with FRP. A comparative study between JBDPA and ACI guidelines was conducted through trial design for strengthening of a column as follows. The shear capacity of an interior square column of 650 x 650 mm dimensions requires upgrade. A complete wrapping scheme (Carbon/Epoxy system) has been selected to upgrade the shear capacity of the column. The ductility index F is estimated as 2.5. Determine the additional reinforcement. The “un-factored” axial forces are Dead Load equal to 1500 kN, Live Load equal to 450 kN, and Seismic Load equal to +/- 15 kN. Figure 6 shows the shear strength as a function of the number of plies wrapping the column. It has shown that the recommendations provided by ACI-440 allow for a larger contribution of the FRP reinforcement shown in the figure. The JBDPA guidelines express the contribution of the shear reinforcement as the square root of the summation of the steel and FRP contributions. Compared to the ACI guidelines, where the shear strength is expressed as the summation of concrete, steel and FRP, this approach increases the difference in the values of FRP shear contribution when the number of plies is increased.

Material Properties : Fc = 21 MPa, σ_y = 345 MPa, σ_{wys} = 295 MPa
Area Longitudinal Bars: 387mm^2, Area Transversal Bars: 64 mm^2 (spacing=200 mm)
FRP Properties : σ_f = 3400 MPa, E_{fd} = 230 GPa, Thickness per ply = 0.167 mm

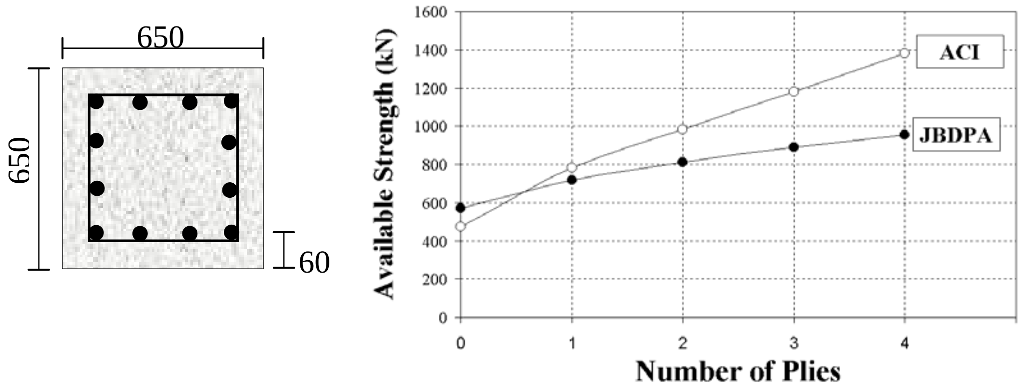

Figure 6: Shear Strength vs. Number of Plies

In Figures 7, to correlate experimental and expected values according to the JBDPA and ACI codes, data obtained from over one hundred columns tested in Japan was used (Tumialan et. al, 2001). Most of these specimens were strengthened with one or two plies of FRP laminates; mainly, carbon and aramid. It should be noted that both codes provide appropriate estimations with proper conservative values. It is also observed that the JBDPA approach provides less data dispersion.

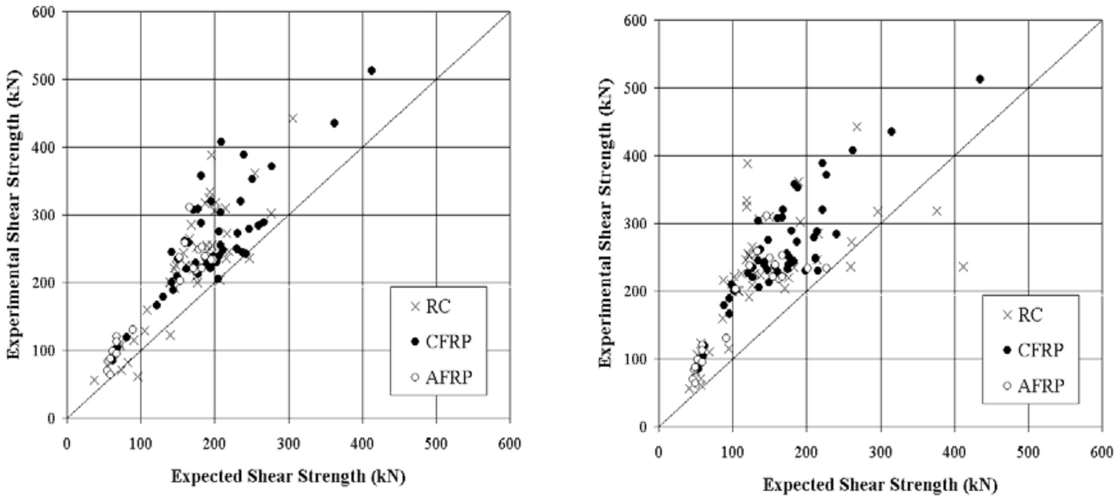

(a) JBDPA Code (b) ACI Code

Figure 7: Experimental vs. Expected Values

FINAL REMARKS

Some of the most important provisions of the Japanese guidelines for the retrofitting of RC building structures with FRP materials are presented. The JBDPA guidelines condense the research on seismic retrofitting of RC building structures using FRP materials, which has been conducted in Japan mainly after the Kobe Earthquake. These provisions deal with the proper handling, design and installation of FRP systems used in Japan. Special considerations as the detailing of anchorage and strengthening of columns in the presence of finishing mortar are described. Comparisons with the guidelines provided by the ACI-440 are also presented.

NOTATION

a_g	:	Overall area of the longitudinal reinforcement of the column (mm^2)
a_t	:	Area of the reinforcement in tension of a column or beam (mm^2)
a_v	:	Area of shear reinforcement within a distance equal to the spacing "s" (mm^2)
b, D	:	Dimensions of the columns ($D \geq b$) (mm)
d	:	Effective depth (Distance from extreme compression fiber to centroid of longitudinal tension reinforcement) (mm)
E_{fd}	:	Modulus of elasticity of the FRP (Mpa)
F	:	Ductility Index
F_c	:	Compressive strength of concrete (Mpa)
g_1	:	Ratio of distance between the centers of longitudinal reinforcement in tension and compression to the column width.
h_o	:	Clear height of column
j	:	Distance between the tensile and compressive force resultants. (In columns: j = 0.80D. In beams: j = $^7/_8$ d)
M_u	:	Ultimate Flexural Capacity (N-mm)
M/Q	:	Shear span (mm). A value equal to half of the column height can be used
N	:	Axial Force in the Column (N)
p_t	:	Ratio of tensile reinforcement = a_t/bd (%)
p_{ws}	:	Ratio of existing shear steel reinforcement to area of contact surface = a_v/bd (%)
p_{wf}	:	Ratio of FRP reinforcement to area of contact surface = Area FRP/bD (%)
Q_{mu}	:	Shear force associated to the ultimate flexural capacity (N)
Q_{su}	:	Ultimate Shear Capacity (N)
ε_{fd}	:	Effective Strain of the FRP, taken as 0.7%
μ	:	Ultimate ductility factor
σ_y	:	Specified yielding strength of the longitudinal reinforcement (MPa) For round steel bars: f_y = 295 MPa For deformed steel bars: f_y = specified strength + 49 (MPa)
σ_{wys}	:	Specified yield strength of the existing transversal reinforcement (MPa)
σ_{fd}	:	Tensile strength of FRP for shear design (MPa)
σ_f	:	Tensile Strength of FRP (MPa)
σ_o	:	Axial stress (MPa), no larger than 7.84 Mpa

REFERENCES

American Concrete Institute (ACI), Committee 440. (2001, document under review), Guide for the Design and Construction of Externally Bonded FRP Systems for Strengthening Concrete Structures

Japan Building Disaster Prevention Association (JPDPA). (1977 revised in 1990), Standards for Seismic Capacity Evaluation of RC Buildings, (in Japanese)

Japan Building Disaster Prevention Association (JPDPA). (1977 revised in 1990), Guidelines for Seismic Rehabilitation of RC Buildings, (in Japanese)

Japan Building Disaster Prevention Association (JPDPA). (1999), Seismic Retrofitting Design and Construction Guidelines for Existing Reinforced Concrete (RC) and Steel-encased Reinforced Concrete (SRC) Buildings with FRP Materials, (in Japanese)

Tumialan G., Nakano K., Fukuyama H., and Nanni A. (2001), Japanese and North American Guidelines for Strengthening Concrete Structures with FRP: a Comparative Review of Shear Provisions, Proceedings of the Fifth International Conference on the use of Fibre Reinforced Plastics for Reinforced Concrete Structures (FRPRCS-5), Thomas Telford Ltd (paper submitted).

Appendix 12

Reference materials of JRC-IPSC

A DISPLACEMENT-BASED MDOF TECHNIQUE TO ACCOUNT FOR THE EFFECTS OF INFILLS IN FRAMED STRUCTURES

Fabio TAUCER[1] and Paolo NEGRO[2]

[1, 2] Research Officer, ELSA Unit, Institute for the Protection and Security of the Citizen (IPSC), European Commission – Joint Research Centre, fabio.taucer@jrc.it / paolo.negro@jrc.it

ABSTRACT: A response spectrum procedure for the global analysis of multi-degree-of-freedom building structures to account for the nonlinear behaviour of structural members as a function of increasing earthquake intensities is presented. The procedure is based on interstorey secant stiffness and damping envelopes and searches for a displacement shape compatible with the structure's secant stiffness and spectral response for the considered earthquake intensity. The procedure is used to study the behaviour of regular and irregular infilled RC building structures in the context of performance based design.

Key Words: performance based design, infill walls, multi-degree-of-freedom response spectrum analysis

INTRODUCTION

The effect of nonstructural masonry infills on the global dynamic behaviour of framed structures is still a controversial issue (Colombo et al. 1998). Even though infills are disregarded in the design process by most codes, they are capable of modifying the behaviour of building structures to a large extent.

The detrimental effects of irregularly arranged infill panels are known, and attempts to account for these effects in design have been made (Fardis et al. 1999a). Even though the relative importance of plan-wise and height-wise irregularities is not completely clear (some studies seem to indicate that the effects of irregularities in plan are not as severe as those of irregularities in elevation) (Fardis et al. 1999b), there is a general consensus about the need to take into account the effects of irregular distributions of infills in design.

On the other hand, the need to account for regularly arranged infills is not very evident. Indeed, the effect of regular infill patterns is typically regarded as positive. Infills can make the structure considerably stiffer and stronger (which is a positive effect in most cases), and can significantly contribute to energy dissipation by progressive damage of the panels, thus protecting the frame from larger damage. The consequence of this point of view is that there is no need to account for the effects of infills in design (as long as they are regularly arranged), and that the infills can be regarded as a second line of defence, which may eventually improve the global seismic behaviour of the structure.

Pseudodynamic tests conducted on a four-storey reinforced concrete (RC) frame have thrown more light into this problem (Negro and Colombo 1997). The seismic response corresponded to a storey-wise progressive failure of the panels, thus transforming the structure into a soft-storey mechanism. Even though the characteristics of the input did not result in excessive deformations, this indicated that regular infill patterns can produce an irregular response. A confirmation of this finding came from the analysis of the damage resulting from the Koçaeli (1999) Earthquake (Dolsek and Fajfar 2001). As an effect of such earthquake, many apparently well designed and constructed uniformly-infilled frames suffered extensive damage, often leading to the collapse of the first storey, and analyses indicated that the reason for the collapse may have remained within the infill panels, in spite of their regular arrangement (see Photo 1, showing a building in Gölçüc which pancaked during the 1999 Koçaeli earthquake with a sort of soft first storey effect, in spite of the fact it was uniformly infilled).

Photo 1 RC Building in Gölçüc which pancaked during the 1999 Koçaeli earthquake.

The storey-wise progression of the failure of the panels cannot be traced by standard single-degree-of-freedom (SDOF) techniques. A new assessment method, based on a simplified multi-degree-of-freedom (MDOF) displacement-based technique, is used to study the behaviour of a three-storey RC infilled frame which will be subjected to pseudodynamic tests. The conditions which correspond to a storey-level mechanism are analysed, and the consequences for the structural behaviour of the frame are discussed. The technique is proposed as a viable means to account for these effects in analysis and design.

ANALYSIS METHODOLOGY

The assessment of the response of a building structure can be performed by means of analytical procedures that can vary in complexity as a function of the methodology used and the level of refinement desired for the computed structural response.

Non-linear dynamic time history analysis by means of Finite Element Models (FEM) offers to date the most realistic description of the response of a structure to earthquake excitation. However, the limitations of such a methodology are many: the constitutive relations that represent the physical properties of the elements that make up the structure can be very complex and not always consider all the factors that determine their behaviour; the analysis procedure is computationally expensive, requires specialised and experienced engineers and may not always lead to a solution; finally the confidence of the available data used as input in the analysis is generally lower than the accuracy of the computed response. For these reasons parametric analyses are prohibitively expensive, thus excluding the possibility of using FEM non-linear dynamic analysis for design purposes.

Response Spectrum Analysis (RSA) methodologies offer a good compromise between accuracy and computational cost. The maximum response is obtained based on fundamental properties of the structure and of the seismic input. This makes the procedure ideal for design, as it allows to perform parametric analyses at different levels of seismic input and different structural configurations.

The limit of RSA lies in the approximations involved in determining the two quantities that govern the response of the structure: period of vibration and equivalent damping. In traditional force-based design methods the period of the structure is obtained either by empirical expressions that take into account the geometry of the structure or by computing the elastic first mode of vibration. A constant level of equivalent damping is assigned as a function of the materials used, while the effect of energy dissipation due to the development of plastic behaviour is taken into account by reducing the elastic spectral forces. Whereas this approach may give a good description of the response of a regular structure with well distributed damage, it falls short in identifying the members that most contribute to energy dissipation, the mode of failure of irregular structures and the actual displacements obtained for the different members of the structure.

The methodology proposed herein is based on response spectrum analysis applied to MDOF systems and on equivalent secant stiffness and damping of the structure as a function of displacement response (Taucer 2000, Taucer et al. 2000). The methodology identifies the effective contributions to damping and stiffness of the different elements that form the structure, thus tracing the damage evolution and failure modes as a function of the earthquake intensity. The proposed approach is ideal for the analysis of infilled regular/irregular structures for which the stiffness and damping contributions of the infill wall can be explicitly taken into account.

Non-linear Response Spectrum Analysis of SDOF Systems

It has been well recognised that the earthquake response of a non-linear SDOF system can adequately be well represented by means of linear analysis of an equivalent system with secant stiffness and hysteretic damping obtained at maximum response (Miranda and Ruiz-Garcia, 2002). Whereas some differences are obtained in the time history response of the non-linear and equivalent linear systems, a very good match is obtained for maximum response, in general sufficient for preliminary assessment and design. It follows that response spectrum analysis of the equivalent linear system will give a good approximation of the maximum earthquake response of the non-linear system.

Let us take a SDOF system described by an inertial mass m and by a given cyclic nonlinear force-displacement constitutive law. Furthermore, the system is discretised into force-displacement and damping-displacement envelope functions f_V and f_D. The force envelope is computed as the resisting force F developed by the system at increasing levels of displacement, considering either monotonic or cyclic behaviour of the constitutive law at the displacement of interest; similarly, the damping envelope is obtained by computing the hysteretic damping with the following expression:

$$\xi_h = \frac{W_D}{4\pi W_s} \tag{1}$$

where W_D is the energy contained by the hysteresis loop of the constitutive law and W_s is the elastic strain energy stored in the system at the considered displacement amplitude d.

The step-by-step procedure to determine the response of a nonlinear system to earthquake excitation is as follows:

Step 1.	Assume trial displacement d^*
Step 2.	$F = f_V[d^*]$ and $\xi_{eq} = f_D[d^*]$

Step 3.

$$k_{eq} = \frac{F}{d^*}$$

Step 4.

$$T_{eq} = 2\pi \sqrt{\frac{m}{k_{eq}}}$$

Step 5.

$$S_d = RS_d\,[a_g, T_{eq}, \xi_{eq}]$$

Step 6.

If $\dfrac{|S_d - d^*|}{S_d} < Tol$ Then

$d = S_d$, analysis has converged.

else

$d^* = S_d$, go to *Step 2*

The procedure is iterative; when convergence is achieved with tolerance *Tol*, the resulting displacement corresponds to the response of the system to a seismic input of peak ground acceleration a_g. Spectral displacement S_d in *Step 5* is computed from displacement spectra RS_d corresponding to a specific soil class and to other parameters that may describe the ground motion.

The step-by-step procedure is repeated for different levels of a_g to obtain the response of the system with increasing levels of the earthquake intensity. Moreover, it is also possible to compute the total damping as the sum of hysteretic and viscous damping, thus giving a better control of the variables that determine the response of the system.

For a SDOF system made up of resisting elements in parallel the procedure is straight forward: there are as many force and damping envelope functions as there are elements in parallel and the total force is obtained as the sum of the resisting forces computed at displacement d. The equivalent damping of the system is computed as the ratio between the weighted sum of the damping contributions of each element in terms of their stored energy and the total elastic energy stored in the system.

For a system formed by M_q members ranging from q = 1 to Q, the total equivalent damping is computed as (Priestley and Calvi 1997):

$$\xi_{eq} = \frac{\sum_{q=1}^{Q} F_{M_q}\, d\, \xi_{M_q}}{\sum_{q=1}^{Q} F_{M_q}\, d} \tag{2}$$

The possibility of assembling the contributions of different elements in parallel is well suited for the analysis of infilled frames, offering the possibility to distinguish the contributions of the infill walls and of the RC frame.

Non-linear Response Spectrum Analysis of MDOF Systems

The transition from non-linear spectral analysis of SDOF systems to MDOF systems is not a trivial one. A MDOF system can be seen as a system in series, where the displacement shape is not known in advance. For the case of multi-storey buildings it is possible to discretise the structure as a system in series made up of as many elements as the number of storeys of the building, and as a system in parallel for the different elements that make up each storey (i.e., infill walls and RC frame elements are subjected to the same interstorey displacement).

Having presented in the previous sub-section the approach to compute the SDOF response of system in parallel, the next step is to compute the MDOF seismic response corresponding to a system in series. In fact, as acknowledged by many researchers, this is one of the main problems that has been faced by displacement based methodologies: the definition of the displacement shape (Fajfar and Krawinkler 1997). A traditional option has been to assume a near to inverted triangular shape for regular buildings, to concentrate most of the deformation where a soft-storey mechanism is expected, or to assume a displaced shape based on capacity design considerations (Miranda 1997, Fajfar et al. 1997, Fardis and Panagiotakos 1997, Priestley and Calvi 1997, Reinhorn 1997). However, these assumptions use as premise the expected response of the structure, which is what the analysis methodology is expected to compute. As an alternative to overcome this problem the following iterative procedure is proposed:

Step 1.	Assume a trial displacement shape.
Step 2.	Compute the resisting force and equivalent damping of all members of the structure by means of the force and damping envelopes as a function of the trial displacement shape.
Step 3.	Assemble the element stiffness into the structure stiffness matrix.
Step 4.	Compute the equivalent damping of the structure by means of Eq. (2).
Step 5.	Compute the eigenvalues and eigenvectors of the structure based on the stiffness matrix computed in *Step 3*.
Step 6.	Enter the response spectra for a given earthquake intensity and compute the modal spectral displacements as a function of the modal periods computed in *Step 5* assuming constant damping (as computed in *Step 4*) for all modes of vibration of the structure.
Step 7.	Compute the modal displacements of the structure based on the eigenvectors computed in *Step 5* and the spectral displacements computed in *Step 6*; obtain the displaced shape by SRSS combination (for faster convergence it is also possible to account for the contribution of the first mode only).
Step 8.	Compare the obtained displaced shape with the trial shape. If the comparison is within the desired tolerance the solution converges, otherwise update the trial displaced shape with the computed displaced shape in *Step 7* and go to *Step* 2.

As with the SDOF system, an assumption is made for the displaced shape, which is updated through the iterative procedure until a solution is found. A set of iterations is performed for each level of the earthquake intensity, using as starting trial displaced shape the converged displaced shape at the previous earthquake intensity.

In essence, the procedure consists in searching a displacement shape that results in a stiffness matrix and equivalent damping such that, when computing the modal properties and entering the response spectra for a given earthquake intensity, a displacement response equal to the trial displacement shape is obtained.

Step-by-Step Analysis Procedure for Multi-Storey Building Structures

The procedure presented for MDOF systems is now presented for the particular case of multi-storey structures. The first assumption that is made is that the behaviour of the building structure can be discretised as shear type, where independent interstorey shear-displacement envelope functions can be computed for each storey.

One way of establishing these envelope functions is by performing pushover analyses on a nonlinear model of the building, where unit interstorey displacements are imposed at the storeys of interest. Another way of calculating these functions is by computing the maximum capacity of the frame at each storey as a function of the member cross sections, setting yield interstorey displacements as a function of interstorey height and interstorey drifts at yield, and establishing the slope of the plastic branch as a function of the detailing or type of cross section of members.

The condensation of the response of a shear type building in the lateral degrees-of-freedom (DOF's) is exact when working in the linear range; however, when working in the nonlinear range the secant stiffness matrix obtained from the pushover analysis or from the stiffness-strength-ductility evaluations changes as a function of the displacement shape considered in the stiffness evaluation itself. However, these changes are usually not too large (Miranda and Ruiz-Garcia, 2002), therefore at this stage of analysis the assumption of being able to calculate nonlinear force-displacement envelopes from unit interstorey deformations is considered satisfactory.

The procedure for computing the response of a multistorey building follows the same step-by- step schemes presented in the previous section. The following nomenclature is introduced, where index *i* denotes the storey number (or mode number) and *n* the total number of storeys (or total number of modes considered in the analysis):

- Storey displacement vector: $\boldsymbol{\psi}$
- Interstorey displacement vector: $\Delta\boldsymbol{\psi}$
- Member interstorey shear force envelopes: $\boldsymbol{V_{Mq}} = f_{V\,Mq}\,[\Delta\boldsymbol{\psi}]$
- Member equivalent damping envelopes: $\boldsymbol{\xi_{Mq}} = f_{\xi\,Mq}\,[\Delta\boldsymbol{\psi}]$

All vectors are of *n* (number of storeys) dimension. The building is composed of *Q* members M_q acting in parallel at each storey level. For example, a reinforced concrete (RC) infilled frame would be composed by two M_q members ($Q = 2$), namely the RC frame (M_1) and the infill walls (M_2). For storey levels where not all M_q members are present, zero interstorey force and damping functions are assigned.

Secant stiffness $\mathbf{K}_{\text{sec}}$ is computed by assembling through the *n* storeys of the structure interstorey secant stiffness $k_{sec\ i}$, obtained as the sum of secant stiffness $k_{sec\ Mq\ i}$ calculated for each of the *Q* members working in parallel at storey level *i*. The secant stiffness of each member M_q is calculated as the ratio between resisting force $V_{Mq\ i}$ and interstorey displacement $\Delta\psi_i$. The structure stiffness matrix $\mathbf{K}_{\text{sec}}$ is then assembled as (for ease of notation, the term $k_{sec\ i}$ in Eq. (3) was replaced by k_i):

$$\mathbf{K}_{\text{sec}} = \begin{bmatrix} k_1 + k_2 & -k_2 & & & & & \\ -k_2 & & & & & & \\ & & & -k_i & & & \\ & & -k_i & k_i + k_{i+1} & -k_{i+1} & & \\ & & & -k_{i+1} & & & \\ & & & & & & -k_n \\ & & & & & -k_n & k_n \end{bmatrix} \tag{3}$$

The mass matrix $\mathbf{M}$ is assumed diagonal, with all cross terms equal to zero and diagonal terms m_{ii} equal to storey mass m_i.

The input data given by the user to start up the analysis procedure are:

- Number of storeys: n
- Member interstorey shear force envelopes: $f_{V\,Mq}$
- Member equivalent damping envelopes: $f_{\xi\,Mq}$
- Storey masses: m_i
- Response spectrum function: $S_a = RS_a\,[a_g, T, \xi]$
- Set of target a_g (of length K): $\boldsymbol{a_g}$
- Trial displacement shape: $\boldsymbol{\psi}_0$
- Convergence tolerance: Tol
- Structure viscous damping: ξ_v

The step-by-step procedure is described as follows:

Step 1. Set $k = 1$

Step 2.

$$a_g^{\,k} = a_{g_k} \quad ; \quad j = 1$$

Step 3. Set trial displacement shape:

If $k = 1$ and $j = 1$ then

$$(\boldsymbol{\psi}^j)^k = \boldsymbol{\psi}_0$$

If $k \neq 1$ and $j = 1$ then

$$(\boldsymbol{\psi}^j)^k = \boldsymbol{\psi}^{k-1}$$

If $k \neq 1$ and $j \neq 1$ then

$$(\boldsymbol{\psi}^j)^k = (\boldsymbol{\psi}^{j-1})^k$$

Step 4. Compute interstorey displacements $(\Delta\boldsymbol{\psi}^j)^k$ corresponding to $(\boldsymbol{\psi}^j)^k$:

$$(\Delta\psi_1^{\,j})^k = (\psi_1^{\,j})^k \quad ; \quad (\Delta\psi_i^{\,j})^k = (\psi_i^{\,j})^k - (\psi_{i-1}^{\,j})^k \quad \text{for } i = 2 \text{ to } n$$

Step 5. Evaluate member interstorey forces $(V_{Mq\;i}{}^j)^k$ at each storey i:

$$(V_{Mq\,i}{}^j)^k = f_{V\,Mq}\,[(\Delta\psi_i^{\,j})^k\,]$$

Step 6. Compute member secant stiffness $(k_{sec\;Mq\;i}{}^j)^k$ at each storey i:

$$(k_{\sec Mq\,i}{}^j)^k = \frac{(V_{Mq\,i}{}^j)^k}{(\Delta\psi_i^{\,j})^k}$$

Step 7. Compute interstorey secant stiffness $(k_{sec\;i}{}^j)^k$ at each storey i:

$$(k_{\sec\,i}{}^j)^k = \sum_{Mq}^{Q} (k_{\sec Mq\,i}{}^j)^k$$

Step 8. Assemble member secant stiffness $(k_{sec\;i}{}^j)^k$ to obtain structure stiffness $(\mathbf{K}_{\sec}{}^j)^k$.

Step 9. Evaluate equivalent damping $(\xi_{Mq\,i}{}^{j})^{k}$ at each storey i:

$$(\xi_{Mq\,i}{}^{j})^{k} = f_{\xi\,Mq}[(\Delta\psi_i{}^{j})^{k}]$$

Step 10. Compute the equivalent damping $(\xi^{j})^{k}$ of the structure:

$$(\xi^{j})^{k} = \frac{\sum_{i}^{n}\sum_{Mq}^{Q}(\xi_{Mq\,i}{}^{j})^{k}\,[(V_{Mq\,i}{}^{j})^{k}\,(\Delta\psi_{Mq}{}^{j})^{k}]}{\sum_{i}^{n}\sum_{Mq}^{Q}(V_{Mq\,i}{}^{j})^{k}\;(\Delta\psi_{Mq}{}^{j})^{k}} + \xi_v$$

Step 11. Solve the eigenvalue problem $\left\|(\mathbf{K}_{\mathrm{sec}}{}^{j})^{k} - [(\omega_i{}^{j})^{k}]^2\,\mathbf{M}\right\| = \mathbf{0}$ and obtain:

Modal angular frequencies $(\omega_i{}^{j})^{k}$ and Modal shapes $(\varphi_i{}^{j})^{k}$

Step 12. Compute modal spectral accelerations $(S_{a\,i}{}^{j})^{k}$ corresponding to $(T_i^{j})^{k}$ and $(\xi^{j})^{k}$ as a function of $a_g{}^{k}$:

$$(T_i{}^{j})^{k} = \frac{2\pi}{(\omega_i{}^{j})^{k}} \quad ; \quad (S_{a\,i}{}^{j})^{k} = RS_a[a_g{}^{k},(T_i^{j})^{k},(\xi^{j})^{k}]$$

Step 13. Compute modal spectral displacement $(S_{d\,i}{}^{j})^{k}$:

$$(S_{d\,i}{}^{j})^{k} = \frac{(S_{a\,i}{}^{j})^{k}}{[(\omega_i{}^{j})^{k}]^2}$$

Step 14. Compute structure modal displacements $(\psi_i^{j})^{k}$ corresponding to $(S_{d\,i}{}^{j})^{k}$:

$$(Y_i^{j})^{k} = \frac{(L_i{}^{j})^{k}}{(M_i{}^{j})^{k}} \quad ; \quad (L_i{}^{j})^{k} = (\boldsymbol{\varphi}_i{}^{j})^{k\,T}\,\mathbf{M}\{\mathbf{1}\} \quad ; \quad (M_i{}^{j})^{k} = (\boldsymbol{\varphi}_i{}^{j})^{k\,T}\,\mathbf{M}\,(\boldsymbol{\varphi}_i{}^{j})^{k}$$

$$(\boldsymbol{\psi}_i{}^{j})^{k} = (\boldsymbol{\varphi}_i{}^{j})^{k}\,(Y_i^{j})^{k}\;(S_{d\,i}{}^{j})^{k}$$

Step 15. Compute the displacements $(\boldsymbol{\psi}^{*j})^{k}$ of the structure by *SRSS* combination of $(\boldsymbol{\psi}_i^{j})^{k}$:

$$(\boldsymbol{\psi}^{*\,j})^{k} = SRSS\;[(\boldsymbol{\psi}_i{}^{j})^{k}]$$

Step 16. Compare computed displacements $(\boldsymbol{\psi}^{*j})^{k}$ with trial displacements $(\boldsymbol{\psi}^{j})^{k}$:

If $\dfrac{(\psi_i{}^{j})^{k} - (\psi_i{}^{*j})^{k}}{(\psi_i{}^{j})^{k}} \le Tol$ for all i DOF

go to *Step 3*

else

$(\boldsymbol{\psi}^{j})^{k} = (\boldsymbol{\psi}^{*j})^{k}$, go to *Step 17*

Step 17. Compute external storey forces $\mathbf{F}_{ext}{}^{k}$:

$$\mathbf{F}_{ext}{}^{k} = \mathbf{K}_{\sec}{}^{k}\ \boldsymbol{\psi}^{k}$$

Step 18. Compute modal effective mass $M_{eff\,i}{}^{k}$:

$$M_{eff\,i}{}^{k} = \frac{(L_i{}^{k})^2}{M_i{}^{k}}$$

Step 19. Compute modal base shear $V_{b\,i}{}^{k}$:

$$V_{b\,i}{}^{k} = M_{eff\,i}\ S_{a\,i}{}^{k}$$

Step 20. Compute total base shear $V_b{}^{k}$ by *SRSS* combination:

$$V_b{}^{k} = SRSS\ [V_{b\,i}{}^{k}]$$

Step 21. If $k < \mathrm{K}$ then

$k = k + 1$, go to *Step 2*

else

Stop

The step-by-step procedure consists of an internal iteration loop denoted by index j and an external cycle loop denoted by index k. The external cycle loop consists of K cycles, each cycle corresponding to a target level of base acceleration a_g. At each cycle k, J^k iterations are performed to reach a converged solution.

From *Step 3* the trial displacement shape is taken either as the last converged state in the previous k cycle or as the last computed state obtained in the previous j iteration. As for the trial displacement shape ψ_0 used to start the procedure it is preferable to use an inverted triangular shape with small displacement values corresponding to elastic behaviour of the structure.

From *Step 10* the total damping of the structure is computed as the sum of the energy-weighted hysteretic damping contributions of structural members and the structure viscous damping ξ_v that remains constant throughout the analysis.

In *Step 13* the spectral displacements are computed from the spectral accelerations computed on *Step 12* from the acceleration spectra RS_a. This option enables the user to use the acceleration spectra as defined by most seismic building codes.

The variables introduced in *Step 14*, namely L_i, M_i and Y_i, are no more than the modal-earthquake excitation factor, modal mass and modal amplitude used in the standard analysis of earthquake response of lumped MDOF systems.

It is also possible to compute other quantities of interest, such as the total interstorey force, or the percentage of equivalent damping proportioned by each storey or by each member type M_q.

EXAMPLE OF A 3-STOREY INFILLED RC BUILDING FRAME

An example of a three storey frame RC building (Photo 2) that will be tested at the European Laboratory for Structural Assessment (ELSA) is presented in the following. The structure is part of a project to study the seismic behaviour of flat-slab buildings designed in accordance with the 1986 Italian national seismic code (Ministero dei Lavori Pubblici 1986). Extensive nonlinear analyses have been performed in preparation for the testing campaign, thus permitting to derive the force and damping envelopes required for the proposed procedure (Negro et al. 2002). In addition, the analytical results will be published before performing the tests in the laboratory, thus giving the opportunity of a "blind" check of the validity of the assessment procedure proposed herein.

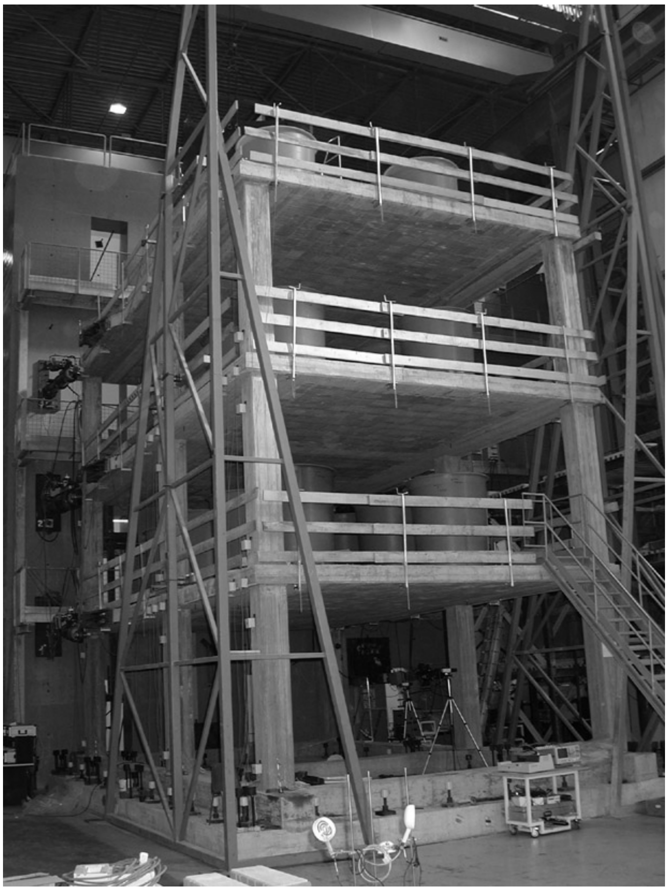

Photo 2 3-Storey RC Flat-slab Building

Description of the structure

The test specimen is a full scale building composed of two frames with two spans of 6 and 4 meters as shown in Fig. 1. The storey heights are 2.82, 5.76 and 8.70 metres measured from the base of columns, with free interstorey heights of 2.70 m. A slab with a thickness of 20 cm and with 4 cm topping was adopted. The beams are 1 m wide, have the same height of the slab and are supported by columns of 40 cm square cross section. An eccentricity of 20 cm exists between the axis of the beam and that of the column. Due to the limited cross section height, beams have rather high reinforcement on both sides, however, only some rebars are anchored or passing through the column the column joint.

The self weight of the slab is 3.5 kN/m^2. An extra permanent load of 2.0 kN/m^2 and a live load of 2.0 kN/m^2 were considered. The inertial masses m used for the seismic design and analysis were of 51.61 Ton for the first and second storeys and of 54.12 Ton for the third storey. The structure was designed for medium seismicity (base shear coefficient 0.07, importance factor 1.0), which corresponds to a peak ground acceleration of 0.25 g.

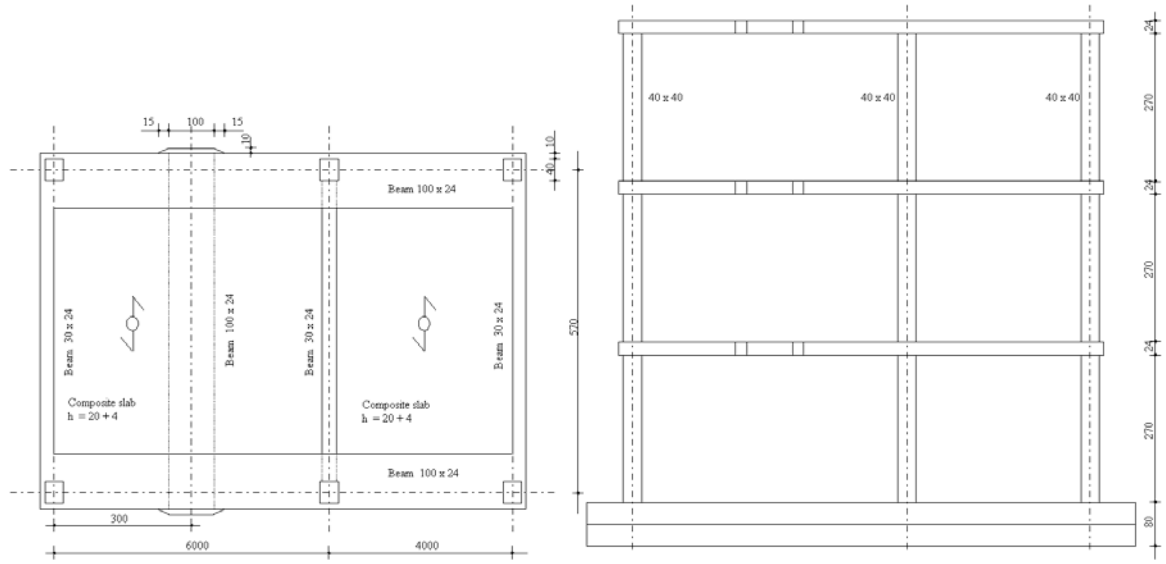

Fig. 1 Lay-out of the RC building frame mock-up

To represent the construction practice before the new Italian code came into effect (Ministero dei Lavori Pubblici 1997), the detailing rules in the current code were intentionally violated. This applies to the eccentricity between beam and column axes, as well as to the width of the beam, which would not have been acceptable. In addition, no rules for ductility were considered: columns have single 8 mm stirrups (with 90° bents) at 20 cm spacing, beams have double 8 mm stirrups at 15 cm spacing. Standard materials were used (concrete C25/30 and steel deformed bars with 440 MPa characteristic yield strength).

Seismic Input

The seismic input used for the analysis corresponds to the elastic response spectrum RS_a given by (Eurocode 8 1998) for sub-soil class B for increasing levels of peak ground acceleration a_g. The damping correction factor η is given by Eq. (4) and was derived as the best fit of the reduction factors proposed by (Boomer and Elnashai 1999) for elastic displacement spectra predicated from attenuation equations. Eq. (4) gives a better estimate than Eurocode 8 of the damping correction factor for large values of damping up to 30%.

$$\begin{aligned} \eta &= \sqrt{\frac{7}{2+\xi}} && \text{for} \quad \xi < 5\% \\ \eta &= \sqrt{\frac{10}{5+\xi}} \geq 0.53 && \text{for} \quad \xi \geq 5\% \end{aligned} \tag{4}$$

Interstorey RC Frame Envelopes

Interstorey envelopes were derived for the RC frame based on analytical results obtained from a nonlinear model of the structure using the FEM computer code IDARC2D (Valles et al. 1996). The standard lumped-plasticity model was used using a trilinear model with pinching behaviour and strength and stiffness degradation; the skeleton curve was modified to include the effect of slippage of the rebars. The parameters of the model were adjusted to fit the experimental behaviour observed on similar RC elements (Negro et al. 2002).

Nonlinear quasi-static cyclic analyses were performed by imposing displacement shapes corresponding to (*d*, *d*, *d*), (0, *d*, *d*) and (0, 0, *d*) for the first, second and third storeys to study the interstorey force-displacement behaviour; displacement *d* corresponded to a cyclic history of increasing amplitudes of 2.0, 5.0, 9.7, 14.8, 20.9 (18.0 for the third interstorey) and 27.0 mm. Three cycles were imposed at each displacement amplitude with the purpose of stabilising the pinching, stiffness and strength degradation effects accounted by the model; the interstorey force-displacement envelope used in this study was obtained from the values obtained at the third cycle.

Force-Displacement Envelope

The interstorey shear-displacement envelopes obtained from the nonlinear analysis were fitted with the expression formulated by (Menegotto and Pinto 1973) to describe the monotonic envelope of the stress-strain uniaxial behaviour of steel reinforcing bars:

$$V_c = k_{c0}\left[b_V + \frac{1-b_V}{\left[1+\left(\dfrac{\Delta\psi}{d_{V\,c0}}\right)^{R_V}\right]^{1/R_V}} \right]\Delta\psi \quad > \quad 0 \tag{5}$$

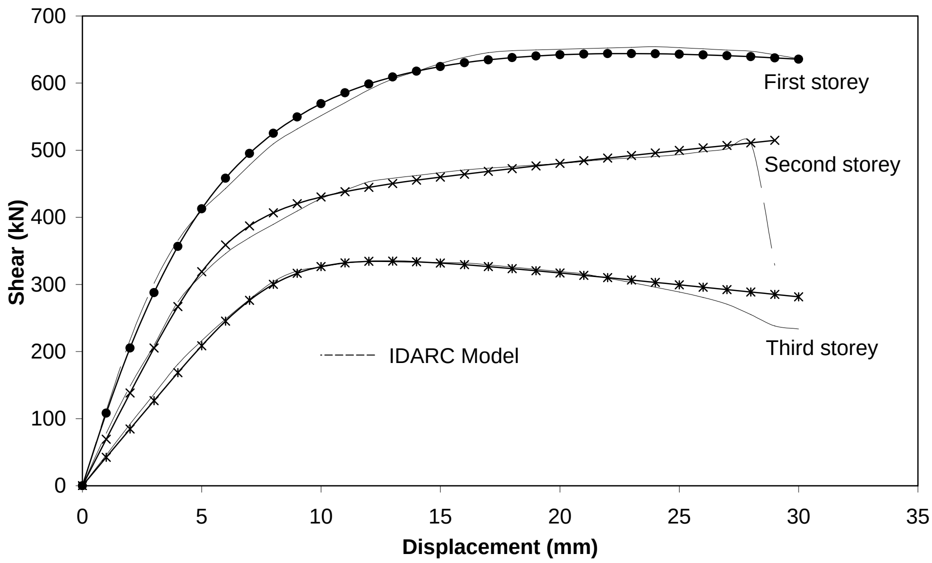

Fig. 2 RC Frame Interstorey Shear-Displacement Envelope

where V_c is the RC frame resisting force corresponding to interstorey displacement $\Delta\psi$, k_{c0} is the initial stiffness, b_V is the post-elastic to initial stiffness ratio, $d_{V\,c0}$ is the “yield” interstorey displacement and R_V is a parameter which can vary from 0 to infinity. Low values of the R_V parameter result in a smooth variation of the slope from initial to post-elastic stiffness, while large values of R_V give a sharp variation of the slope resulting in a curve that mimics a bi-linear behaviour. The advantage of this formulation is that it is continuous and closed-form and requires parameters that are well related with the force-displacement envelope of a structure. Eq. (5) corresponds to the member interstorey shear force envelope function $f_{V\,Mq}$ proposed in the step-by-step procedure. For ease of notation index M_q has been changed to c to denote the RC frame. The force-displacement envelopes are shown in Fig. 2 and the parameters used in Eq. (5) are given in Table 1.

Table 1 RC Frame Menegotto-Pinto Parameters of Interstorey Shear-Displacement Envelopes

Storey	k_{co} kN/mm	b_V	$d_{V\,c0}$ mm	R_V
1	113.4	-0.038	7.0	1.6
2	69.35	0.054	6.2	4.0
3	42.35	-0.086	8.5	5.0

Damping-Displacement Envelope

The interstorey damping-displacement envelope is computed from Eq. (1) based on the area contained by the hysteresis loops of the cyclic numerical nonlinear response of the numerical model described in the previous sub-section using IDARC2D. The equivalent damping was computed for the third cycle at each of the imposed displacement amplitudes, resulting in lower values than those expected for the first cycle, thus recognising some amount of degradation in the RC frame. The damping envelopes were also fitted with the Menegotto and Pinto formulation, the expression is now reformulated into Eq. (6) to account for the different parameters given as input to define the member storey shear force envelope function $f_{\xi\,Mq}$ proposed in the step-by-step procedure:

$$\xi_c = \frac{\xi_{c0}}{d_{\xi\,c0} - d_{\xi\,cs}} \left[b_\xi + \frac{1 - b_\xi}{\left[1 + \left(\dfrac{\Delta\psi - d_{\xi\,cs}}{d_{\xi\,c0} - d_{\xi\,cs}} \right)^{R_\xi} \right]^{1/R_\xi}} \right] \left(\Delta\psi - d_{\xi\,cs} \right) \;>\; 0 \quad \text{for} \quad \Delta\psi \geq d_{\xi\,cs} \tag{6}$$

$$b_\xi = \frac{\dfrac{\xi_{cu}}{\xi_{c0}} - 1}{\dfrac{d_{\xi\,cu} - d_{\xi\,cs}}{d_{\xi\,c0} - d_{\xi\,cs}} - 1} \tag{7}$$

Table 2 RC Frame Menegotto-Pinto Parameters of Interstorey Damping-Displacement Envelope

Storey	$d_{\xi\,cs}$	$d_{\xi\,c0}$ mm	$d_{\xi\,cu}$	ξ_{c0}	ξ_{cu} %	R_ξ
1	2	7.2	27	8.4	5.9	5.0
2	2	6.0	27	5.0	5.8	3.5
3	2	4.8	8.7	8.5	3.2	2.5

where ξ_c is the RC frame equivalent damping corresponding to interstorey displacement $\Delta\psi$, ξ_{c0} is the damping related to displacement $d_{\xi\,c0}$ and R_ξ is a parameter which can vary from 0 to infinity.

Parameter b_ξ is computed from Eq. (7), ξ_{cu} is the damping related to displacement $d_{\xi\,cu}$ and $d_{\xi\,cs}$ is the displacement corresponding to loss of linearity; for $\Delta\psi < d_{\xi\,cs}$ the hysteretic equivalent damping ξ_c is equal to zero. The damping-displacement envelopes are shown in Fig. 3 and the parameters used in Eqs. (6) and (7) are given in Table 2.

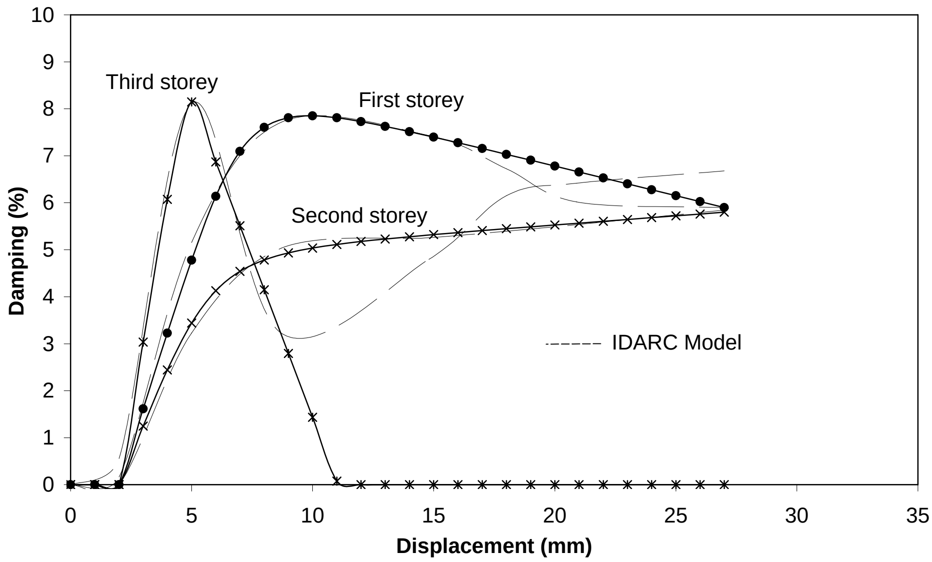

Fig. 3 RC Frame Interstorey Damping-Displacement Envelope

Interstorey Infill Wall Envelopes

The infill wall envelopes were computed from the infill macromodel developed at the University of Patras by Panagiotakos and Fardis and described in (ECOEST-PREC8 1996).

Force-Displacement Envelope

The force displacement envelope is a trilinear function with the following properties:

$$k_{w0} = \frac{G_w A_w}{H_w} \quad ; \quad A_w = L_w t_w \tag{8}$$

$$k_{wu} = \frac{E_w W_{eff} t_w}{\sqrt{L^2 + H^2}} \cos^2\theta \quad ; \quad \theta = \arctan(H/L) \tag{9}$$

$$W_{eff} = 0.175(\lambda_h H)^{-0.4}\sqrt{L^2 + H^2} \quad ; \quad \lambda_h = \sqrt[4]{\frac{E_w t_w \sin 2\theta}{4\, E_c I_c H_w}} \tag{10}$$

$$V_{w0} = \tau_{w\,cr}\, A_w \quad \text{and} \quad V_{wu} = 1.3\, V_{w0} \tag{11}$$

where k_{w0} is the intial stiffness, k_{wu} is the secant ultimate stiffness at ultimate shear strength V_{wu} and V_{w0} is the shear cracking strength corresponding to the change of secant stiffness from initial to ultimate. The input parameters needed to compute these values are: G_w, E_w and $\tau_{w\,cr}$ corresponding to the shear modulus (1240 MPa), elastic modulus in the horizontal (weak) direction (2520 MPa) and diagonal cracking strength (0.28 MPa) of masonry; L_w, H_w and t_w corresponding to the length (3.60 and 5.60 m), height (2.70 m for all storeys) and thickness (11.2 cm) of the infill wall; H and L corresponding interstorey height (2.94 m for all storeys) and bay length (4 and 6 m) of the RC frame; E_c and I_c corresponding to the elastic modulus of concrete (30000 MPa) and the moment of inertia of columns (213000 cm^4). Other parameters derived from the above equations are the cross section area A_w of the infill wall and the effective width W_{eff} of the equivalent strut inclined at an angle θ with respect to the horizontal.

The linear unloading branch after reaching V_{wu} is replaced by the exponential strength decay proposed by (Klingner and Bertero 1976), where ν is the strength decay coefficient (0.035 mm^{-1}), υ is the elongation of the compression strut and d_{wu} is the displacement corresponding to maximum strength V_{wu}:

$$V_w = V_{wu}\, e^{-\nu\upsilon} \quad \text{for} \quad \Delta\psi > d_{wu} \quad ; \quad \upsilon = \frac{\Delta\psi - d_{wu}}{\cos\theta} \quad \text{and} \quad d_{wu} = \frac{V_{wu}}{k_{wu}} \tag{12}$$

The shear-displacement envelope of the infill wall is shown in Fig. 4 and was computed as the sum in parallel of the contributions of the two sections of 3.60 and 5.60 meters of length. The parameters that result from Eqs. (9), (11) and (12) are given in Table 3 and describe the infill wall shear-displacement envelope $f_{V\,w}$ function used in the step-by-step procedure.

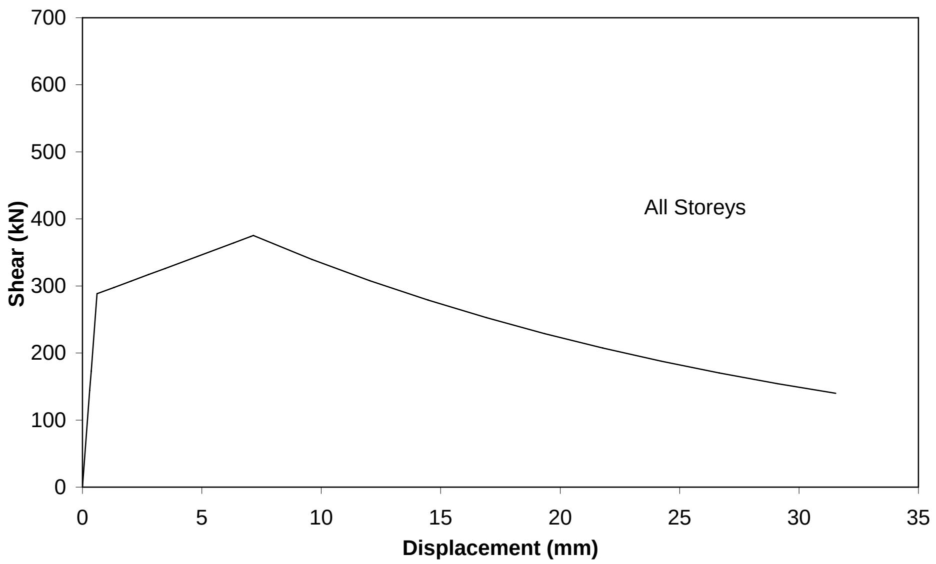

Fig. 4 Infill Wall Interstorey Shear-Displacement Envelope

Table 3 Infill Wall Parameters of Interstorey Shear-Displacement Envelopes

Storey	k_{w0}	k_{wu}	V_{w0}	V_{wu}	θ	ν
	kN/mm		kN		rad	mm^{-1}
1, 2, 3	473	52.4	289	375	0.53	0.035

It is also possible to reduce the shear capacity of the infill wall to account for cyclic damage by using the following expression, where a (~0.025) and κ (exponent that accounts for half cycle ductility accumulation) are parameters derived from tests and set to zero for the present analysis:

$$V_w = V_w \, e^{-2a(\Delta\psi / d_{w0})^{\kappa}} \quad ; \quad d_{w0} = \frac{V_{w0}}{k_{w0}} \tag{13}$$

Damping Displacement-Envelope

The damping envelope of the infill wall is computed from the expression given in Eq. (14) in terms of ductilities μ_w and μ_{wu} as defined in Eq. (15), stiffness ratios p and p_1 as defined in Eq. (16) and parameters α, β and γ, defining the unloading brach; the damping formulas apply for reloading cycles after the first. Damping ξ_w is equal to zero for $\mu_w < 1$.

The infill wall damping envelope function $f_{\xi\,w}$ defined by Eq. (14) is shown in Fig. 5 and was derived with the parameters given on Table 4. The values of α, β and γ correspond to those recommended in (ECOEST-PREC8 1996).

$$\xi_w = \frac{(1-p)(\mu_w - 1)}{\pi\,\mu} \, \frac{\beta + 0.5(1-\alpha)(1-\gamma)[1 + p(\mu_w - 1)]}{1 + p(\mu - 1)} \quad \text{for} \quad \mu_w < \mu_{wu}, \quad \text{else}$$

$$\xi_w = \frac{\mu_w - 1 - p\,(\mu_{wu} - 1) + p_1(\mu_w - \mu_{wu})}{\pi\,\mu} \, \frac{\beta + 0.5(1-\alpha)(1-\gamma)[1 + p(\mu_{wu} - 1) - p_1(\mu_w - \mu_{wu})]}{1 + p(\mu_{wu} - 1) - p_1(\mu_w - \mu_{wu})} \tag{14}$$

$$\mu_w = \frac{\Delta\psi}{d_{w0}} \quad \text{and} \quad \mu_{wu} = \frac{d_{wu}}{d_{w0}} \tag{15}$$

$$p = \frac{V_{wu} - V_{w0}}{d_{wu} - d_{w0}} \, \frac{1}{k_{wo}} \quad \text{and} \quad p_1 = \frac{V_{wu}\left(e^{-1.5\,\nu\, d_{wu} / \cos\theta} - 1\right)}{1.5\, d_{wu}\, k_{wo}} \tag{16}$$

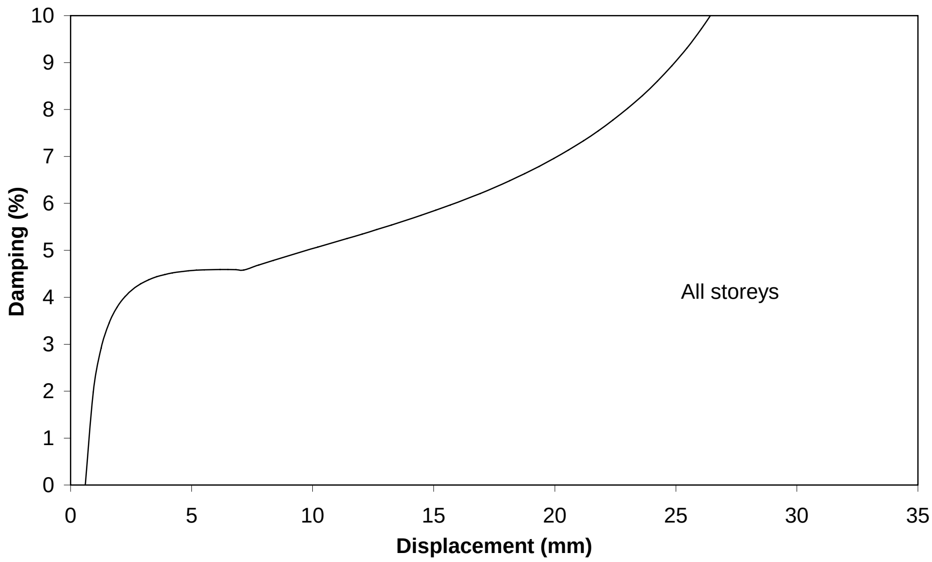

Fig. 5 Infill Wall Interstorey Damping-Displacement Envelope

Table 4 Infill Wall Parameters of Interstorey Damping-Displacement Envelope

Storey	α	β	γ	p	p_1
1, 2, 3	0.15	0.10	0.80	0.0279	0.0275

Response of the Regularly and Irregularly Infilled RC Frame

The proposed step-by-step procedure is used to analyse the response of the RC building considered in this example for a series of increasing peak ground accelerations a_g up to a maximum of 0.35g (length of $\mathbf{a_g}$ vector: K = 60, i.e. intervals of 0.00583g). The properties of the RC frame and infill walls were given in the previous sections. The remaining values given as input to start-up the analysis procedure are: number of storeys n = 3, trial displacement shape ψ_0 equal to a constant drift of 0.05%, convergence tolerance *Tol* of 0.01% and constant viscous damping ξ_v of 2.5%.

The analysis results are presented in terms of interstorey displacements versus peak ground acceleration. The plots are presented against a performance criteria (a dashed line) for visually assessing the state of the structure, with no influence on the analysis results. The performance criteria corresponds to a polynomial curve defined by interstorey drifts of 0.15% (4.41 mm), 0.45% (13.3 mm) and 0.75% (22.1 mm) at a_g values of 0.07g, 0.25g and 0.35g, allowing for minor, medium and extensive damage for small, medium and large periods of return of the earthquake. For a_g less than 0.07g the interstorey drift criteria is constant and equal to 0.15%.

The results for the regularly infilled frame are shown in Fig. 6, and show that the structure satisfies the assumed performance criteria up to a maximum interstorey displacement at first storey of 8.2 mm, when the infill wall enters into the unloading branch and the structure develops an unstable soft-storey mechanism at 0.28g.

The analysis of the response of the bare frame and of irregular storey-wise infilled wall configurations give further insight into the problem. In Fig. 7 the response of the bare frame is shown, showing that interstorey drifts are largest at the second storey, exceeding the performance criteria at a_g equal to 0.175g with an interstorey displacement of 8.8 mm; the structure becomes unstable when the first storey also develops a mechanism at a_g equal to 0.25g. In Fig. 8 shows the response of the frame with infills at second and third storeys only, showing that in this case all deformations are concentrated in the first storey, exceeding the performance criteria at a_g equal to 0.16g with a displacement of 7.8 mm and becoming unstable at a_g equals to 0.19g.

On Table 5 the response quantities relative to the external storey force (F_{ext}), interstorey shear (V_{int}), interstorey secant stiffness ($k_{sec\ int}$) and interstorey equivalent damping (ξ_{int}) contributions of the RC frame and infill wall members for a_g equal to 0.175g are given for the three structural configurations corresponding to the regularly infilled frame, bare frame and first soft storey frame. The response quantities in terms of interstorey displacement, structure damping, first mode period, spectral displacement and spectral acceleration, and structure base shear are given in Table 6 for a_g equal to 0.175g for all the possible combinations of regularly and irregularly infilled frames.

Focusing on the first three configurations represented in Figs. 6, 7 and 8, it is possible to conclude what has been observed from previous experimental tests, nonlinear time history analyses and field observations: the regularly infilled frame can sustain base accelerations 50% larger than the bare frame, however, the failure mode of the latter is more "ductile" when compared with the sudden failure that takes place when the first storey infill wall reaches its maximum capacity. The soft storey configuration develops a mechanism at about the same base acceleration as the bare frame, yet with mechanisms that are intrinsically different: the bare frame develops a mechanism at the second storey, confirming the results obtained from preliminary time history nonlinear analyses.

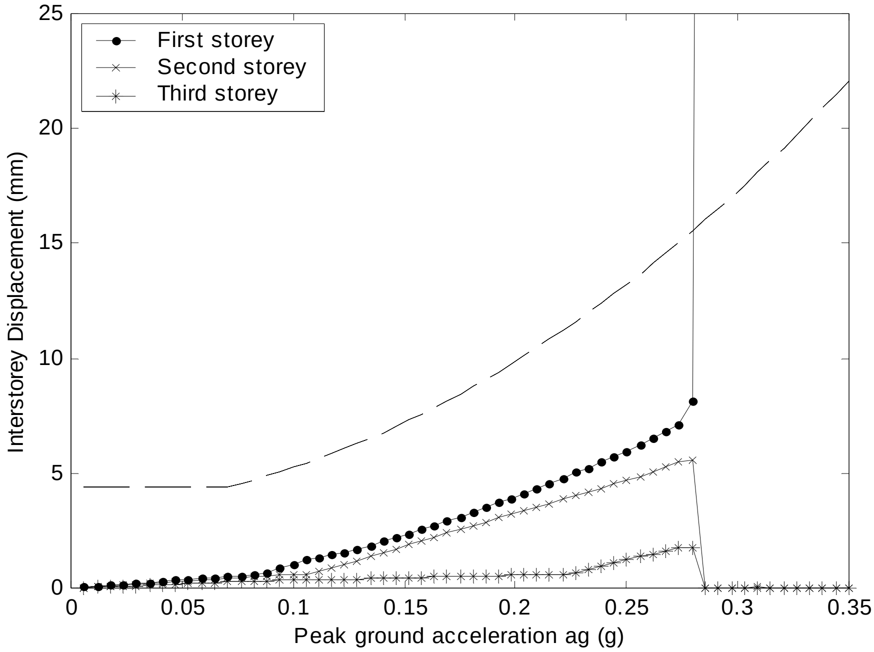

Fig. 6 Regularly Infilled RC Frame Displacement Response

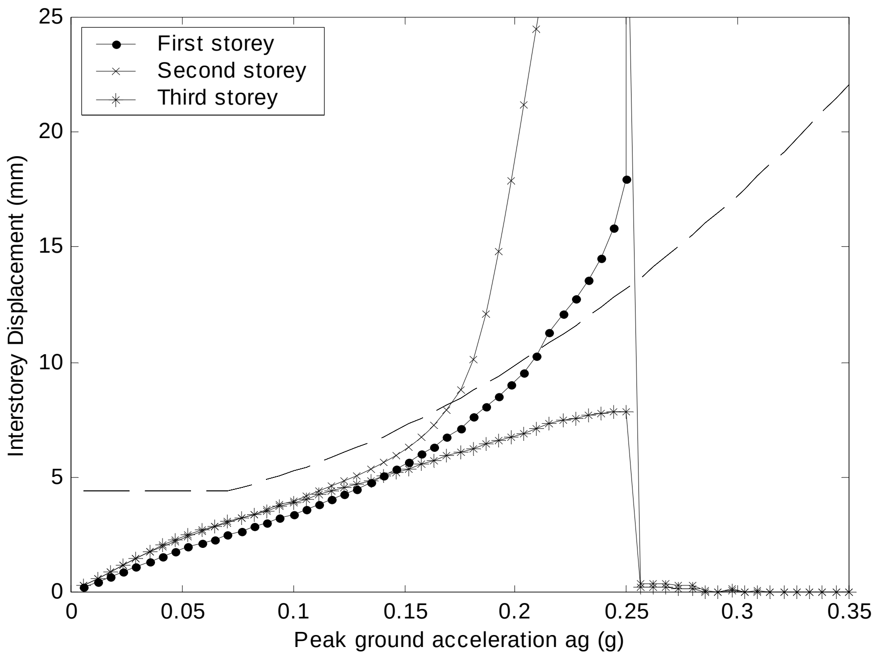

Fig. 7 Bare RC Frame Displacement Response

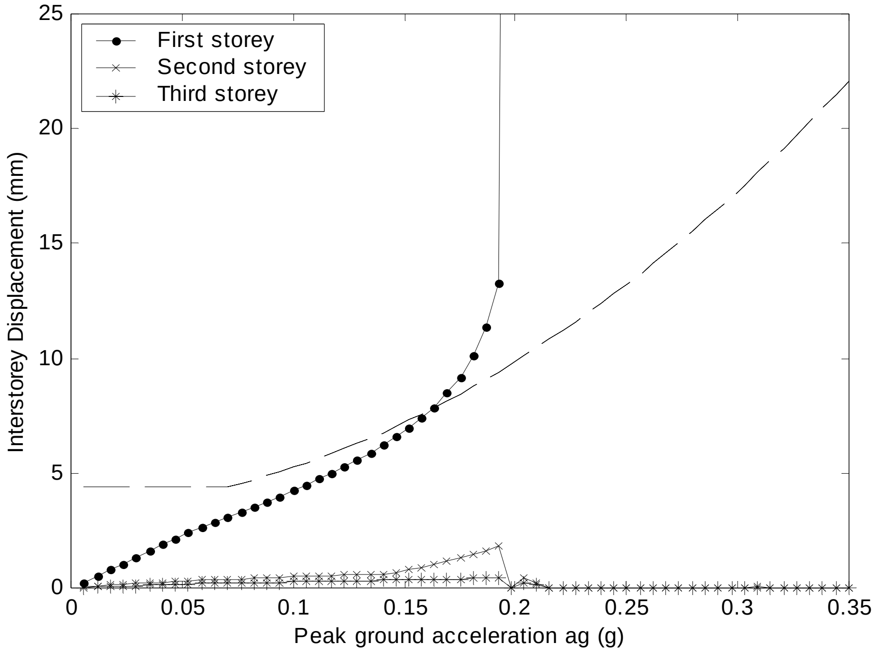

Fig. 8 1st Soft Storey RC Frame Displacement Response

Table 5 RC Frame Response for 3 Infilled Configurations for a_g = 0.175g

Storey n	***F_{ext} (kN)***			***V_{int} (kN)***			***$k_{sec\ int}$ (kN/mm)***			***ξ_{int} (%)***		
	Total	*RC*	*Infill*	*Total*	*RC*	*Infill*	*Total*	*RC*	*Infill*	*Total*	*RC*	*Infill*
Regularly Infilled												
3rd	262	22	241	262	22	241	515	42	473	0.00	0.00	0.00
2nd	228	155	74	491	176	315	192	69	123	1.11	0.09	1.01
1st	127	120	7	618	296	322	199	95	104	1.81	0.50	1.31
Bare Frame												
3rd	248	248	0	248	248	0	41	41	0	1.17	1.17	0.00
2nd	170	170	0	418	418	0	48	48	0	2.06	2.06	0.00
1st	82	82	0	500	500	0	70	70	0	2.94	2.94	0.00
1st Soft Storey												
3rd	203	17	187	203	17	187	515	42	473	0.00	0.00	0.00
2nd	187	75	112	390	92	298	295	69	225	0.21	0.00	0.21
1st	163	462	-298	554	554	0	60	60	0	7.01	7.01	0.00

Table 6 RC Frame Response for all Possible in-height Infilled Configurations / a_g = 0.175g

Infill wall?	3rd	yes	no	yes	yes	no	no	no	yes
	2nd	yes	no	yes	no	yes	no	yes	no
	1st	yes	no	no	yes	yes	yes	no	no
Interstorey Dislacement (mm)									
3^{rd} Storey		0.51	6.07	0.39	0.44	5.69	6.28	6.17	0.43
2^{nd} Storey		2.56	8.77	1.32	10.42	0.55	7.43	1.35	9.73
1^{st} Storey		3.11	7.14	9.19	1.66	0.71	1.24	7.72	7.99
ξ_S (%)		5.42	8.66	9.72	7.06	8.12	7.46	9.33	8.74
1^{st} Mode Period (s)		0.224	0.435	0.339	0.343	0.248	0.353	0.360	0.418
1^{st} Mode S_d (mm)		5.36	17.58	10.27	11.67	5.83	12.16	11.74	16.17
1^{st} Mode S_a (m/s^2)		4.20	3.67	3.54	3.91	3.75	3.85	3.59	3.66
Base Shear (kN)		618	500	554	477	369	430	517	525

CONCLUSIONS

The analysis methodology presented herein offers a valuable tool to analyse and assess the seismic response of multi-storey structures. The methodology is based on stiffness and equivalent damping envelopes in terms of the interstorey displacements of the different members that constitute the structure (RC and masonry walls for the example presented). The analysis procedure allows to study the evolution of structural response for increasing levels of earthquake base excitation to different structural configurations at very low computing costs, thus offering a valuable tool not only for assessment, but for structural design as well.

The results confirm the observations gathered in recent years from the study of infilled frames: the design of a RC frame must take into account the presence of infilled masonry walls in order to account for the effective modes of failure that take place at different levels of earthquake excitation. The proposed methodology offers the means to analyse/design such structures in the framework of performance base design.

ACKNOWLEDGMENTS

The authors acknowledge the contribution of Marcin Kowalski in performing the pushover nonlinear analyses for generating the RC frame envelopes. The discussions with Eugenio Gutiérrez on the use of equivalent damping/stiffness were of most value for developing the proposed procedure.

REFERENCES

Boomer, J. J. and Elnashai, A. S. (1999). “Displacement Spectra for Seismic Design”. *Journal of Earthquake Engineering* , Vol. 3, No.1, 1-32.

Colombo A., Negro P. and Verzeletti G. (1998). “Infilled Frames: Certainties and Uncertainties”. *11th European Conference on Earthquake Engineering*, 6-11 September, Paris.

Dolsek, M. and Fajfar, P. (2001). “Soft Storey Effects in Uniformly Infilled Reinforced Concrete Frames”. *Journal of Earthquake Engineering*, Vol. 5, No. 1, 1-12.

Eurocode 8, (1998). "General Rules and Rules for Buildings–Seismic Actions and General Requirements for Structures". *European Committee for Standardisation* , ENV 1988-1-1: 1994 E, 14-19.

ECOEST- PREC 8 (1996). "Experimental and Numerical Investigations on the Seismic Response of RC Infilled Frames and Recommendations and Provisions". *European Consortium of Earthquake Shaking Tables – Prenormative Research in Support of Eurocode 8*, Report No. 6, November 96, Edited by M. Fardis and 9-24.

Fajfar, P., Gašperšič, P. and Drobnič D. (1997). "A Simplified Nonlinear Method for Seismic Damage Analysis of Structures". *International Workshop on Seismic Design Methodologies for the Next Generation of Codes*, Bled – Slovenia, 24-27 June, 183-193.

Fajfar, P. and Krawinkler / Editors (1997) "Seismic Design Methodologies for the Next Generation of Codes". *Proceedings of the International Workshop*, Bled – Slovenia, 24-27 June.

Fardis, M. N. and Panagiotakos, T. B. (1997). "Displacement-based design of RC buildings: Proposed Approach and Application", *International Workshop on Seismic Design Methodologies for the Next Generation of Codes*, Bled – Slovenia, 24-27 June, 195-206.

Fardis M. N, Negro P., Bousias S. N. and Colombo A. (1999a). "Seismic Design of Open-Storey Infilled RC Buildings". *Journal of Earthquake Engineering*, Vol. 3, No. 2, 173-199.

Fardis M. N, Bousias, S. N., Franchioni, G. and Panagiotakos, T.B.(1999b). "Seismic Response and Design of RC Structures with Plan-Eccentric Masonry Infills". *Earthquake Engineering & Structural Dynamics,* 28(2), 173-191.

Miranda, E. (1997). "Estimation of Maximum Interstorey Drift Demands in Displacement-Based Design". *International Workshop on Seismic Design Methodologies for the Next Generation of Codes*, Bled – Slovenia, 24-27 June, 253-264.

Miranda, E. and Ruiz-Garcia, J. (2002). "Evaluation of approximate Methods to estimate maximum Inelastic Displacement Demands". *Earthquake Engineering and Structural Dynamics*, 31, 539-560.

Negro P. and Colombo A. (1997). "Irregularities Induced by Nonstructural Masonry Panels in Framed Buildings", *Engineering Structures*, Vol. 19, No. 7, 576-585.

Negro P., Vukazich S. and Colombo A. (2002). "Seismic Assessment of Flat Slab Buildings: The Case of Old Italian Practice". *European Laboratory for Structural Assessment*, Special Publication (to appear), Joint Research Centre, Ispra – Italy.

Valles R. E., Reinhorn A. M., Kunnath, S. K., Li, C. and Madan, A. (1996). "IDARC2D Version 4.0: A Computer Program for the Inelastic Damage Analysis of Buildings". *National Center for Earthquake Engineering Research*, Technical Report NCEER-96-0010, State University of New York at Buffalo (http://civil.eng.buffalo.edu/idarc2d50/).

Klingner, R. E. and Bertero, V. V. (1976). "Infilled Frames in Earthquake Resistant Construction". *Earthquake Engineering Research Center*, Report No. EERC 76-32, University of California at Berkeley.

Menegotto, M. and Pinto, P. (1973). "Method of Analysis for Cyclically Loaded RC Plane Frames Including Changes in Geometry and Non-elastic Behaviour of Elements Under Combined Normal Force and Bending". *IABSE*, Symposium on the Resistance and Ultimate Deformability of Structures Acted on by Well Defined Repeated Loads, Zurich, 15-22.

Ministero dei Lavori Pubblici (1986). *Norne Tecniche Relative alle Costruzioni Sismiche*, Decreto 16 e 24, Gennaio 1986.

Ministero dei Lavori Pubblici (1996). *Istruzioni per l'Applicazione delle Norme per le Costruzioni in Zone Sismiche di cui al D.M. 16 Gennaio 1996*, Circolare 10 Aprile 1997 n. 65.

Priestley M. J. N. and Calvi G. M. (1997). "Concepts and Procedures for Direct Displacement Based-Design and Assessment". *International Workshop on Seismic Design Methodologies for the Next Generation of Codes*, Bled – Slovenia, 24-27 June, 171-181.

Reinhorn, A. (1997). "Inelastic Analysis Techniques in Seismic Evaluations". *International Workshop on Seismic Design Methodologies for the Next Generation of Codes*, Bled – Slovenia, 24-27 June, 277-287.

Taucer, F. (2000). “Displacement Based Design of Infilled Frames Protected with Energy Dissipation Devices – Excel Implementation Procedure”. *European Laboratory for Structural Assessment*, Technical Note No. I.00.37, Joint Research Centre, Ispra – Italy.

Taucer, F. and Marazzi, F. (2000) “Displacement Based Design of Infilled Frames Protected with Energy Dissipation Devices”. *Second European Conference on Structural Control*, Champs-sur-Marne – France, July 3-6.

国土技術政策総合研究所資料
Ｎｏ．１０４　　　　2003 **年** 3 **月**

編集･発行　©国土技術政策総合研究所

本資料の転載･複写の問い合わせは
〒305－0804　茨城県つくば市旭1番地
企画部研究評価･推進課　TEL　029－864－2675

Technical Note of NILIM
No.104　　March 2003

Edited and published by NILIM, MLIT, JAPAN
All rights reserved, Copyright ©

Details and advice about the copy or transmission of this book can be obtained from the Copyright Holder, Research Administration and Evaluation Division of NILIM.

Address: 1, Asahi, Tsukuba-city, Ibaraki-prefecture, JAPAN, 305-0804
Telephone: +81-(0)29-864-2675